



저작자표시-비영리-변경금지 2.0 대한민국

이용자는 아래의 조건을 따르는 경우에 한하여 자유롭게

- 이 저작물을 복제, 배포, 전송, 전시, 공연 및 방송할 수 있습니다.

다음과 같은 조건을 따라야 합니다:



저작자표시. 귀하는 원저작자를 표시하여야 합니다.



비영리. 귀하는 이 저작물을 영리 목적으로 이용할 수 없습니다.



변경금지. 귀하는 이 저작물을 개작, 변형 또는 가공할 수 없습니다.

- 귀하는, 이 저작물의 재이용이나 배포의 경우, 이 저작물에 적용된 이용허락조건을 명확하게 나타내어야 합니다.
- 저작권자로부터 별도의 허가를 받으면 이러한 조건들은 적용되지 않습니다.

저작권법에 따른 이용자의 권리는 위의 내용에 의하여 영향을 받지 않습니다.

이것은 [이용허락규약\(Legal Code\)](#)을 이해하기 쉽게 요약한 것입니다.

[Disclaimer](#)

이학박사 학위논문

**Development of hepatitis C virus NS5A
inhibitors using SuFEx chemistry and
development of effective treatments for
hepatitis C genetic mutations based on fluorene
structures**

**SuFEx 화학을 이용한 C 형 간염 바이러스
NS5A 저해제 개발 및 플루오렌을 바탕으로
한 유전적 돌연변이에 효과적인 C 형 간염
치료제 개발**

2019 년 8 월

서울대학교 대학원

화학부 유기화학 전공

유 영 수

Abstract

Hepatitis C virus (HCV) infection is a serious and continuing threat to human health. The infection by the HCV can lead to liver cirrhosis and eventually hepatocellular carcinoma, which often results in death. Recently efforts have been concentrated towards developing direct acting agents (DAA's) targeting several gene products of HCV. Among several gene products of HCV, non-structural protein 5A (NS5A) is known to be essential for HCV proliferation and considerable efforts have been made in developing anti-HCV drugs targeting NS5A. We report in this thesis the discovery of a new series of potent hepatitis C virus non-structural protein 5A (NS5A) inhibitors containing biaryl sulfone or sulfate cores and substituted fluorenyl cores.

First, for the synthesis of HCV NS5A inhibitors containing a sulfate core structure, highly efficient, chemoselective coupling reactions between an arylsulfonyl fluoride and an aryl silyl ether, known as the sulfur(VI) fluoride exchange (SuFEx) reaction, were utilized. Among the inhibitors prepared based on the SuFEx chemistry, several compounds exhibited two-digit picomolar EC_{50} values against GT-1b and single digit or sub-nanomolar activities against HCV GT-2a strain. Nonsymmetrical inhibitors containing an imidazole and amide moieties on each side of the sulfate core structures were also synthesized. Structure-activity relationship (SAR) studies on inhibitors containing various substitution patterns of the sulfate or sulfone core structure established that *m,m'*-substituted biaryl sulfate core-based inhibitors containing an amide

moiety (**BMK-21014**) or an imidazole moiety (**BMK-21025**) showed extremely high potency. **BMK-21014** demonstrated double-digit pM potencies against both genotype 1b (GT-1b) and 2a (GT-2a). **BMK-21025** also exhibited double-digit pM potencies against GT-1b and sub nM potencies against GT-2a. Furthermore, **BMK-21014** and **BMK-21025** exhibited no cardiotoxicity in an hERG ligand binding assay and showed acceptable plasma stability and no mutagenic potential in the Ames test. In addition, these compounds showed distinctive additive effects in combination treatment with the non-structural protein 5B (NS5B) targeting drug sofosbuvir (Sovaldi®). The results of this study showed that the **BMK-21014** and **BMK-21025** could be effective HCV inhibitors.

In addition, a biotinylated probe targeting NS5A protein was prepared for labeling using the same synthetic methodology. These compounds also showed higher inhibitory effects than previously reported compounds. These results showed that compounds with biaryl sulfate core skeleton could be effective HCV inhibitors.

While several NS5A inhibitors in combination with inhibitors of other gene products have been effective, NS5A inhibitor resistances caused by mutants have become a major issue. To overcome the low efficacy of known inhibitors on a specific genotype and the low resistance barrier, we have generated many different derivatives of NS5A inhibitors and investigated their effects on HCV proliferation using *in vitro* as well as *in vivo* assay systems. Among several different types of inhibitors, we generated NS5A inhibitors with fluorene

prolinamide structures and found that they are highly effective on resistance mutants HCV or pan-genotype HCV. Also, we identified a close structure activity relationship (SAR) between the specific part of compounds such as fluorene core or L-proline derivatives towards daclatasvir resistance mutants. From this study, we developed compounds **BMK-21054** and **BMK-21075** that are effective for genotype 3a and drug resistance mutants. Based on these results, we were able to identify new NS5A inhibitors containing the fluorene core skeleton and substituted L-proline derivatives, which exhibit excellent inhibitory activities against various genotypes and mutant strains of HCV.

Key words: HCV, NS5A inhibitor, antiviral agent, biarylsulfate, SuFEx, structure-activity relationship, fluorene, resistance mutation

CONTENTS

Abstract	i
List of Publications	iii
List of Figures	iv
List of Schemes	vi
List of Tables	vii

Chapter 1.

Introduction on the development of hepatitis C virus and non-structural 5A protein inhibitors

1. Introduction	10
2. Non-structural 5A protein	11
3. Development of NS5A inhibitors	13

Chapter 2.

Development of potent HCV NS5A inhibitors based on a biaryl sulfate core structure

1. Introduction	17
2. Results and Discussion	21
3. Conclusion	45
4. Experimental	46

Chapter 3.

Development of effective treatments for hepatitis C genetic mutations based on fluorene structures

1. Introduction	93
2. Results and Discussion	94
3. Conclusion	115
4. Experimental	117
References	122
국문초록	129

List of Publication

1. New potent biaryl sulfate-based hepatitis C virus inhibitors, Yongsu You^{*}, Hee Sun Kim^{*}, Il Hak Bae, Seung Gi Lee, Min Hyeok Jee, Gyochang Keum, Sung Key Jang^{} and B. Moon Kim^{**}, *European Journal of Medicinal Chemistry*, **2017**, 125, 87-100**

2. Sulfur(VI) fluoride exchange as a key reaction for synthesizing biaryl sulfate core derivatives as potent hepatitis C virus NS5A inhibitors and their structure–activity relationship studies, Yongsu You, Hee Sun Kim, Jung Woo Park, Gyochang Keum, Sung Key Jang and B. Moon Kim^{}, *RSC Advances*, **2018**, 8, 31803-31821**

** These two individuals contributed equally to this work.*

*** Corresponding author.*

List of Figures

Figure 1. X-ray crystal structures of NS5A protein

Figure 2. Structure of NS5A inhibitors in market or clinical trials

Figure 3. Strategy for designing new potent HCV NS5A inhibitors

Figure 4. Biaryl sulfate core based nonstructural 5A (NS5A) inhibitors and modification using sulfur(VI) fluoride exchange (SuFEx) chemistry

Figure 5. Docking of inhibitor compounds to an NS5A (3FQQ) dimer model

Figure 6. Combination index values of compounds **22** and **26**

Figure 7. The structure of replicon NK5.1-Gluc

Figure 8. Representative ^1H NMR (400 MHz, DMSO- d_6) Analysis of Fosylation and SuFEx

Figure 9. Representative ^{19}F NMR (400 MHz, DMSO- d_6) Analysis of Fosylation and SuFEx

Figure 10. Representative ^{13}C NMR (400 MHz, DMSO- d_6) Analysis of Fosylation and SuFEx

Figure 11. 2D-interaction docking model of compounds in an NS5A dimer model

Figure 12. Superposed model of inhibitors inside NS5A dimer model

Figure 13. Superposed model of inhibitors inside NS5A dimer model

Figure 14. Structure of **BMK-21001** and Ames results of metabolite

Figure 15. Design strategy of new NS5A inhibitors

Figure 16. Schematic structure of replicons

Figure 17. Colony formation assay on NK5.1 replicon HCV

Figure 18. Colony formation assay on S52 replicon HCV

Figure 19. Genotype 3a HCV inoculated to humanized mice

Figure 20. Colony formation assay for combination with grazoprevir

Figure 21. Colony formation assay for combination with grazoprevir on S52 replicon HCV

Figure 22. Docking studies of an inhibitor compound and NS5A dimer model

List of Schemes

Scheme 1. Synthesis of NS5A inhibitors; reagents and conditions

Scheme 2. Synthesis of intermediates; reagents and conditions

Scheme 3. Synthesis of intermediates; reagents and conditions

Scheme 4. Synthesis of compound **43 (BMK-21060)**

Scheme 5. Synthesis of compound **44 (BMK-21057)**

Scheme 6. Synthesis of biotin-tagged, biaryl sulfate core based NS5A inhibitor

List of Tables

Table 1. *In silico* calculation of the distance between two capping group sterogenic centers of the NS5A inhibitors

Table 2. Preparation of fluorosulfate monomers

Table 3. Preparation of biaryl sulfate core structures using sulfur(VI) fluoride exchange (SuFEx) chemistry

Table 4. *In vitro* activities of inhibitors containing a *p*-,*p*'-disubstituted biaryl sulfone or sulfate core

Table 5. *In vitro* activities of inhibitors containing an *m*-,*m*'-disubstituted biaryl sulfate core

Table 6. Synthesis and *in vitro* antiviral activities of inhibitors comprising an amide linked biaryl sulfate core

Table 7. Synthesis and *in vitro* antiviral activities of sulfate core inhibitors equipped with imidazole moieties

Table 8. Results of hERG ligand binding assay

Table 9. Plasma stability

Table 10. Results of bacterial reverse mutation assay with compounds **22** and **26**

Table 11. The EC₅₀ values of inhibitors containing a fluorene core

Table 12. The EC₅₀ values of inhibitors containing 9,9-dibutylfluorene and pyrrolidine derivatives

Table 13. The EC₅₀ values of inhibitors containing 9,9-dipentylfluorene and pyrrolidine derivatives

Table 14. Pharmacokinetics results about compounds **47** and **54** at CD1 mice

Table 15. Combination index of NS5A inhibitors and grazoprevir

Chapter 1.

Introduction on the development of hepatitis C virus and non-structural 5A protein inhibitors

1. Introduction

HCV affects essential liver health leading to infectious hepatitis.^[1, 2] Since the first identification of HCV in 1989, approximately 3 to 4 million people are newly infected annually and 160-200 million people have been infected worldwide so far. Nearly 20 percent of those patients develop liver cirrhosis and some eventually hepatocellular carcinoma (HCC).^[3, 4] In 2014, the World Health Organization (WHO) announced that hepatitis C-related liver diseases kill 350-500 thousand people each year.^[5]

Most people were mainly infected the HCV through contact with the blood of an infected person such as the use of non-sterile apparatuses, heterosexual contact and blood transfusion.^[6] The possibility of diagnosing the HCV RNA level 1~3 weeks after infection and no symptoms in the early stages of the disease have made the infected patients increase rapidly.^[6]

To date, HCV strain has been classified into 7 genotypes and about 70 subtypes. Because of the intrinsic lack of proof-reading of HCV RNA dependent RNA polymerase (RDRP), genomic diversity of HCV has grown. According to recent estimates, genotype 1a and 1b are distributed mostly (46.2%) in the world, followed by genotype 3 (30.1%). Genotypes 2, 4 and 6 account for 22.8% of all HCV cases.^[7]

HCV is an encased RNA virus in the Flaviviridae family comprising of a 9.6-kb single (+) strand RNA.^[8] The genome of HCV consists of a single open reading frame (ORF) containing 9024~9111 nucleotides.^[9] This genome encodes 10 proteins which are synthesized in double membranous vesicle and translated into cytosol by binding of host translation initiation factors on internal ribosome entry site (IRES) region of 5' untranslated region (UTR).^[10] The translated polyprotein is made up with about 3,000 amino acid, which is cleaved to non-structural (P7, NS2, NS3, 4A, NS4B, NS5A, and NS5B) proteins and structural (Core, E1 and E2) proteins by both viral and cellular proteases, which are necessary for viral proliferation.^[11]

The core protein and two envelope glycoproteins (E1 and E2) are structural proteins which form the viral nucleocapsid by surrounding the HCV RNA genome. The p7 transmembrane polypeptide, which form the hexamers and regulate the ion-channel activity, play a crucial role for viral particle maturation and release.^[12] The NS2 cysteine protease participate in cleavage the NS2-NS3 junction in the polyprotein. And it also regulates cell cycle and proliferation for the host cell.^[13] The NS3 has two enzymatic roles: N-terminal protease and a C-terminal helicase.^[13] Especially, serine protease domain in NS3 play an important role in the cleavage of four junctions in HCV polyprotein.^[14] NS4A is cofactor of NS3 protease and NS4B is an integral membrane protein having four transmembrane domains that participate in establishment the membranous web.^[6] The NS5A protein is about 447-amino acid, hydrophilic phosphorylated zinc- metalloprotein. It conducts formation of RNA replication complex and assembly for new virions. The NS5B is the RNA dependent RNA polymerase (RDRP), which fulfills the replication of the HCV RNA using the positive RNA strands.^[15]

2. Non-structural 5A protein

NS5A is known as a non-enzymatic, multifunctional protein involved in viral replication and assembly.^[16] Though it has no enzymatic activity, it is essential for the formation of RNA replication complex.^[17] It regulates virus particle assembly in a phosphorylation dependent manner.^[18] NS5A is phosphorylated by cellular kinases to the basal and hyper phosphorylated form in order to regulate virus life cycle.^[19] NS5A protein has several interactions with host factors that lead to developing of liver disease such as carcinoma.^[20, 21] NS5A consists of three distinct domains I, II and III. Especially, domain I and II are involved in RNA replication and domain III is region that related to package and releasing of viral particles.^[17, 22]

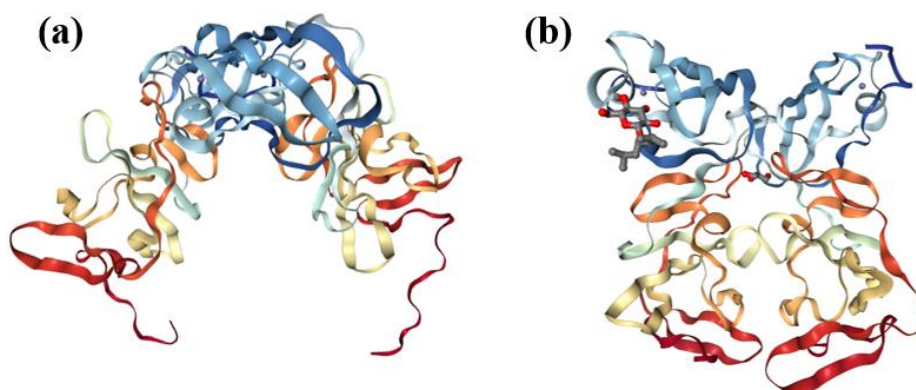


Figure 1. X-ray crystal structures of NS5A protein. (a) Open form (PDB : 1ZH1) (b) Closed form (PDB : 3FQQ).

Two X-ray crystal structures of NS5A protein were revealed for the domain I of NS5A excluding 1~31 amino acids, which consist of the amphipathic alpha helix region (AH) at the N-terminal part (figure 1).^[21] However, full form of NS5A domain 1 structure has not been elucidated yet.^[3, 22]

Recently, biochemical studies suggested a mechanism of action for NS5A inhibitor. It is reported that potent NS5A inhibitors block the viral replication by interrupting the formation of membranous web at an early stage in virus replication cycle.^[23] In addition, *in-vitro* analysis has shown that NS5A inhibitors appear to compete with HCV RNA for binding purified NS5A protein. However, resistance mutant forms of NS5A protein reduced binding affinity with NS5A inhibitor. Subsequently, *in-silico* docking studies were performed with an NS5A inhibitor and NS5A protein to predict the docking region.^[24]

3. Development of NS5A inhibitors

In accordance with international therapy guidelines, the first standard of care (SOC) against HCV comprised a combination of pegylated interferon (PEG-IFN) α series ($\alpha 2a$ or $\alpha 2b$) and ribavirin (RBV), a nucleoside-type drug.^[25, 26] Nevertheless, this remedy has not only 50% cure rate for the common GT-1 patients, but also other severe adverse effects such as insomnia, depression, neutropenia, flu-like symptoms, fatigue, lymphopenia, and other unexpected drug interactions.^[27, 28] Therefore, many pharmaceutical companies and laboratories worldwide have widely studied Direct Acting Antivirals (DAA's) as next-generation therapies to overcome drawbacks of conventional treatments.^[21] DAAs therapies have higher SVR rate to HCV compared to IFN-based therapy and are found to be relatively safer than the IFN treatments.^[14] The major targets of DAAs are NS3/4A protease, NS5B RNA-dependent RNA polymerase (RDRP) and NS5A protein.^[29, 30] Because of non-enzymatic property, the NS5A protein was not attractive target protein for early stage in drug discovery. However, replicon systems demonstrated that NS5A functions in HCV life cycle such as participating in viral genome replication and encapsidation.^[31]

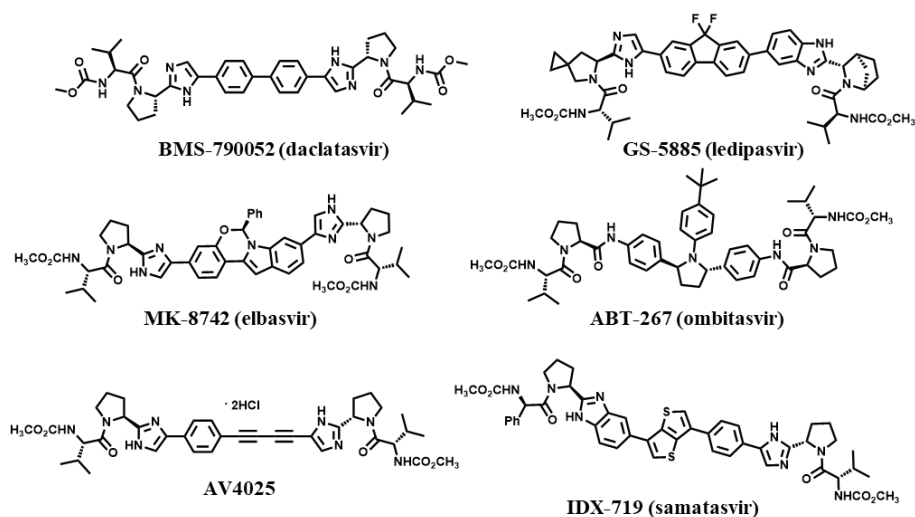


Figure 2. Structure of NS5A inhibitors in market or clinical trials.

Currently, six NS5A inhibitors are on the market for use with ribavirin, NS3/NS4A protease inhibitors, or NS5B inhibitors.^[32] In 2014, the US Food and Drug Administration (FDA) approved ledipasvir (GS-5885) with the NS5B inhibitor, sofosbuvir.^[33] Ombitasvir (ABT-267) was also approved by the FDA in combination with paritaprevir (NS3/4A protease inhibitor), ritonavir (protease inhibitor), and dasabuvir (NS5B inhibitor) for HCV genotype 1 infections.^[34] Daclatasvir (BMS-790052) in combination with sofosbuvir (2015), elbasvir (MK-8742) in combination with grazoprevir (NS3/4A protease inhibitor), and velpatasvir (GS-5816) along with sofosbuvir in 2016 are among another FDA-approved HCV DAAs.^[35] Recently, the FDA approved Vosevi® in 2017, which is a combination of sofosbuvir, velpatasvir, and voxilaprevir (NS3/4A inhibitor); a new pan-genotype drug, Mavyret® (glecaprevir/pibrentasvir), was also approved in the same year.^[36]

A new NS5A inhibitor, daclatasvir (BMS790052, Daklinza®), was first reported in 2010 and approved in Europe in 2014 (Figure 2). As a suppressor of the NS5A replication complex, daclatasvir showed impressive results at single-digit picomolar effective concentrations (EC₅₀) (9 pM and 50 pM against GT-1b and GT-1a, respectively). It effected 2-fold decreases in levels of viral RNA within 6 h of oral administration in clinical trials.^[37, 38] Consequently, the NS5A phosphoprotein became one of the most desirable drug targets of HCV for many pharmaceutical companies.^[38]

Daclatasvir has a C-2 symmetric structure that consists of a biphenyl core linked to a 2-(1*H*-imidazol-2-yl)-pyrrolidine moiety, and an *N*-(methoxycarbonyl)-L-valine capping group (Figure 2). In particular, the imidazole and carbamate groups play an important role in the interaction of daclatasvir with the HCV NS5A complex.^[39, 40] Although daclatasvir had no reported serious side-effects or drug-drug interactions (DDI), resistance to the drug appeared in patients infected with GT-1a and GT1-b HCV.^[20] The main amino acid mutations were Y93H and L31V in GT-1b, which resulted in 19-fold and 23-fold increases in resistance to daclatasvir, respectively.^[41] When

there was combination of both Y93H and L31V mutations in GT-1b, resistance to daclatasvir increased 8,336-fold. To address this issue, many research groups have developed HCV NS5A targeting drug candidates. ^[41]

Chapter 2.

Development of potent HCV NS5A inhibitors based on a biaryl sulfate core structure

1. Introduction

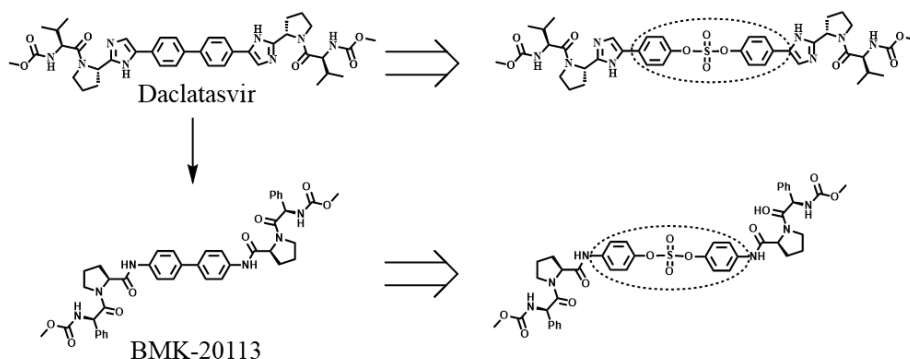
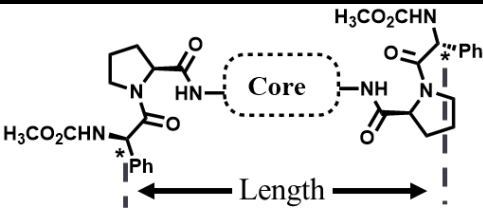
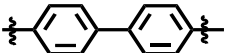
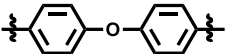
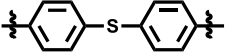
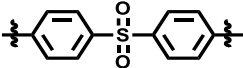
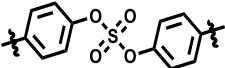


Figure 3. Strategy for designing new potent HCV NS5A inhibitors.

Our laboratory reported a series of NS5A inhibitors represented by **BMK-20113** (EC₅₀ against GT-1b and GT-2a strains: 28 pM and 260 pM, respectively), which comprises a benzidine prolinamide skeleton and an *N*-(methoxycarbonyl)-D-phenylglycine based capping group (Figure 3).^[15]

Y. A. Ivanenkov and coworkers reported that the length between chiral carbons of two capping groups in NS5A inhibitors having high inhibitory activities are 19 ~ 21 Å by calculation *in silico*.^[42] Considering the structural features of BMK-20113, we hypothesized that a longer biaryl core might improve the inhibitory activity of the HCV NS5A replication complex as shown with ombitasvir (ABT-267), elbasvir (MK-8742) and ledipasvir (GS-5885).

Table 1. *In silico* calculation of the distance between two capping group stereogenic centers of the NS5A inhibitors.

		
Core	Log P (calculated) ^a	Length ^b (calculated) ^c
 (BMK-20113)	4.00	16.4 Å
	4.09	17.3 Å
	4.36	17.9 Å
	3.27	18.2 Å
	3.43	19.8 Å
Daclatasvir (BMS-790052)	4.58	17.5 Å
Ombitasvir (ABT-267)	5.60	18.5 Å
Elbasvir (MK-8742)	6.02	19.0 Å
Ledipasvir (GS-5885)	5.57	22.3 Å
Samatasvir (IDX-719)	6.42	20.5 Å

^aALOGPS 2.1

^bLength is the distance between two chiral centers of capping groups

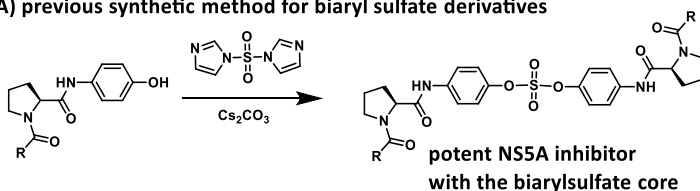
^cSpartan (v14, B3LYP, 6-31G*)

We calculated the lengths between two capping group stereogenic centers in BMK series inhibitors and commercial drugs for the purpose of finding optimal distance of the optimized core structure (Table 1). In addition, we investigated the logP values to predict the solubility of the inhibitor compounds. Finally, the

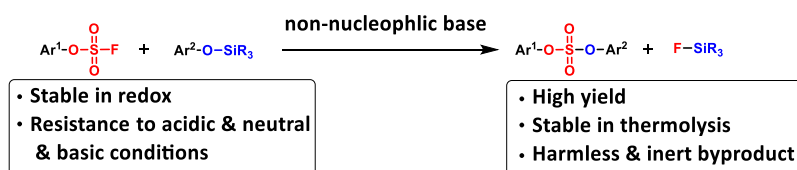
NS5A inhibitors equipped with biaryl sulfone or sulfate core structures showed optimal scores for the length and logP *in silico*.

Herein, we report the design and synthesis of new NS5A inhibitors embedding biaryl sulfone or sulfate core structures (Ar-SO₂-Ar, ArO-SO₂-OAr) with imidazole or amide connections.

(A) previous synthetic method for biaryl sulfate derivatives



(B) Sulfur(VI) fluoride exchange (SuFEx)



(C) Synthesis of NS5A inhibitors using the SuFEx chemistry)

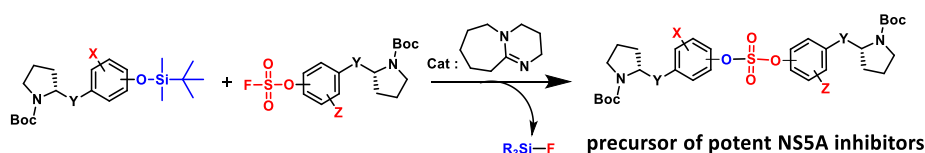


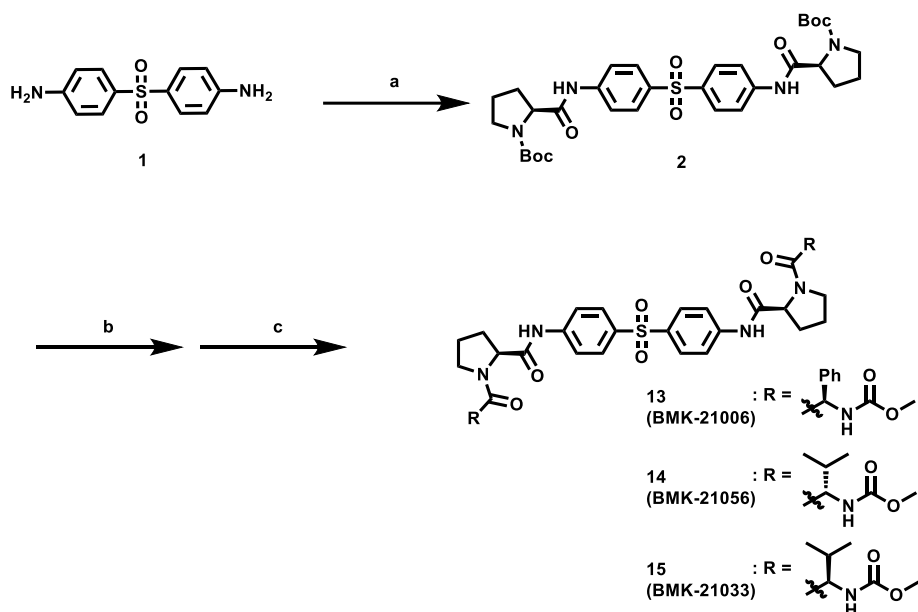
Figure 4. Biaryl sulfate core based nonstructural 5A (NS5A) inhibitors and modification using sulfur(VI) fluoride exchange (SuFEx) chemistry.

We also optimized the biaryl sulfate core part and carried out further SAR studies based on the sulfate core structures. During this investigation, we discovered that some substituted biaryl sulfate core structures were not readily accessible from traditional coupling reactions with sulfonyl diimidazole (SDI). For example, in the cross-coupling reactions of *o*-fluorophenol derivatives with SDI, only a monomeric aryloxy sulfonyl imidazole was obtained. Likewise, the sulfonyl diimidazole coupling strategy would not be appropriate for selective construction of nonsymmetrical biaryl sulfate core structures (Figure 4).^[43]

Although the first-generation DAA's HCV drugs have symmetrical structures similar to daclatasvir, many next-generation DAA's developed to treat multi-genotype strains tend to possess nonsymmetric structures.^[42, 44] Since there have been reports of NS5A inhibitors with a high degree of variation at the center core, we envisioned that nonsymmetrical biaryl sulfate core structures with substituted aryl groups would be worth investigating and, thus, were included in our SAR studies.^[39, 45] For the synthesis of the nonsymmetrical biaryl sulfate core structures, SuFEx chemistry appeared to be an extremely attractive strategy.^[46] Therefore, we report the fruitful exploitation of SuFEx chemistry for the construction of symmetrical and nonsymmetrical biaryl sulfate-based HCV NS5A inhibitors, which exhibit extremely high inhibitory activities.

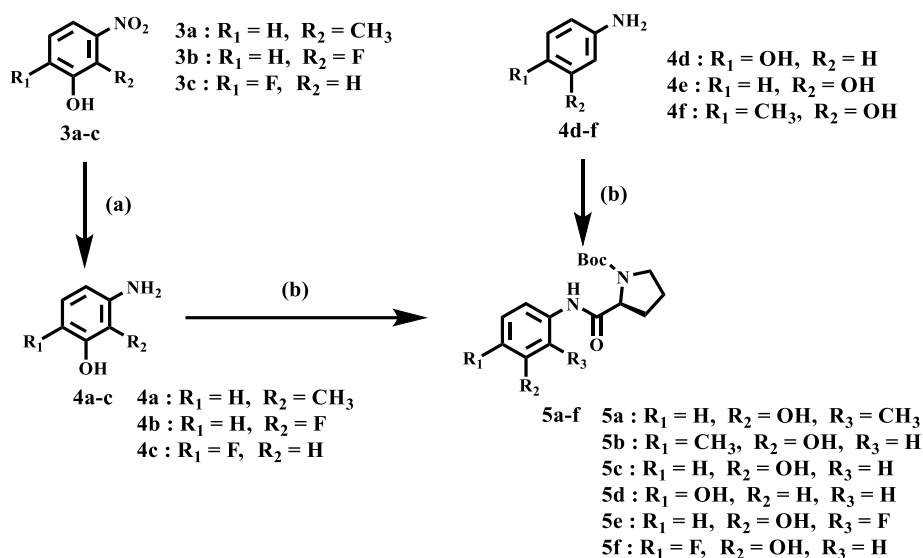
In 2014, Sharpless and coworkers introduced the SuFEx click reaction for chemoselectively linking two different phenol derivatives.^[47] The sulfate coupling reaction was accomplished through the reaction of an aryl fluorosulfate and an aryl silyl ether in the presence of a catalytic amount of 1,8-diazabicyclo(5.4.0) undec-7-ene (DBU).^[47, 48] The synthesis of sulfate compounds from the S^{VI}-F group proceeded with high yields and at a fast rate because of the driving force that formed the strong Si-F and S-O bond.^[48] Furthermore, the resulting compounds exhibited considerably high stabilities against hydrolysis, nucleophilic substitution, thermolysis, and reduction.^[49, 50] Moreover, this useful coupling reaction produces only inert silyl fluorides as by-products.^[49-52] We envisioned that this chemoselective SuFEx reaction could be used for the synthesis of novel HCV NS5A inhibitors containing biaryl sulfates possessing various substitution at the *o*-position of the phenol derivatives or a nonsymmetric biaryl sulfate core structures.

2. Results and Discussion



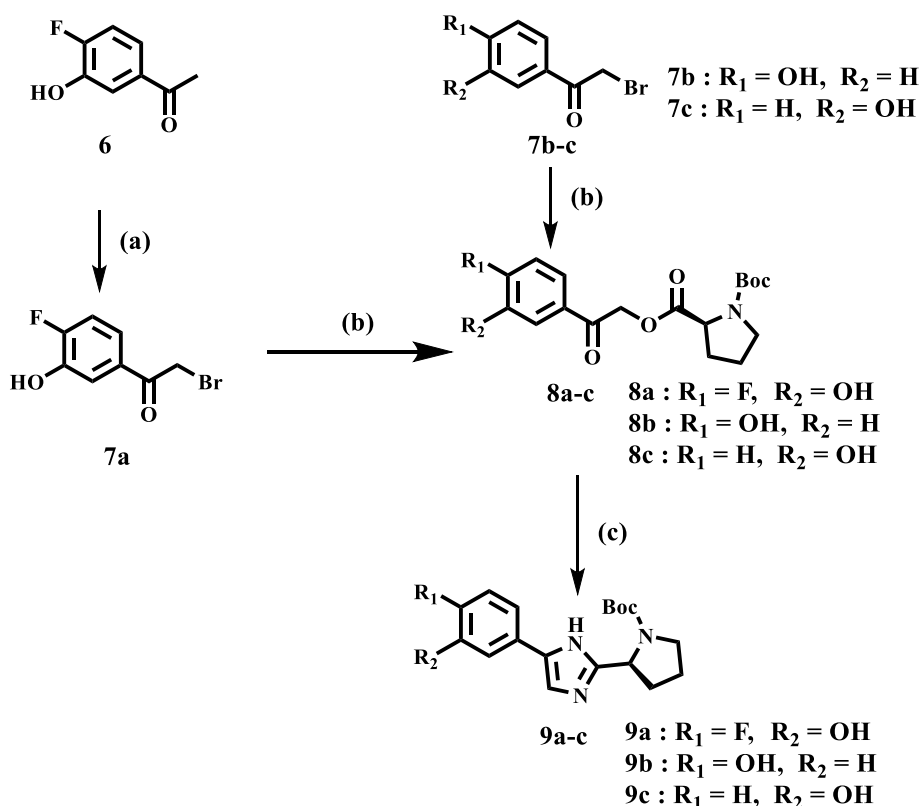
Scheme 1. Synthesis of NS5A inhibitors; reagents and conditions: (a) EDCI, *N*-Boc-L-proline, CH₂Cl₂, rt, 4 h, 44%; (b) TFA, CH₂Cl₂, rt, 30 m; (c) HOBT, EDCI, DIPEA, Capping group, CH₂Cl₂, rt, 16 h, 50-55%

Compounds containing a biaryl sulfone core were prepared following a general amide synthesis procedure as shown in Scheme 1.^[33] Coupling of 4,4'-diaminodiphenyl sulfone **1** with *N*-Boc-L-proline in the presence of 1-ethyl-3-(3-dimethylaminopropyl)carbodiimide (EDCI) provided *N*-Boc-protected intermediate **2** in moderate yield (44%). After removal of the Boc group, free amine moieties were coupled with D-phenylglycine, D-valine, or L-valine, each of which was capped with an *N*-(methoxycarbonyl) group^[53] furnishing the final compounds **13**, **14**, and **15** at yields of 50%, 53%, and 55%, respectively.



Scheme 2. Synthesis of intermediates; reagents and conditions: (a) Pd/C, H₂, MeOH, rt, 24 h, 99%; (b) EDCI, *N*-Boc-L-proline, CH₂Cl₂, rt, 4 h, 59-99%.

Synthesis of prolinamide precursors **5a-f** for the sulfate class inhibitors was accomplished according to Scheme 2. Various aminophenol derivatives (**4a-f**), which were either commercially available or prepared from reduction (Pd/C, H₂) of nitrophenol derivatives **3a-c**, were coupled with *N*-Boc-L-proline through a standard amide coupling method to yield prolinamide derivatives **5a-f** in moderate to excellent yields (59-99%).^[54]

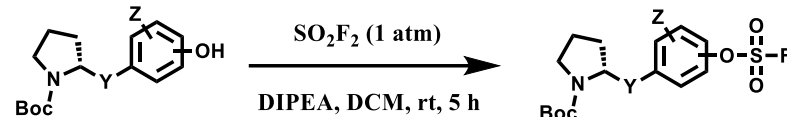
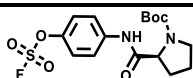
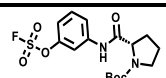
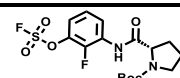
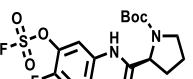
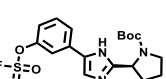
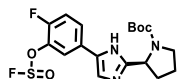
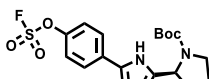


Scheme 3. Synthesis of intermediates; reagents and conditions: (a) CuBr_2 , EA/CHCl_3 , reflux, 8 h, 81%; (b) *N*-Boc-L-proline, *N,N*-Diisopropylethylamine (DIPEA), acetonitrile, rt, 5 h, 72–91%; (c) NH_4OAc , toluene, 95 °C, 20 h, 45–52%.

We also prepared various imidazole-containing phenol derivatives (**9a-c**) as substrates for the SuFEx reaction (Scheme 3).^[33, 55] The imidazole-linked monomers **7a-c** were prepared from the acetophenone derivatives following an established procedure.^[40] α -Bromination of acetophenone **6** was carried out in the presence of copper(II) bromide to provide α -bromoacetophenone **7a** in an 81% yield.^[56] Then, the resulting product **7a-c** was treated with *N*-Boc-L-proline in the presence of DIPEA to yield ester **8a**.^[40] Likewise, commercially available α -bromoacetophenone derivatives **7b** and **7c** were converted to the corresponding esters **8b** and **8c**, respectively. Synthesis of the imidazole

derivatives **9a-c** was accomplished by the reaction of **8a-c** with ammonium acetate.^[40]

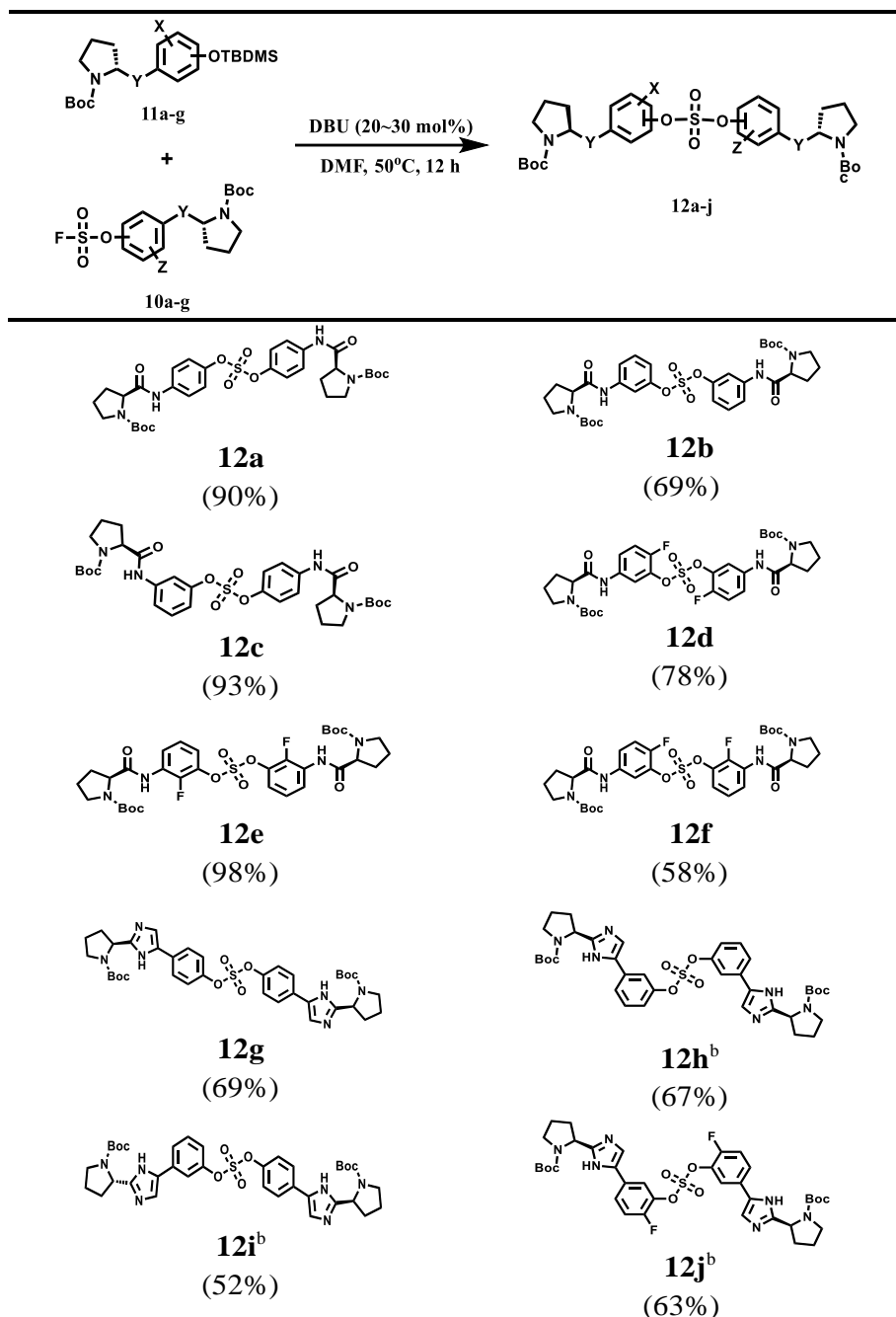
Table 2. Preparation of fluorosulfate monomers.^a

		
5a-f, 9a-c	10a-g	
		
10a (90%)	10b (87%)	10c (83%)
		
10d (90%)	10e (80%)	10f (92%)
		
10g (80%)		

^a Yields of isolated products.

The introduction of a fluorosulfonyl (fosyl) group was achieved by the reaction of the corresponding phenol derivatives with sulfuryl fluoride (SO_2F_2) and 1.7 equiv DIPEA in dichloromethane (Table 2).^[48] Since SO_2F_2 is a gas, the reaction mixture was stirred rapidly ($> 1,000$ rpm) to enhance the liquid-gas contact.^[50] The reaction was complete within 5 h, monitored using thin layer chromatography (TLC). The structures of the fosylated products were confirmed using proton (^1H), ^{13}C , and ^{19}F nuclear magnetic resonance (NMR) spectroscopy; especially, ^{19}F NMR chemical shifts of fluorine at fosyl group ranged from ca. 31 to 40 ppm.^[57] These fluorosulfate derivatives exhibited good stability against hydrolysis and could be stored on the shelf for months.^[58] Compounds **10a-g** were obtained in good yields ($> 80\%$) as shown in Table 2.

Table 3. Preparation of biaryl sulfate core structures using sulfur(VI) fluoride exchange (SuFEx) chemistry^a



^aYields of isolated products.

^bThe reactions were carried out with DBU (2.2-2.3 equiv).

We then constructed the sulfate core structures using aryl silyl ether counterparts through SuFEx chemistry (Table 3).^[51] Silylation of phenol groups was achieved using the standard method with *tert*-butyldimethylsilyl chloride (TBDMSCl) and imidazole.^[59] The coupling reaction between an aryl fosylate and aryl silyl ether was carried out in the presence of DBU in dimethyl formamide (DMF) according to Sharpless' protocol.^[46, 48] Then, the mixture was stirred at 50 °C for 12 h. The biaryl sulfate products (compounds **12a-f**) were formed in good to excellent yields in the presence of catalytic amounts of DBU (20-30 mol%).^[46, 48] However, in case of the coupling reactions involving the silyl ether or fluorosulfate monomer containing an imidazole moiety (compounds **12g-j**), 2.2-2.3 equiv DBU was used for the SuFEx coupling products.

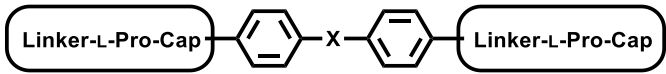

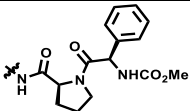

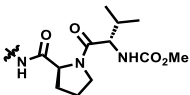
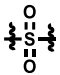
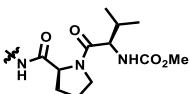
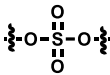
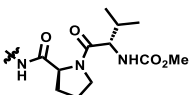
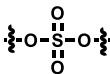
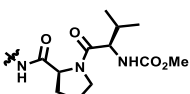
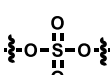
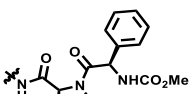
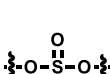
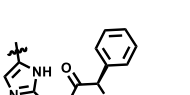
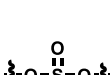
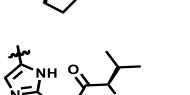
We synthesized biaryl sulfate based NS5A inhibitors using appropriate precursors. The *tert*-butoxycarbonyl (Boc)-protecting group for the proline moiety was deprotected with 50% (v/v) TFA in CH₂Cl₂.^[15] Volatiles were removed from the reaction mixture under reduced pressure and the residue was directly coupled with a capping group such as *N*-methyloxycarbonyl-protected valine (val) or phenylglycine (phg) in the presence of EDCI and HOBT.^[60] Finally, the biaryl sulfate based HCV NS5A inhibitors were obtained after purification of the crude products using silica gel chromatography.^[60]

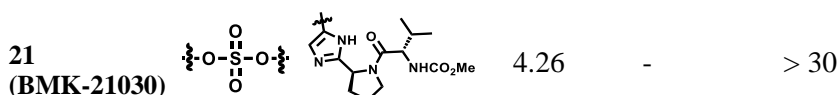
To determine the antiviral activities of each compound, we measured the EC₅₀ of inhibitors for genotype-1b (GT-1b) and 2a (GT-2a) using the HCV replicon and HCV cell culture (HCVcc) systems, respectively.^[53] We used the human hepatoma Huh 7.5.1 cell line to investigate the EC₅₀ of the compounds in the HCV replicon systems for GT-1b, which encodes the bicistronic *NK5.1* gene and Gaussia luciferase (*Gluc*) reporter gene.^[61]

On the other hand, the inhibitory activities of GT-2a were measured using the HCVcc system with JFH 5a-Rluc-ad34, which is a derivative of JFH5a-Rluc-ad34 (a variant of JFH1 with 2 cell culture-adaptive mutations) was added to Huh7.5.1.^[62] After infection for 4 h, Huh7.5.1 cells were added to culture medium containing compounds of interest at different concentrations. After the

cells were incubated for 3 d, EC₅₀ values of compounds were measured using luciferase assays.^[53, 63]

Table 4. *In vitro* activities of inhibitors containing a *p,p'*-disubstituted biaryl sulfone or sulfate core.

					
Compounds	X	Linker-L-Pro-Cap	GT-1b (nM)	GT-2a (nM)	Cytotoxicity (μM)
13 (BMK-21006)			36.1	-	> 30
14 (BMK-21056)			> 10 ⁵	-	> 30
15 (BMK-21033)			> 10 ⁵	-	> 30
16 (BMK-21057)			2,570	-	> 30
17 (BMK-21013)			575	-	> 30
18 (BMK-21007)			0.0100	0.128	> 30
19 (BMK-21016)			0.270	0.147	> 30
20 (BMK-21015)			417	427	> 30



The EC₅₀ values of tested compounds against GT-1b and GT-2a are listed in Table 4. Compounds showing good potencies against GT-1b were selected for further testing against GT-2a. The inhibitory activity of compound **13**, which features a biarylsulfone core with a D-phenylglycine capping group was 36.05 nM against GT-1b, whereas both **14** and **15**, which contain valine isomers, showed no apparent inhibitory activities against GT-1b. Since the inhibitors containing a biaryl sulfone core did not appear to be effective as NS5A inhibitors, compounds with a biaryl sulfate core were examined. compound **16** containing a biaryl sulfate core with an L-valine capping group exhibited poor inhibitory activity in the GT-1b assay. When the L-valine moiety compound **16** was replaced with an enantiomer **17**, a slight increase in inhibition (EC₅₀ 574.8 nM) was observed. The inhibitory activities of compound **15** and **17** provide a direct comparison of the influence between the sulfone and sulfate core structures and appear to indicate that the sulfate core is more effective. However, when the D-valine residue in **17** was replaced by a D-phenylglycine moiety as in compound **18**, excellent sub nanomolar activities were observed in both GT-1b and GT-2a assays. The replacement of the amide moiety in compound **18** with an imidazole ring as in compound **19**, a replacement that may improve the water solubility of the inhibitor molecule, decreased the inhibitory activity 27-fold in the GT-1b assay. Likewise, similar inhibitory activity was observed for compound **20** and **17** in the GT-1b assay. However, the L-valine diastereomer **21** showed an enhanced activity against GT-1b.

inhibitory activities (EC_{50} of GT-2a and GT-1b: 0.0199 nM and 0.01983 nM, respectively). This is significant since this activity is an approximate 6-fold improvement relative to that of the *p*-,*p*'-disubstituted biaryl sulfate **17** against GT-2a. When the D-phenylglycine capping of compound **22** was replaced with L-*tert*-leucine moiety **23**, 4- and 47-fold decreased activity, respectively, against GT-1b and GT-2a were surveyed. In the case of inhibitors containing an imidazole linker instead of an amide one, compound **24** possessing an *N*-(methoxycarbonyl)-D-phenylglycine capping group, proved to be 18- and 503-fold less potent against GT-1b and GT-2a, respectively, than compound **22**. The compound **25**, which had an L-*tert*-leucine capping group, showed significantly decreased activity (EC_{50} : 37.1 nM) in the GT-1b assay. Notably, compound **26**, which has an imidazole linker with L-valine capping, showed the highest increase in inhibitory activity (132-fold) in the GT-1b assay when compared with **21** which has a *p*-,*p*'- substituted biaryl sulfate core structure.

According to our SAR study, the *m*-,*m*'-disubstituted biaryl sulfate moiety was confirmed to be the best structure for the sulfate core part. Earlier observations have suggested that hindered free rotation around the biaryl moiety significantly influences the inhibitory activity against NS5A.^[53] We therefore evaluated whether blocking the free rotation around the sulfate group may affect the inhibitory potency. We introduced a methyl substitution at the *ortho*-position of the biaryl groups. Of the compounds containing the *m*-,*m*'-disubstituted aryl sulfate with prolinamide linker, those possessing an *o*-methyl group were first investigated. However, compound **27** and **28**, which have methyl substitution at the 2- and 2'-positions (compound **27**) and 6- and 6'-positions of the aryl group (compound **28**), respectively, showed a significant loss in inhibitory activity. For compound **27**, the EC_{50} was 22.9 nM against GT-1b, and for compound **28**, the EC_{50} was 109 pM against GT-1b and 2.23 nM against GT-2a. None of the inhibitors listed in Table 4 and Table 5 were cytotoxic at 20 μ M.

Table 6. Synthesis and in vitro antiviral activities of inhibitors comprising an amide linked biaryl sulfate core.^a

<div style="text-align: center;"> <p>12a-f</p> <p>(a) TFA, CH₂Cl₂, rt, 30 m (b) EDCI, HOBt, Capping group, CH₂Cl₂, rt, 16 h, 39 - 83%</p> </div>				
Compounds	Biaryl sulfate group	Capping group	GT-1b (nM) ^b	GT-2a (nM) ^b
18 (BMK-21007)		(<i>R</i>)-Phenyl	0.0100	0.128
22 (BMK-21014)		(<i>R</i>)-Phenyl	0.0198	0.0199
27 (BMK-21028)		(<i>R</i>)-Phenyl	23.0	- ^d
28 (BMK-21020)		(<i>R</i>)-Phenyl	0.110	2.23
29 (BMK-21022)		(<i>R</i>)-Phenyl	0.361	0.129
30 (BMK-21023)		(<i>R</i>)-Isopropyl	> 100 ^c	- ^d
31 (BMK-21036)		(<i>R</i>)-Phenyl	0.0204	> 10.0 ^c
32 (BMK-21024)		(<i>R</i>)-Phenyl	0.0224	1.22
33 (BMK-21047)		(<i>R</i>)-Phenyl	0.0241	0.627
34 (BMK-21027)		(<i>R</i>)-Isopropyl	> 100 ^c	- ^d
35 (BMK-21048)		(<i>R</i>)-Isopropyl	> 100 ^c	- ^d
36 (BMK-21038)		(<i>R</i>)-Isopropyl	> 1.00 ^c	- ^d

^aEC₅₀, half-maximal (50%) effective concentration; GT-1b, genotype-1b; GT-2a, genotype-2a.

^bAll experiments were performed three times except for compounds that exhibited > 1 nM EC₅₀ for GT-1b.

^cExperiment was performed once.

^dNot determined.

The antiviral activities (EC₅₀) of the tested compounds containing amide groups on both side of the sulfate core against replicon (GT-1b) and HCVcc (GT-2a) are listed in Table 6. We first selected the compounds that exhibited < 1 nM EC₅₀ for GT-1b, and then measured the HCVcc EC₅₀ for GT-2a. In the amide linker series, the D-valine or D-phenylglycine derivatives were chose as only capping groups because these groups showed the highest levels of antiviral activities in our previous study.^[60]

We first carried out the SAR studies of inhibitors containing a non-symmetric sulfate core. The compound **29** containing 3-aminophenyl (4-aminophenyl) sulfate derivative equipped with a D-phenylglycine capping moiety showed 36-fold lower potency against the GT-1b than the symmetric *p,p'*-substituted inhibitor **18** did, while the antiviral activities on GT-2a were reduced by > 6-fold compared to those of the symmetrically *m,m'*-substituted biaryl sulfate inhibitor **22**. The replacement of the D-phenylglycine with D-valine moieties as shown in **30** induced no apparent inhibitory activity against GT-1b at 100 nM concentration.

We next investigated the inhibitors containing *o*-fluoro substituted biaryl groups, expecting increased potency based on the restricted rotational conformation around the sulfate core. In a previous study, compound **27**, which was substituted with methyl at 2- and 2'-positions, showed activity at two-digit nanomolar levels in GT-1b.^[60] However, replacement of the methyl groups of compound **27** with fluorine **31** improved the inhibitory activity against GT-1b strain with 0.0204 nM EC₅₀. This result, surprisingly, was a 1,127-fold higher inhibitory activity than that of compound **27** was, suggesting that the *o*-position in the biaryl groups is extremely important for increasing the potency.

The C_2 symmetric 6,6'-difluoro-substituted phenol derivatives containing the D-phenylglycine moieties **32** also showed increased inhibitory activities against both GT-1b and GT-2a, compared to **28**, which has *o*-methyl groups at 6- and 6'-positions of the biaryl group.^[60] Although the inhibitory activities against GT-1b were increased, compound **32** showed low GT-2a inhibitory activity (single nanomolar level EC_{50}) and compound **31** showed no inhibitory activities at 10 nM.

Nonsymmetrically substituted difluorobiarylsulfate **33** with 2- and 2'-fluoro-substitution exhibited 5-fold weaker activity for GT-1b and 2-fold higher potency for GT-2a compared to symmetric compound **31**. The replacement of the D-phenylglycine with D-valine moiety (compound **34** and **35**) showed lower inhibitory activities except for compound **36**, which had GT-1b potency to single nanomolar range. The fact that the SAR results were highly dependent on the substitution and the sulfate linking the position of the biaryl groups indicates that the inhibitory activity of various HCV genotype is highly sensitive to the structural features of the core moiety. These results indicate that *ortho*-substitution in a phenyl group with fluorine blocks the free rotation, which lowers the antiviral activities against GT-1b. Nevertheless, replacing it with hydrogen, which lacks steric hindrance relatively, enhanced the inhibitory activities against the GT-2a gene.

Table 7. Synthesis and in vitro antiviral activities of sulfate core-inhibitors equipped with imidazole moieties.^a

(a) TFA, CH₂Cl₂, rt, 30 m
(b) EDCI, HOBt, Capping group, CH₂Cl₂, rt, 16 h, 35 - 86%

Compounds	Biaryl sulfate group	Capping group	GT-1b (nM) ^b	GT-2a (nM) ^b
26 (BMK-21025)		(S)-Isopropyl	0.0323	0.882
37 (BMK-21046)		(R)-Isopropyl	> 100 ^c	- ^d
38 (BMK-21044)		(S)-Isopropyl	> 10.0 ^c	- ^d
39 (BMK-21045)		(R)-Phenyl	0.584	9.70
40 (BMK-21040)		(R)-Phenyl	0.139	3.59
41 (BMK-21043)		(R)-Isopropyl	> 100 ^c	- ^d
42 (BMK-21039)		(S)-Isopropyl	0.260	> 10.0 ^c

^aEC₅₀, half-maximal (50%) effective concentration; GT-1b, genotype-1b; GT-2a, genotype-2a.

^bAll experiments were performed three times except for compounds that exhibited > 1 nM EC₅₀ for GT-1b.

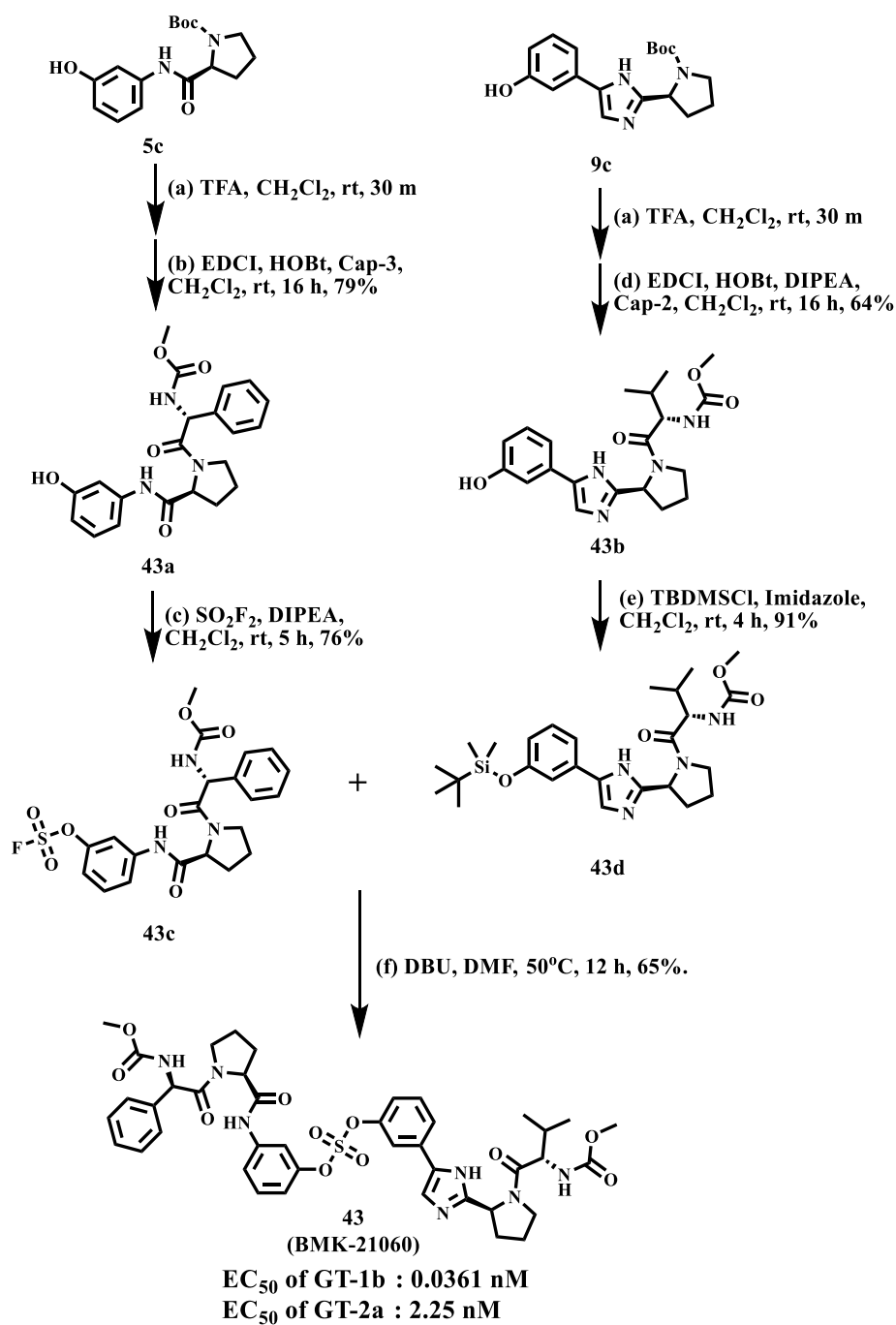
^cExperiment was performed once.

^dNot determined.

As shown in Table 7, we designed the NS5A inhibitor series consisting of imidazole linkers with the aim of enhancing the antiviral activities and solubility.^[64] In our previous report, the imidazole linked biaryl sulfate

inhibitors containing an L-valine capping group **26** showed good activities against GT-1b and GT-2a.^[60] Thus, we introduced nonsymmetric or substituted sulfate core structures in imidazole-linked inhibitors to determine if it would influence the inhibitory activities and the results are summarized in Table 7. Compound **37**, containing *o*-fluoro substituted biaryl sulfate with D-valine derivative, showed no inhibitory activity at 100 nM against replicon GT-1b. Compound **38** with an *N*-methoxycarbonyl-L-valine capping group resulted in two-digit nM EC₅₀ on GT-1b. The replacement of the L-valine moiety with D-phenylglycine moiety as in compound **39** dramatically enhanced the antiviral activity against GT-1b. However, these results showed 25-fold lower activity than that of inhibitors linked with amides such as compound **33**. Introduction of *m,p'*-disubstituted biaryl sulfate core as in compound **40** demonstrated that the potencies for both GT-1b and GT-2a were better than that of compound **39** with an *o*-fluoro substituent. While the D-valine derivative **41** showed no inhibition at 100 nM, the opposite stereoisomeric L-valine derivative **42** showed improved potency for GT-1b, respectively. However, it showed no marked antiviral activity against GT-2a.

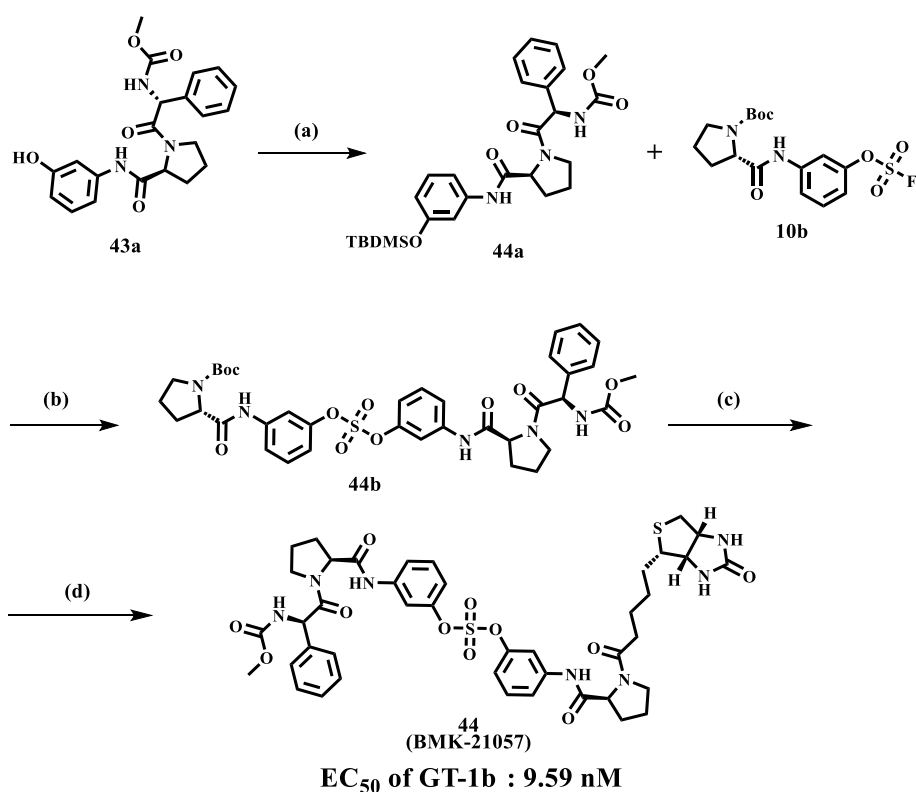
Based on the SAR study, it can be concluded that compounds with asymmetric biaryl sulfate core and D-phenylglycine capping derivatives (compound **29** and **40**) showed the best inhibitory activities for both genotypes. We proceeded to synthesize nonsymmetric compounds, exploiting the chemoselectivity of SuFex chemistry.



Scheme 4. Synthesis of compound **43** (BMK-21060).

In our previous study, we have found that *m,m'*-biaryl sulfate derivatives exhibit high inhibitory activities against NS5A.^[60] Especially, *C*₂-symmetric

biaryl sulfate comprising amide **22** and imidazole **26** linkers showed extremely high antiviral activities against two genotypes. Based on these results, we synthesized compound **43** having a hybridized structure of the two compounds. Due to the orthogonality of SuFEx, we were able to synthesize the biaryl sulfate compound containing imidazole-proline-L-valine carbamate derivative and amide-proline-D-phenylglycine carbamate derivative in moderate yields as shown in Scheme 4.^[65] The nonsymmetric **43** exhibited excellent inhibitory activity for GT-1b. However, it exhibited nanomolar levels of antiviral activity against GT-2a, which indicated no dramatic change in activity.



Scheme 5. Synthesis of compound **44** (BMK-21057); reagents and conditions: (a) TBDMSO, Imidazole, CH₂Cl₂, rt, 4 h, 81%; (b) DBU, DMF, 50 °C, 12 h, 75%; (c) TFA, CH₂Cl₂, rt, 30 m; (d) EDCI, HOBT, DIPEA, Biotin, CH₂Cl₂, rt, 16 h, 96%.

We also used SuFEx chemistry to prepare the biotin-tagged, biaryl sulfate core based NS5A inhibitor as shown in Scheme 5. Biotin binds specific proteins such as streptavidin and avidin with extremely high affinity.^[20] Because of this specificity, biotinylation of NS5A inhibitors has been reported.^[66] The introduction of biotin into one proline was readily carried out using SuFEx chemistry. Although the NS5A inhibitor containing the biaryl sulfate with biotin-tag **44** showed a slightly decreased EC₅₀ against genotype-1b (9.59 nM), it was 10 times higher than the previously reported biotinylated tag molecules based on BMS compound (BMS-671 and BMS-690).^[20, 31, 66]

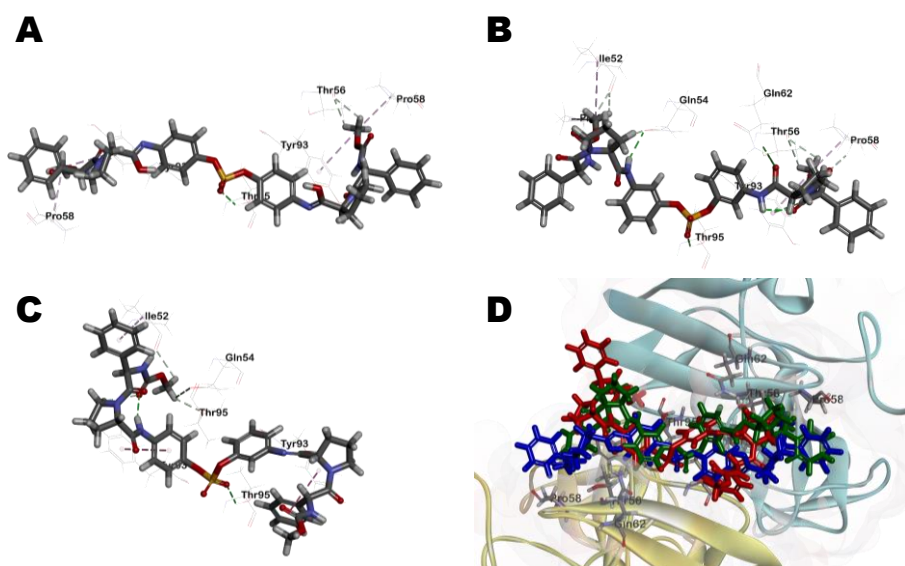


Figure 5. Docking of inhibitor compounds to an NS5A (3FQQ) dimer model. (A) compound **18**, (B) compound **22**, and (C) compound **29** to an NS5A (3FQQ) dimer model. For clarity purpose, only residues having interactions were shown. Compound **18**, **22**, and **29** are shown in stick and surrounding residues were shown in line. Various interactions are shown in dashes (for more clarity see Figure 11). (D) Superposed model of inhibitors inside 3FQQ dimer model. Compound **18**, **22**, and **29** are shown blue, green and red, respectively.

To understand the observed antiviral activities (EC_{50}) of inhibitors from a 3D structural perspective, three representative inhibitors, compound **18**, **22**, and **29**, were docked in an NS5A protein dimer model. The model was constructed using the NS5A domain 1 crystal structure (3FQQ)^[22] and amino terminal alpha helical NMR structure (1R7G).^[67] Figure 5 illustrates the 3D-interaction models of compound **18**, **22**, and **29** with the NS5A dimer. The docking model demonstrates that inhibitors bound across the dimer interface with Thr95A, which forms a hydrogen bond with the nonsymmetric biaryl sulfate core. The interactions of inhibitors and the residues at the binding site are detailed in two dimensional (2D) docking representation (Figure 11). In the case of compound **18**, the biaryl sulfate moiety can engage in hydrophobic interaction with Gln54A and Gln54B, whereas the methyl groups of the carbamate groups make π -alkyl interaction with Pro58 and Tyr93 of the NS5A protein dimer (Figure 5A and Figure 11A). The amide linkers of compound **22** make hydrogen bond with Gln54, Thr56, and Gln62, whereas both methyl groups of the carbamates involve π -alkyl interaction with Pro58 and Tyr93 (Figure 5B and Figure 11B). In compound **29** (Figure 5C), the sulfate moiety appears to interact with Thr95 by hydrogen bonding. Interestingly, Tyr93A has π -alkyl interaction with the pyrrolidine ring and the methyl moiety of methyl carbamate, whereas Tyr93B shows π -donor hydrogen bond interaction with the phenyl group of D-phenylglycine. There are no interactions with the residues of Pro58 (Figure 11C).

As shown in a superposed model (Figure 5D and Figure 11A-B), the symmetric inhibitors **18** and **22** pose reduced steric hindrance of D-phenylglycine moiety compared to nonsymmetrical inhibitor **29**, where only one methyl group of the carbamates is involved in π -alkyl interaction with Tyr93A. Also, CDocker interaction energies of compound **18**, **22**, and **29** are -58.41, -57.20, and -46.19 kcal/mol, respectively, which suggests that compound **18** and **22** might be better placed in the binding mode compared to **29**. In the case of inhibitor **40**, hydrogen bond interactions are found not only between the sulfate and Gly54A but also between the imidazole and Thr56

(Figure 11D). Both ends of the carbamate groups appear to show π -alkyl interaction with Tyr93A and Tyr93B, and especially Tyr93A is engaged in hydrogen bond interaction with the carbonyl moiety of one carbamate. Interestingly, one methyl group of the carbamate makes hydrophobic interaction with Pro58B, whereas the other side correlates with Pro97B. Therefore, the D-phenylglycine of inhibitor **40** poses reduced steric hindrance compared to inhibitor **29** due to the hydrogen bonding of the carbamate group (Figure 13). CDocker interaction energy of inhibitor **40** is -54.76 kcal/mol, which bodes well with its EC₅₀ activity.

Table 8. Results of hERG ligand binding assay.^a

Treatment	Concentration (μ M)	% inhibition
22 (BMK-21014)	10	2.73 ± 3.16
26 (BMK-21025)	10	18.7 ± 4.58
Astemizole (positive control)	10	66.0 ± 5.22

^amean \pm SD, n=3

Based on these results, we evaluated the top two compounds, **22** and **26**, which contain the amide and imidazole linker, respectively, in a battery of pharmacological studies. First, we assessed the hERG ligand binding of compounds **22** and **26** at 10 μ M (Table 8). The hERG ligand binding assay is used for the evaluation of potential heart related safety issues.^[33, 68] By using “red fluorescent hERG channel ligand tracer”, the inhibition potential of test compounds could be evaluated.^[54] In the case of hERG inhibiting chemicals, the tracers do not bind to the membrane resulting in low polarization.^[33, 55] The % inhibition values of compounds on hERG ligand binding are listed in Table 8. Compounds having inhibition value more than 50% of the positive control such as astemizole are considered to possess potential cardiotoxicity.^[69]

However, compounds **22** and **26** showed no significant inhibition potential in this study.

Table 9. Plasma stability.^a

Treatment	Rat (%)	Human (%)
22 (BMK-21014)	76.7 ± 10.6	86.3 ± 12.3
26 (BMK-21025)	87.2 ± 12.6	92.6 ± 9.69
Enalapril (Positive control)	0.032 ± 0.003	-
Procaine (Positive control)	-	0.003 ± 0.002

^a% remaining after 4 h incubation at 37°C

Next, we measured the stabilities of compounds **22** and **26** against hydrolytic enzymes, such as aldolase, cholinesterase, acid phosphatase, alkaline, dehydropeptidase and lipase in rat and human plasma (Table 9). Because the hydrolysis of candidate molecules in plasma can result in low stability, it is important to assess liability of test compounds.^[13, 70] When compounds **22** and **26** were tested, results showed high stability in rat and human plasma when compared with positive controls (Table 9).

Table 10. Results of bacterial reverse mutation assay with compounds **22** and **26**.

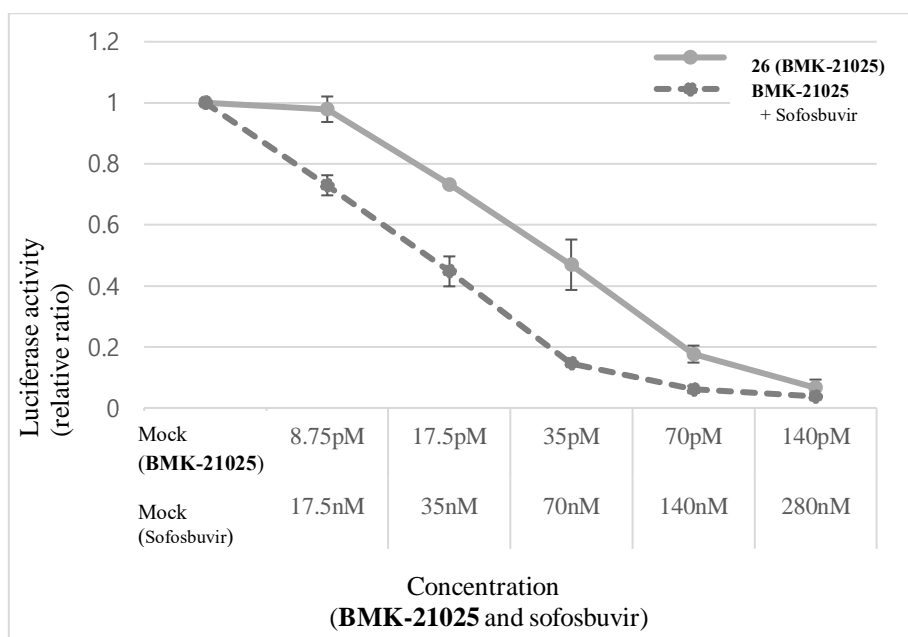
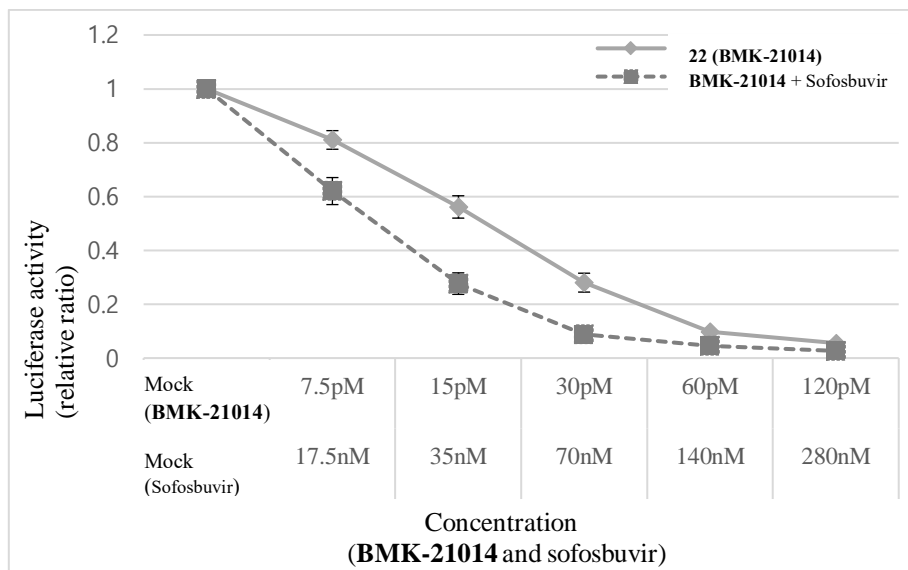
Tester strain	compound	Dose ($\mu\text{g}/\text{plate}$)	Revertant colonies/plate (Mean \pm SD) ^b	
			Without S-9 mix	With S-9 mix
TA98	vehicle control	0	21 \pm 1	25 \pm 3
	22 (BMK-21014)	1,000	26 \pm 3	29 \pm 2
	26 (BMK-21025)	1,000	28 \pm 4	29 \pm 4
	Bis(4-aminophenyl) sulfate	5,000	1 \pm 1 (vehicle control: 1 \pm 1)	1 \pm 1 (vehicle control: 1 \pm 1)
TA100	vehicle control	0	125 \pm 9	129 \pm 3
	22 (BMK-21014)	1,000	126 \pm 7	130 \pm 9
	26 (BMK-21025)	1,000	125 \pm 12	110 \pm 2
	Bis(4-aminophenyl) sulfate	5,000	10 \pm 7 (vehicle control: 7 \pm 2)	8 \pm 1 (vehicle control: 5 \pm 2)
	Positive control	Dose	Without S-9 mix	With S-9 mix
TA98	2-nitrofluorene	1 $\mu\text{g}/\text{plate}$	183 \pm 24	ND
	Benzo(a)pyrene	2 $\mu\text{g}/\text{plate}$	ND ^a	198 \pm 15
TA100	Sodium azide	1	748 \pm 25	ND
	Benzo(a)pyrene	2	ND	778 \pm 14

^aND: Non Determined.^bMean \pm SD, n=3

We then proceeded to evaluate the two compounds for genotoxicity in the Ames test (Table 10). We chose the commonly used *Salmonella typhimurium* strains TA98 and TA100 for the detection of frameshift mutations and base substitution mutations, respectively.^[61] In this study, the positive controls increased the amount of revertant colonies significantly in TA98 and TA100.^{[12,}
^{62]} There was no increase in the quantity of revertant colonies observed when compounds **22** or **26** (1,000 $\mu\text{g}/\text{plate}$) were applied. In other words, neither test

compound had mutagenic potential against TA98 and TA100. In addition, the evaluation of bis(4-aminophenyl) sulfate, which is a potential metabolite of compound **22**, in the Ames MPF™ 98/100 Mutagenicity Assay showed no mutagenicity at up to 5 mg/plate.

Figure 6. Combination index values of compounds **22** and **26**.



Combination Index	ED ₅₀	ED ₇₅	ED ₉₀	ED ₉₅
BMK-21014 + sofosbuvir	0.87160	0.90939	0.94888	0.97676
BMK-21025 + sofosbuvir	0.98005	1.06148	1.16322	1.24630

To evaluate compounds **22** and **26** in combination with a representative NS5B inhibitor, sofosbuvir, we adopted the Chou method.^[71-73] Compound **22** or **26** was tested at a constant ratio of sofosbuvir to NK5.1 Gluc replicon and, each inhibition effect was measured through the Gaussia luciferase assay. We calculated the relative inhibition effect of cells treated with single or combination administrations compared with mock treated replicon cells (Figure 6). To evaluate the combination index (CI) values, such as effective dose (ED) at each point (ED₅₀, ED₇₅, ED₉₀, and ED₉₅), we used the Compusyn Freeware Program (ComboSyn, Inc). Compound **22** showed CI values below 1 at 50%, 75%, 90%, and 95% ED concentrations. On the other hand, compound **26** exhibited CI values almost similar to 1 in ED₅₀ and ED₇₅, and above 1 in ED₉₀ and ED₉₅. In conclusion, we suggest that compound **22** has a synergic effect with sofosbuvir, but that compound **26** shows a dose-dependent additive effect (CI > 1: antagonism effect, CI=1: additive effect, CI <1: synergistic effect).

3. Conclusion

In summary, we investigated new compounds containing biaryl sulfone or sulfate cores as inhibitors of the hepatitis C virus NS5A protein. Especially, using SuFEx chemistry we achieved chemoselective coupling of aryl fluorosulfates and aryl silyl ethers in the presence of a catalytic amount of a DBU as a base. Furthermore, this method was used to synthesize new NS5A inhibitors containing various substituted sulfate core structures with high yields. These compounds exhibited high inhibitory activities against HCV viral proliferation by binding NS5A protein. We easily synthesized inhibitors containing nonsymmetric or *o*-fluoro substituted biaryl sulfate core structures using the SuFEx reaction in a “click chemistry” manner. Based on these results, SuFEx chemistry proved to be highly useful in constructing symmetric and nonsymmetric sulfate core-containing NS5A inhibitors, and could potentially be applied to the synthesis of a wider range of compounds in medicinal

chemistry. Through SAR study, we discovered that two compounds containing an *m*-,*m*'-disubstituted biaryl sulfate core, **22** or **26**, exhibit excellent inhibitory potencies against both GT-1b and GT-2a. In hERG ligand binding inhibition assays, no inhibition activity was detected for either **22** or **26**. These compounds showed high plasma stability and no mutagenic potential as evaluated by the Ames test. In addition, compounds **22** or **26** had synergistic or nearly additive combination effect with sofosbuvir, respectively. Based on these encouraging results, further studies are being pursued in our research laboratory.

4. Experimental

General chemical methods

The ^1H and ^{13}C NMR-spectra were measured with a Varian/Oxford As-500 (500 MHz), and an Agilent 400-MR DD2 Magnetic Resonance System (400 MHz) spectrophotometer. Chemical shifts were measured as part per million (δ values) from Tetramethylsilane (TMS) as an internal standard at probe temperature in CD_3OD or CDCl_3 or DMSO-D_6 for neutral compounds. Coupling constants are provided in Hz, with the following spectral pattern designations: s, singlet; d, doublet; t, triplet; q, quartet; quint, quintet; m, multiplet; br, broad; app, apparent. Reactions were conducted, purified, and analyzed according to methods widely practiced in the field, while taking necessary precautions in the exclusion of moisture and/or oxygen where appropriate. Evaporation of solvents was performed at reduced pressure using a rotary evaporator. TLC was performed using silica gel 60F254 coated on an aluminum sheet (E. Merck, Art.5554). High resolution mass spectra (HRMS) were recorded on a ThermoFinnigan LCQTM Classic, Quadrupole Ion-Trap Mass Spectrometer. HPLC analyses were carried out on an Agilent HP1100 system (Santa Clara, CA, USA), composed of an auto sampler, quaternary pump, photodiode array detector (DAD), and HP Chemstation software. The separation was carried out on a poroshell 120 EC-C18 column 50 X 4.6 mm,

2.7 μm with acetonitrile (A), 0.1% TFA in water (B), as a mobile phase at a flow rate of 1 mL/min at 20 $^{\circ}\text{C}$. Method: 5% A and 95% B (0 min), 50% A and 50% B (15 min), 95% A and 5% B (24min), 95% A and 5% B (25min), 5% A and 95% B (26 min), 5% A and 95% B (27 min). All materials were purchased from a commercial supplier and used without further purification unless otherwise noted.

(Methoxycarbonyl)-D-valine (Cap-1). Na_2CO_3 (276 mg, 2.6 mmol) was added to aq NaOH (5 mL of 1 M/ H_2O , 5 mmol) solution of D-valine (586 mg, 5.00 mmol) and the resulting solution was cooled with ice-water bath. Methyl chloroformate (0.420 mL, 5.40 mmol) was added dropwise, the cooling bath was removed and the reaction mixture was stirred at ambient temperature for 3.25 h. The reaction mixture was washed with ether (3x9 mL), and the aqueous phase was cooled with ice-water bath and acidified with conc HCl to a pH region of 1-2, and extracted with CH_2Cl_2 (3x9 mL). The organic phase was dried (MgSO_4), filtered, and concentrated in vacuo to afford **Cap-1** as a white solid (760 mg, 87%). ^1H NMR ($\text{DMSO}-d_6$, $\delta=2.5$ ppm, 300 MHz): 12.54 (s, 1H), 7.32 (d, 1H), 3.84 (t, 1H), 3.54 (s, 3H), 2.03 (m, 1H), 0.87 (d, 6H).

(Methoxycarbonyl)-L-valine (Cap-2). Yield 5.0 g (86%); ^1H NMR ($\text{DMSO}-d_6$, $\delta=2.5$ ppm, 400 MHz): 12.51 (br s, 1H), 7.32 (d, 1H), 3.84 (t, 1H), 3.54 (s, 3H), 2.03 (m, 1H), 0.88 (d, $J=12$, 6H).

(R)-2-((methoxycarbonyl)amino)-2-phenylacetic acid (Cap-3). Yield 1.4 g (67%); ^1H NMR ($\text{DMSO}-d_6$, $\delta=2.5$ ppm, 500 MHz): 12.79 (br s, 1H), 7.96 (d, $J=12$, 1H), 7.40-7.29 (m, 5H), 5.13 (d, $J=12$, 1H), 3.55 (s, 3H).

(S)-2-((methoxycarbonyl)amino)-3,3-dimethylbutanoic acid (Cap-4). Yield 670 mg (71%); ^1H NMR (CDCl_3 , $\delta=7.26$ ppm, 500 MHz): 9.57 (br s, 1H), 5.31 (d, 1H), 4.20 (d, 1H), 3.70 (s, 3H), 1.03 (s, 9H).

Di-tert-butyl 2,2'-(((sulfonylbis(4,1-phenylene))bis(azanediyl))bis(carbonyl))(2*S*,2'*S*)-bis(pyrrolidine-1-carboxylate) (2). A mixture of 4,4'-Diaminodiphenyl Sulfone **1** (481 mg, 1.94 mmol), *N*-Boc-L-proline (1.00 g, 4.65 mmol), and EDCI (945 mg, 5.03 mmol) in CH₂Cl₂ (10 mL) was stirred at room temperature for 16 h. The mixture was then poured in 1 N aq. HCl solution and extracted with CH₂Cl₂. The organic layer dried over magnesium sulfate, filtered, and concentrated in vacuo. Then without any purification, *tert*-Butyl (*S*)-2-(((4-(((4-((*R*)-1-(*tert*-butoxycarbonyl)pyrrolidine-2-carboxamido)phenyl)sulfonyl)phenyl)carbonyl)pyrrolidine-1-carboxylate **2** was obtained as white solid (544 mg, 44%). ¹H NMR (DMSO-*d*₆, δ=2.5 ppm, 400 MHz): 10.43 (s, 2H), 7.89-7.79 (m, 8H), 4.27-4.18 (m, 2H), 3.44-3.39 (m, 4H), 2.19-2.16 (m, 2H), 1.99-1.78 (m, 6H), 1.38-1.23 (app br s, 18H). ¹³C NMR (DMSO-*d*₆, δ=39.52 ppm, 100 MHz): 172.3, 153.0, 143.4, 135.3, 128.5, 119.2, 113.0, 78.6, 62.8, 60.4, 46.5, 45.1, 33.1, 30.9, 30.1, 27.9, 26.7, 26.6, 24.0, 23.4, 13.1. HRMS (ESI) *m/z*: Anal. calcd. for [M+Na]⁺ C₃₂H₄₂N₄NaO₈S: 665.2616; found 665.2613.

Dimethyl ((1*R*,1'*R*)-((2*S*,2'*S*)-(((sulfonylbis(4,1-phenylene))bis(azanediy))bis(carbonyl))bis(pyrrolidine-2,1-diyl))bis(2-oxo-1-phenylethane-2,1-diyl))dicarbamate (13, BMK-21006). Yield 111 mg (50 %); ¹H NMR (DMSO-*d*₆, δ=2.5 ppm, 400 MHz): 10.37 (s, 2H), 7.87-7.85 (d, 4H), 7.82-7.80 (d, 4H), 7.73-7.57 (q, 2H), 7.40-7.29 (m, 9H), 7.20-6.99 (q, 1H), 5.50-5.48 (d, 2H), 4.38-4.37 (d, 2H), 3.80-3.70 (m, 2H), 3.52 (s, 6H), 3.20-3.14 (q, 2H), 2.02-1.94 (m, 4H), 1.91-1.78 (m, 4H). ¹³C NMR (DMSO-*d*₆, δ=39.52 ppm, 100 MHz): 171.0, 168.3, 156.0, 143.4, 137.2, 135.3, 128.6, 128.0, 119.2, 60.7, 56.6, 51.6, 46.9, 29.2, 24.3. HRMS (ESI) *m/z*: Anal. calcd. for [M+Na]⁺ C₄₂H₄₄N₆NaO₁₀S: 847.2732; found 847.2734.

Dimethyl ((2*S*,2'*S*)-((2*S*,2'*S*)-(((sulfonylbis(4,1-phenylene))bis(azanediy))bis(carbonyl))bis(pyrrolidine-2,1-diyl))bis(3-methyl-1-oxobutane-1,2-diyl))dicarbamate (14, BMK-21056). Yield 65.8 mg (53 %); ¹H NMR (DMSO-

d_6 , $\delta=2.5$ ppm, 400 MHz): 10.49 (s, 2H), 7.85-7.76 (m, 8H), 7.33-7.32 (d, 2H), 4.43 (s, 2H), 4.04-4.02 (t, 2H), 3.80 (s, 2H), 3.61 (s, 2H), 3.52 (s, 6H), 2.16 (s, 2H), 1.96-1.87 (m, 8H), 0.93-0.87 (m, 12H). ^{13}C NMR (DMSO- d_6 , $\delta=39.52$ ppm, 100 MHz): 171.2, 170.4, 156.8, 143.5, 135.2, 128.4, 119.0, 60.3, 57.9, 51.5, 51.4, 47.2, 29.8, 29.3, 24.7, 18.9, 18.6. HRMS (ESI) m/z : Anal. calcd. for $[\text{M}+\text{H}]^+$ $\text{C}_{36}\text{H}_{49}\text{N}_6\text{O}_{10}\text{S}$: 757.3225; found 757.3228.

Dimethyl ((2R,2'R)-((2S,2'S)-(((sulfonylbis(4,1-phenylene))bis(azanediy))bis(carbonyl))bis(pyrrolidine-2,1-diyl))bis(3-methyl-1-oxobutane-1,2-diyl))dicarbamate (15, BMK-21033). Yield 53.1 mg (55 %); ^1H NMR (DMSO- d_6 , $\delta=2.5$ ppm, 500 MHz): 10.72-10.24 (app s, 2H), 7.99-7.84 (m, 4H), 7.82-7.71 (m, 4H), 7.56-7.33 (m, 2H), 4.41-4.40 (d, 2H), 4.10-4.07 (t, 2H), 3.78-3.68 (m, 2H), 3.63-3.59 (m, 1H), 3.54 (s, 6H), 3.46-3.44 (t, 1H), 2.18-2.09 (m, 2H), 2.04-1.82 (m, 8H), 0.88-0.85 (t, 10H), 0.77-0.76 (d, 1H), 0.68-0.67 (d, 1H). ^{13}C NMR (DMSO- d_6 , $\delta=39.52$ ppm, 125 MHz): 171.2, 170.2, 156.9, 143.3, 135.3, 128.4, 119.1, 60.3, 57.9, 51.6, 47.7, 29.7, 29.3, 24.3, 19.1, 18.3. HRMS (ESI) m/z : Anal. calcd. for $[\text{M}+\text{Na}]^+$ $\text{C}_{36}\text{H}_{48}\text{N}_6\text{NaO}_{10}\text{S}$: 779.3045; found 779.3045.

General procedure for synthesis of aminophenol

A stirred mixture of Nitro phenol (12.7 mmol) in MeOH (50 mL) at room temperature was treated with 10 wt% palladium on charcoal (100 mg). Hydrogen gas was passed through the mixture for 24 h, and then the palladium on charcoal was removed by filtration through Celite. The filtrate was concentrated in vacuo, and was obtained as solid product.

3-Amino-2-methylphenol (4a). Yield (1.62 g, 99%); ^1H NMR (CD_3OD , $\delta=3.31$ ppm, 400 MHz): 6.77-6.73, (t, 1H), 6.29-6.27 (d, 1H), 6.22-6.20 (d, 1H), 2.02 (s, 3H). ^{13}C NMR (CD_3OD , $\delta=49.00$ ppm, 100 MHz): 156.7, 147.5, 127.2, 110.9, 108.8, 106.7, 9.2. HRMS (ESI) m/z : Anal. calcd. for $[\text{M}+\text{H}]^+$ $\text{C}_7\text{H}_{10}\text{NO}$: 124.0757; found 124.0759.

3-Amino-2-fluorophenol (4b). Yield (1.65 g, 99%); ^1H NMR (CD_3OD , $\delta=3.31$ ppm, 400 MHz): δ 6.69-6.65 (t, 1H), 6.34-6.25 (m, 2H); ^{13}C NMR (CD_3OD , $\delta=49.00$ ppm, 100 MHz): δ 146.13, 143.90, 141.59, 124.71, 109.49, 107.95; ^{19}F NMR (CD_3OD , 376 MHz): δ -161.96; HRMS (ESI) m/z : Anal. calcd. for $[\text{M}+\text{H}]^+$ $\text{C}_6\text{H}_7\text{FNO}$: 128.0506; found 128.0482.

5-Amino-2-fluorophenol (4c). Yield (809 mg, 99%); ^1H NMR (CD_3OD , $\delta=3.31$ ppm, 400 MHz): δ 6.78-6.73, (t, 1H), 6.34-6.31 (q, 1H), 6.17-6.13 (m, 1H); ^{13}C NMR (CD_3OD , $\delta=49.00$ ppm, 100 MHz): δ 147.94, 145.65, 145.15, 116.60, 107.67, 106.22; ^{19}F NMR (CD_3OD , 376 MHz): δ -152.91; HRMS (ESI) m/z : Anal. calcd. for $[\text{M}+\text{H}]^+$ $\text{C}_6\text{H}_7\text{FNO}$: 128.0506; found 128.0508.

General procedure for synthesis of amide linked intermediate

A mixture of Amino phenol (12.6 mmol), *N*-Boc-L-proline (3.25 g, 15.1 mmol), and EDCI (2.11 g, 16.4 mmol) in CH_2Cl_2 (30 mL) was stirred at room temperature for 4 h. The mixture was then poured in 1 N aq HCl solution and Extracted with CH_2Cl_2 . The organic layer dried over magnesium sulfate, and then was purified by the column chromatography (n-hexane / ethyl acetate). The residue was obtained as solid product.

***tert*-Butyl (S)-2-((3-hydroxy-2-methylphenyl)carbamoyl)pyrrolidine-1-carboxylate (5a).** Yield (1.76 g, 99%); ^1H NMR ($\text{DMSO}-d_6$, $\delta=2.5$ ppm, 400 MHz): 9.36-9.24 (t, 2H), 6.94 (s, 1H), 6.82-6.78 (d, 1H), 6.65 (s, 1H), 4.29 (s, 1H), 3.42-3.32 (m, 2H), 2.23-2.14 (d, 1H), 1.99 (s, 3H), 1.89-1.81 (m, 3H), 1.42-1.37 (app br s, 9H). ^{13}C NMR ($\text{DMSO}-d_6$, $\delta=39.52$ ppm, 100 MHz): 171.3, 155.7, 153.3, 137.1, 125.5, 119.3, 116.2, 111.8, 78.5, 60.0, 46.6, 31.4, 28.1, 23.3, 10.7. HRMS (ESI) m/z : Anal. calcd. for $[\text{M}+\text{Na}]^+$ $\text{C}_{17}\text{H}_{24}\text{N}_2\text{NaO}_4$: 343.1628; found 343.1627.

***tert*-Butyl (S)-2-((3-hydroxy-4-methylphenyl)carbamoyl)pyrrolidine-1-carboxylate (5b).** Yield 1.92 g (74%); ¹H NMR (DMSO-*d*₆, δ=2.5 ppm, 400 MHz): 9.73 (s, 1H), 9.27 (s, 1H), 7.21 (s, 1H), 6.94-6.92 (d, 1H), 6.86-6.84 (d, 1H), 4.23-4.13 (m, 1H), 3.39 (s, 2H), 2.20-2.17 (d, 1H), 2.04 (s, 3H), 1.86-1.80 (m, 3H), 1.39-1.23 (app br s, 9H). ¹³C NMR (DMSO-*d*₆, δ=39.52 ppm, 100 MHz): 171.1, 155.2, 153.2, 137.6, 130.2, 118.6, 109.9, 106.2, 78.4, 60.3, 46.5, 31.0, 28.0, 23.4, 15.5. HRMS (ESI) *m/z*: Anal. calcd. for [M+Na]⁺ C₁₇H₂₄N₂NaO₄: 343.1628; found 343.1626.

***tert*-Butyl (S)-2-((3-hydroxyphenyl)carbamoyl)pyrrolidine-1-carboxylate (5c).** Yield 5.41 g (96%); ¹H NMR (DMSO-*d*₆, δ=2.5 ppm, 400 MHz): 9.83 (s, 1H), 9.36 (s, 1H), 7.18 (s, 1H), 7.08-7.04 (t, 1H), 6.96-6.94 (d, 1H), 6.45-6.43 (d, 1H), 4.24-4.15 (m, 1H), 3.37 (m, 1H), 3.33-3.32 (m, 1H), 2.17-2.08 (m, 1H), 1.86-1.75 (m, 3H), 1.39-1.27 (app br s, 9H). ¹³C NMR (DMSO-*d*₆, δ=39.52 ppm, 100 MHz): 171.4, 157.6, 153.2, 140.2, 129.3, 110.4, 110.1, 106.6, 78.5, 60.4, 46.6, 31.1, 28.0, 23.4. HRMS (ESI) *m/z*: Anal. calcd. for [M+Na]⁺ C₁₆H₂₂N₂NaO₄: 329.1472; found 329.1474.

***tert*-Butyl (S)-2-((4-hydroxyphenyl)carbamoyl)pyrrolidine-1-carboxylate (5d).** Yield 5.36 g (87%). ¹H NMR (DMSO-*d*₆, δ=2.5 ppm, 400 MHz): 9.68 (s, 1H), 9.16 (s, 1H), 7.37-7.34 (d, 2H), 6.70-6.67 (d, 2H), 4.22-4.12 (m, 1H), 3.43-3.37 (m, 1H), 3.35-3.29 (m, 1H), 2.19-2.12 (m, 1H), 1.91-1.74 (m, 3H), 1.39-1.28 (app br s, 9H). ¹³C NMR (DMSO-*d*₆, δ=39.52 ppm, 100 MHz): 170.8, 153.3, 130.7, 121.0, 115.0, 78.4, 60.3, 46.6, 31.0, 30.2, 28.0, 24.0, 23.4. HRMS (ESI) *m/z*: Anal. calcd. for [M+Na]⁺ C₁₆H₂₂N₂NaO₄: 329.1472; found 329.1472.

***tert*-Butyl (S)-2-((2-fluoro-3-hydroxyphenyl)carbamoyl)-pyrrolidine-1-carboxylate (5e).** Yield (3.79 g, 93%); ¹H NMR (DMSO-*d*₆, δ=2.5 ppm, 500 MHz): δ 9.84 (s, 1H), 9.63 (s, 1H), 7.32-7.21 (m, 1H), 6.90-6.89 (d, 1H), 6.71-6.70 (d, 1H), 4.42-4.33 (m, 1H), 3.40 (s, 1H), 3.36-3.32 (m, 1H), 2.20-2.12 (m, 1H), 1.87-1.78 (m, 3H), 1.40-1.31 (app br s, 9H); ¹³C NMR (DMSO-*d*₆, δ=39.52 ppm, 126 MHz): δ 171.90, 153.34, 145.34,

142.79, 127.08, 123.46, 114.31, 113.46, 78.66, 60.03, 46.67, 31.23, 28.02, 23.43; ^{19}F NMR (DMSO- d_6 , 376 MHz): δ -147.91, -149.01; HRMS (ESI) m/z : Anal. calcd. for $[\text{M}+\text{Na}]^+$ $\text{C}_{16}\text{H}_{21}\text{FN}_2\text{NaO}_4$: 347.1378; found 347.1379.

***tert*-Butyl (S)-2-((4-fluoro-3-hydroxyphenyl)carbamoyl)pyrrolidine-1-carboxylate (5f).** Yield (748 mg, 59%); ^1H NMR (DMSO- d_6 , δ =2.5 ppm, 400 MHz): δ 9.83 (s, 2H), 7.38-7.36 (d, 1H), 7.05-7.00 (t, 1H), 6.95-6.91 (m, 1H), 4.23- 4.13 (m, 1H), 3.44-3.38 (m, 1H), 3.35-3.32 (m, 1H), 2.23-2.12 (m, 1H), 1.91-1.75 (m, 3H), 1.39-1.28 (app br s, 9H); ^{13}C NMR (DMSO- d_6 , δ =39.52 ppm, 100 MHz): δ 171.19, 153.11, 148.05, 146.15, 144.59, 135.46, 115.49, 109.99, 109.09, 78.40, 60.30, 46.49, 30.92, 30.09, 28.09, 27.89, 23.87, 23.29; ^{19}F NMR (DMSO- d_6 , 376 MHz): δ -141.97; HRMS (ESI) m/z : Anal. calcd. for $[\text{M}+\text{Na}]^+$ $\text{C}_{16}\text{H}_{21}\text{FN}_2\text{NaO}_4$: 347.1378; found 347.1379.

2-Bromo-1-(4-fluoro-3-hydroxyphenyl)ethan-1-one (7a). A mixture of 4-Fluoro-3-hydroxyacetophenone (100 mg, 0.649 mmol), copper (II) bromide (174 mg, 0.779 mmol) in Ethyl acetate (5 mL) / Chloroform (5 mL) was heated and refluxed for 8 h. The mixture was then filtered to remove the copper (I) bromide. The filtrate was concentrated in vacuo, and was obtained as yellow solid (123 mg, 81%); ^1H NMR (CDCl_3 , δ =7.26 ppm, 400 MHz): δ 7.67-7.64 (m, 1H), 7.56-7.51 (m, 1H), 7.19-7.13 (m, 1H), 5.63 (s, 1H), 4.38 (s, 2H); ^{13}C NMR (CDCl_3 , δ =77.16 ppm, 100 MHz): δ 190.18, 155.97, 153.50, 144.29, 131.19, 122.62, 118.44, 116.35, 30.63; ^{19}F NMR (CDCl_3 , 376 MHz): -130.70; HRMS (ESI) m/z : Anal. calcd. for $[\text{M}+\text{Na}]^+$ $\text{C}_8\text{H}_6\text{BrFN}_2\text{NaO}_2$: 254.9427; found 254.9428.

General procedure for synthesis of keto ester derivatives

2-Bromo-acetophenone (0.416 mmol) and *N*-Boc-L-proline (0.499 mmol) in Acetonitrile (10 mL) put into the flask. Diisopropylethylamine (0.541

mmol) was added dropwise to the mixture and was stirred at room temperature for 5 h. The mixture was then poured in 1 N aq HCl solution and extracted with CH₂Cl₂. The organic layer dried over magnesium sulfate, and then was purified by the column chromatography (n-hexane / ethyl acetate). The residue was obtained as white solid.

1-(tert-Butyl) 2-(2-(4-fluoro-3-hydroxyphenyl)-2-oxoethyl) (S)-pyrrolidine-1,2-dicarboxylate (8a). Yield (110 mg, 72%); ¹H NMR (DMSO-d₆, δ=2.5 ppm, 400 MHz): δ 10.43 (s, 1H), 7.55-7.48 (m, 2H), 7.34-7.29 (m, 1H), 5.56-5.36 (m, 2H), 4.35-4.39/4.08-4.03 (2 m, 0.86H+0.28H), 3.41-3.34 (m, 1H), 3.28-3.16 (m, 1H), 2.32-2.09 (m, 1H), 1.92-1.76 (m, 3H), 1.36 (app br s, 9H); ¹³C NMR (DMSO-d₆, δ=39.52 ppm, 100 MHz): δ 191.37, 172.33, 155.97, 153.00, 145.44, 130.79, 120.36, 116.90, 116.55, 79.06, 66.41, 58.56, 46.22, 30.47, 29.55, 27.96, 23.88, 23.12; ¹⁹F NMR (DMSO-d₆, 376 MHz): δ -127.51; HRMS (ESI) m/z: Anal. calcd. for [M+Na]⁺ C₁₈H₂₂FNNaO₆: 390.1323; found 390.1323.

1-(tert-Butyl) 2-(2-(4-hydroxyphenyl)-2-oxoethyl) (S)-pyrrolidine-1,2-dicarboxylate (8b). Yield (1.20 g, 74%); ¹H NMR (DMSO-d₆, δ=2.5 ppm, 400 MHz): 10.49 (s, 1H), 7.86-7.85 (d, 2H), 6.88-6.86 (t, 2H), 5.53-5.32 (m, 2H), 4.32-4.29 (m, 1H), 3.11 (m, 2H), 2.29-2.14 (m, 2H), 1.90-1.85 (m, 2H), 1.36 (app br s, 9H). ¹³C NMR (DMSO-d₆, δ=39.52 ppm, 100 MHz): 190.5, 172.3, 162.7, 153.0, 130.4, 125.4, 115.4, 78.9, 66.1, 58.6, 46.2, 30.4, 27.9, 23.1. HRMS (ESI) m/z: Anal. calcd. for [M+Na]⁺ C₁₈H₂₃NNaO₆: 372.1418; found 372.1419.

1-(tert-Butyl) 2-(2-(3-hydroxyphenyl)-2-oxoethyl) (S)-pyrrolidine-1,2-dicarboxylate (8c). Yield 1.47 g (91%); ¹H NMR (DMSO-d₆, δ=2.5 ppm, 400 MHz): 9.88 (s, 1H), 7.45-7.43 (d, 1H), 7.37-7.33 (m, 2H), 7.10-7.08 (d, 1H),

5.58-5.38 (m, 2H), 4.37-4.31 (m, 1H), 3.41-3.31 (m, 2H), 2.34-2.10 (m, 2H), 1.92-1.82 (m, 2H), 1.40-1.37 (app br s, 9H). ¹³C NMR (DMSO-d₆, δ=39.52 ppm, 100 MHz): 192.4, 172.3, 157.8, 153.0, 135.2, 130.0, 121.1, 118.7, 113.9, 79.0, 66.6, 58.6, 46.2, 30.5, 29.6, 28.1, 27.9, 23.9, 23.1. HRMS (ESI) *m/z*: Anal. calcd. for [M+Na]⁺ C₁₈H₂₃NNaO₆: 372.1418; found 372.1417.

General procedure for synthesis of imidazole linked intermediate

A mixture of keto ester (0.554 mmol) and Ammonium acetate (8.30 mmol) were suspended in Toluene (10 mL). The reaction mixture was heated to 90 °C and stirred for 20 h. The mixture was then poured in H₂O and extracted with ethyl acetate. The organic layer dried over magnesium sulfate and evaporated in vacuo. After evaporation, the residue was purified by the column chromatography (n-hexane / ethyl acetate). Then product was obtained as yellow solid.

tert-Butyl (S)-2-(5-(4-fluoro-3-hydroxyphenyl)-1H-imidazol-2-yl)pyrrolidine-1-carboxylate (9a). yield (101 mg, 52%); ¹H NMR (DMSO-d₆, δ=2.5 ppm, 400 MHz): δ 12.06/11.83-11.76 (s/d, 0.16H+0.76H), 9.70 (s, 1H), 7.35 (s, 2H), 7.10-7.01 (m, 2H), 4.80-4.73 (d, 1H), 3.52 (s, 1H), 2.32-2.15 (m, 1H), 1.97-1.76 (m, 4H), 1.39-1.15 (app br s, 9H); ¹³C NMR (DMSO-d₆, δ=39.52 ppm, 100 MHz): δ 153.39, 150.76, 144.58, 138.79, 131.95, 115.97, 115.18, 113.60, 111.31, 78.60, 58.75, 55.20, 46.28, 33.32, 27.88, 23.88, 23.14; ¹⁹F NMR (DMSO-d₆, 376 MHz): δ -138.76, -140.30; HRMS (ESI) *m/z*: Anal. calcd. for [M+H]⁺ C₁₈H₂₃FN₃O₃: 348.1718; found 348.1719.

tert-Butyl (S)-2-(5-(4-hydroxyphenyl)-1H-imidazol-2-yl)-pyrrolidine-1-carboxylate (9b). Yield (887 mg, 47%); ¹H NMR (DMSO-d₆, δ=2.5 ppm, 400 MHz): δ 11.76 (br s, 1H), 9.48 (br s, 1H), 7.53 (s, 2H), 7.20 (s, 1H), 6.77-6.75 (d, 2H), 4.83-4.76 (d, 1H), 3.54-3.35 (d, 2H), 2.20-1.81 (m, 4H),

1.39-1.17 (app br s, 9H); ^{13}C NMR (DMSO- d_6 , $\delta=39.52$ ppm, 100 MHz): δ 155.93, 153.82, 153.47, 150.09, 125.54, 115.30, 78.23, 55.26, 46.34, 33.41, 31.88, 27.93, 23.85, 23.16; HRMS (ESI) m/z : Anal. calcd. for $[\text{M}+\text{Na}]^+$ $\text{C}_{18}\text{H}_{23}\text{N}_3\text{NaO}_3$: 352.1632; found 352.1634.

***tert*-Butyl (S)-2-(5-(3-hydroxyphenyl)-1H-imidazol-2-yl)-pyrrolidine-1-carboxylate (9c).** Yield (456 mg, 45%); ^1H NMR (DMSO- d_6 , $\delta=2.5$ ppm, 400 MHz): δ 11.88 (br s, 1H), 9.41 (br s, 1H), 7.34-7.11 (m, 4H), 6.60 (s, 1H), 4.85-4.77 (d, 1H), 3.55 (s, 1H), 3.35 (s, 1H), 2.22-2.14 (m, 1H), 1.99-1.82 (m, 3H), 1.39-1.16 (app br s, 9H); ^{13}C NMR (DMSO- d_6 , $\delta=39.52$ ppm, 100 MHz): δ 157.66, 153.51, 129.43, 115.25, 113.14, 111.25, 78.32, 55.33, 48.72, 46.42, 33.49, 31.93, 27.96, 23.93, 23.25; HRMS (ESI) m/z : Anal. calcd. for $[\text{M}+\text{Na}]^+$ $\text{C}_{18}\text{H}_{23}\text{N}_3\text{NaO}_3$: 352.1632; found 352.1634.

General procedure for synthesis of fosylated intermediate

A mixture of phenol derivative (0.800 mmol) and *N,N*-Diisopropylethylamine (1.20 mmol) in CH_2Cl_2 (5 mL) was stirred under sulfuryl fluoride at room temperature for 5 h. The mixture was then poured in 1 N aq HCl solution and extracted with CH_2Cl_2 . The organic layer dried over magnesium sulfate, filtered, and concentrated in vacuo. Without any purification, the residue was obtained as an oil.

***tert*-Butyl (S)-2-((4-((fluorosulfonyl)oxy)phenyl)carbamoyl)-pyrrolidine-1-carboxylate (10a).** Yield (278 mg, 90%); ^1H NMR (DMSO- d_6 , $\delta=2.5$ ppm, 400 MHz): δ 10.31 (s, 1H), 7.82-7.80 (d, 2H), 7.53-7.51 (d, 2H), 4.28-4.21 (m, 1H), 3.42 (s, 2H), 2.21 (s, 1H), 1.89-1.79 (m, 3H), 1.38-1.27 (app s, 9H); ^{13}C NMR (DMSO- d_6 , $\delta=39.52$ ppm, 100 MHz): δ 171.97, 153.13, 144.74, 139.67, 121.53, 120.75, 78.57, 60.46, 46.58, 31.01, 30.16, 27.92, 23.99, 23.39; ^{19}F NMR (CD_3OD , 376 MHz): 31.23; HRMS (ESI) m/z : Anal. calcd. for $[\text{M}+\text{Na}]^+$ $\text{C}_{16}\text{H}_{21}\text{FN}_2\text{NaO}_6\text{S}$: 411.0997; found 411.1001.

***tert*-Butyl (S)-2-((3-((fluorosulfonyl)oxy)phenyl)carbamoyl)pyrrolidine-1-carboxylate (10b).** Yield (1.66 g, 87%); ¹H NMR (DMSO-d₆, δ=2.5 ppm, 400 MHz): δ 10.43-10.41 (d, 1H), 7.98 (s, 1H), 7.62-7.59 (t, 1H), 7.55-7.50 (m, 1H), 7.26-7.24 (d, 1H), 4.27-4.17 (m, 1H), 3.46-3.40 (m, 1H), 3.37-3.31 (m, 1H), 2.24-2.16 (m, 1H), 1.94-1.77 (m, 3H), 1.39-1.25 (app s, 9H); ¹³C NMR (DMSO-d₆, δ=39.52 ppm, 100 MHz): δ 172.23, 153.06, 149.63, 141.01, 131.00, 119.33, 115.30, 111.07, 78.61, 60.48, 46.57, 30.91, 30.11, 27.87, 23.98, 23.39; ¹⁹F NMR (CD₃OD, 376 MHz): 38.49; HRMS (ESI) m/z: Anal. calcd. for [M+Na]⁺ C₁₆H₂₁FN₂NaO₆S: 411.0997; found 411.0998.

***tert*-Butyl (S)-2-((2-fluoro-3-((fluorosulfonyl)oxy)phenyl)-carbamoyl)-pyrrolidine-1-carboxylate (10c).** Yield (364 mg, 83%); ¹H NMR (DMSO-d₆, δ=2.5 ppm, 400 MHz): δ 10.18 (s, 1H), 8.04-7.95 (d, 1H), 7.54 (s, 1H), 7.39-7.35 (t, 1H), 4.45-4.36 (m, 1H), 3.42 (s, 1H), 3.37-3.33 (m, 1H), 2.23-2.16 (m, 1H), 1.92-1.80 (s, 3H), 1.40-1.31 (app s, 9H); ¹³C NMR (DMSO-d₆, δ=39.52 ppm, 100 MHz): δ 172.20, 153.08, 146.52, 144.00, 136.75, 128.31, 124.97, 118.45, 78.61, 59.87, 46.55, 31.04, 29.94, 27.86, 23.94, 23.30; ¹⁹F NMR (DMSO-d₆, 376 MHz): δ 39.69, -139.30, -140.16; HRMS (ESI) m/z: Anal. calcd. for [M+Na]⁺ C₁₆H₂₀F₂N₂NaO₆S: 429.0902; found 429.0902.

***tert*-Butyl (S)-2-((4-fluoro-3-((fluorosulfonyl)oxy)phenyl)carbamoyl)-pyrrolidine-1-carboxylate (10d).** Yield (260 mg, 90%); ¹H NMR (DMSO-d₆, δ=2.5 ppm, 400 MHz): δ 10.42 (s, 1H), 8.14-8.12 (d, 1H), 7.64-7.56 (m, 2H), 4.24-4.15 (m, 1H), 3.41 (s, 1H), 3.31 (s, 1H), 2.22-2.17 (m, 1H), 1.93-1.78 (m, 3H), 1.39-1.25 (app s, 9H); ¹³C NMR (DMSO-d₆, δ=39.52 ppm, 100 MHz): δ 172.14, 153.63, 153.05, 149.36, 146.90, 136.55, 135.74, 135.60, 120.93, 118.14, 113.36, 78.65, 60.46, 46.59, 30.92, 30.11, 27.90, 24.00, 23.40; ¹⁹F NMR (DMSO-d₆, 376 MHz):

δ 39.41, -136.14; HRMS (ESI) m/z : Anal. calcd. for $[M+Na]^+$ $C_{16}H_{20}F_2N_2NaO_6S$: 429.0902; found 429.0900.

***tert*-Butyl (S)-2-(5-(3-((fluorosulfonyl)oxy)phenyl)-1H-imidazol-2-yl)pyrrolidine-1-carboxylate (10e).** Yield (49.8 mg, 80%); 1H NMR (DMSO- d_6 , δ =2.5 ppm, 400 MHz): δ 8.31-8.25 (d, 2H), 8.14-8.10 (t, 1H), 7.74-7.70 (t, 1H), 7.63-7.61 (d, 1H), 5.17-5.13 (t, 1H), 3.66-3.61 (m, 1H), 3.44-3.37 (m, 1H), 2.43-2.34 (m, 1H), 2.11-1.90 (m, 3H), 1.38-1.16 (app s, 9H); ^{13}C NMR (DMSO- d_6 , δ =39.52 ppm, 100 MHz): δ 153.82, 152.56, 150.85, 150.11, 131.82, 130.54, 125.80, 121.20, 117.86, 116.57, 79.34, 53.31, 46.54, 32.94, 27.73, 23.45, 17.96, 16.69, 12.20. ^{19}F NMR (DMSO- d_6 , 376 MHz): 38.53; HRMS (ESI) m/z : Anal. calcd. for $[M+H]^+$ $C_{18}H_{23}FN_3O_5S$: 412.1337; found 412.1339.

***tert*-Butyl (S)-2-(5-(4-fluoro-3-((fluorosulfonyl)oxy)phenyl)-1H-imidazol-2-yl)pyrrolidine-1-carboxylate (10f).** Yield (59.6 mg, 92%); 1H NMR (DMSO- d_6 , δ =2.5 ppm, 400 MHz): δ 12.07-12.00 (d, 1H), 8.03-8.01 (d, 1H), 7.91-7.87 (m, 1H), 7.66-7.64 (m, 1H), 7.58-7.54 (t, 1H), 4.82-4.77 (d, 1H), 3.53 (s, 1H), 3.34-3.29 (m, 1H), 2.22 (s, 1H), 1.96-1.85 (m, 3H), 1.39-1.15 (app s, 9H); ^{13}C NMR (DMSO- d_6 , δ =39.52 ppm, 100 MHz): δ 153.36, 151.81, 151.06, 149.33, 136.79, 133.63, 125.85, 118.19, 113.46, 78.26, 55.23, 46.31, 33.29, 31.84, 27.86, 23.83, 23.10; ^{19}F NMR (DMSO- d_6 , 376 MHz): δ 39.85, -134.19; HRMS (ESI) m/z : Anal. calcd. for $[M+H]^+$ $C_{18}H_{22}F_2N_3O_5S$: 430.1243; found 430.1243.

***tert*-Butyl (S)-2-(5-(4-((fluorosulfonyl)oxy)phenyl)-1H-imidazol-2-yl)pyrrolidine-1-carboxylate (10g).** Yield (100 mg, 80%); 1H NMR (DMSO- d_6 , δ =2.5 ppm, 500 MHz): δ 12.50 (s, 1H), 7.93-7.91 (d, 2H), 7.68-7.64 (d, 1H), 7.57-7.56 (d, 2H), 4.88-4.79 (m, 1H), 3.56-3.53 (t, 1H), 3.39-3.35 (m, 1H), 2.28-2.17 (m, 1H), 1.99-1.85 (m, 3H), 1.39-1.15 (app s, 9H); ^{13}C NMR (DMSO- d_6 , δ =39.52 ppm, 126 MHz): δ 153.22, 151.07,

147.88, 126.11, 121.25, 78.35, 54.90, 46.32, 33.23, 31.81, 28.15, 27.83, 23.82, 23.12; ^{19}F NMR (DMSO- d_6 , 376 MHz): 38.27; HRMS (ESI) m/z : Anal. calcd. for $[\text{M}+\text{H}]^+$ $\text{C}_{18}\text{H}_{23}\text{FN}_3\text{O}_5\text{S}$: 412.1337; found 412.1340.

General procedure for silyl protection.

A mixture of phenol derivative (2.29 mmol), *tert*-butyldimethylsilyl chloride (3.44 mmol), imidazole (6.87 mmol) in THF (10 mL) was stirred at room temperature for 4 h. The mixture was then poured in H_2O and extracted with CH_2Cl_2 . The organic layer dried over magnesium sulfate, and then was purified by the column chromatography (n-hexane / ethyl acetate). The residue was obtained as sticky oil.

***tert*-Butyl (S)-2-((3-((*tert*-butyldimethylsilyl)oxy)phenyl)carbamoyl)pyrrolidine-1-carboxylate (11a).** Yield (759 mg, 95%); ^1H NMR (DMSO- d_6 , $\delta=2.5$ ppm, 400 MHz): δ 9.93 (s, 1H), 7.35-7.24 (d, 1H), 7.16-7.09 (m, 2H), 6.52-6.51 (d, 1H), 4.23-4.13 (m, 1H), 3.44-3.38 (m, 1H), 3.32-3.30 (m, 1H), 2.21-2.12 (m, 1H), 1.90-1.75 (m, 3H), 1.39-1.26 (app s, 9H), 0.93 (s, 9H), 0.17 (s, 6H); ^{13}C NMR (DMSO- d_6 , $\delta=39.52$ ppm, 100 MHz): δ 171.50, 155.27, 153.11, 140.22, 129.48, 114.63, 112.27, 110.84, 78.44, 60.40, 46.56, 30.95, 27.89, 25.55, 23.43, 17.95, -4.53; HRMS (ESI) m/z : Anal. calcd. for $[\text{M}+\text{Na}]^+$ $\text{C}_{22}\text{H}_{36}\text{N}_2\text{NaO}_4\text{Si}$: 443.2337; found 443.2337.

***tert*-Butyl (S)-2-((3-((*tert*-butyldimethylsilyl)oxy)-4-fluorophenyl)carbamoyl)pyrrolidine-1-carboxylate (11b).** Yield (318 mg, 73%); ^1H NMR (DMSO- d_6 , $\delta=2.5$ ppm, 400 MHz): δ 9.95 (s, 1H), 7.51-7.38 (q, 1H), 7.09 (s, 2H), 4.22-4.12 (m, 1H), 3.42-3.39 (m, 1H), 3.35-3.30 (m, 1H), 2.21-2.12 (m, 1H), 1.87-1.75 (m, 3H), 1.39-1.25 (app br s, 9H), 0.95 (s, 9H), 0.17 (s, 6H); ^{13}C NMR (DMSO- d_6 , $\delta=39.52$ ppm, 100 MHz): δ 171.38, 153.08, 150.51, 148.14, 142.08, 135.72, 115.92, 113.02, 78.41, 60.40, 46.55, 30.94, 27.85, 25.34, 23.42, 17.95, -4.89; ^{19}F NMR (DMSO- d_6 , 376

MHz): δ -138.76; HRMS (ESI) m/z : Anal. calcd. for $[M+Na]^+$ $C_{22}H_{35}FN_2NaO_4Si$: 461.2242; found 461.2242.

tert-Butyl (S)-2-((3-((tert-butyldimethylsilyl)oxy)-2-fluorophenyl)carbamoyl)pyrrolidine-1-carboxylate (11c). Yield (294 mg, 73%); 1H NMR (DMSO- d_6 , δ =2.5 ppm, 400 MHz): δ 9.71 (s, 1H), 7.54-7.38 (m, 1H), 7.02-6.98 (t, 1H), 6.78-6.74 (t, 1H), 4.40-4.33 (m, 1H), 3.43-3.38 (m, 1H), 2.24-2.08 (m, 1H), 1.91-1.77 (m, 3H), 1.40-1.30 (app br s, 9H), 0.96 (s, 9H), 0.17 (s, 6H); ^{13}C NMR (DMSO- d_6 , δ =39.52 ppm, 100 MHz): δ 171.82, 153.14, 142.85, 127.23, 123.61, 123.56, 117.48, 116.90, 78.51, 59.85, 46.54, 31.05, 27.88, 25.38, 23.32, 18.00, -4.84; ^{19}F NMR (DMSO- d_6 , 376 MHz): δ -143.28, -144.70; HRMS (ESI) m/z : Anal. calcd. for $[M+Na]^+$ $C_{22}H_{35}FN_2NaO_4Si$: 461.2242; found 461.2242.

tert-Butyl (S)-2-(5-(4-((tert-butyldimethylsilyl)oxy)phenyl)-1H-imidazol-2-yl)pyrrolidine-1-carboxylate (11d). Yield (269 mg, 60%); 1H NMR (DMSO- d_6 , δ =2.5 ppm, 500 MHz): δ 11.77 (s, 1H), 7.60-7.59 (d, 2H), 7.30 (s, 1H), 6.81-6.80 (d, 2H), 4.83-4.75 (m, 1H), 3.56-3.50 (m, 1H), 3.37-3.34 (m, 1H), 2.23-2.12 (m, 1H), 2.03-1.83 (m, 3H), 1.39-1.16 (app br s, 9H), 0.95 (s, 9H), 0.18 (s, 6H); ^{13}C NMR (DMSO- d_6 , δ =39.52 ppm, 126 MHz): δ 153.70, 153.37, 139.36, 128.82, 125.44, 119.76, 78.12, 55.20, 46.25, 33.30, 31.76, 27.88, 25.57, 23.79, 23.05, 17.94, -3.21, -4.52; HRMS (ESI) m/z : Anal. calcd. for $[M+H]^+$ $C_{24}H_{38}N_3O_3Si$: 444.2677; found 444.2679.

tert-Butyl (S)-2-(5-(3-((tert-butyldimethylsilyl)oxy)-4-fluoro-phenyl)-1H-imidazol-2-yl)pyrrolidine-1-carboxylate (11e). Yield (638 mg, 69%); 1H NMR (DMSO- d_6 , δ =2.5 ppm, 400 MHz): δ 12.12-11.81 (m, 1H), 7.43 (s, 1H), 7.35-7.31 (m, 2H), 7.23-7.10 (m, 1H), 4.83-4.76 (m, 1H), 3.53 (s, 1H), 2.21-2.10 (m, 1H), 1.98-1.84 (m, 3H), 1.39 (s, 4H), 1.15 (s, 9H), 0.97 (s, 9H), 0.18 (s, 6H); ^{13}C NMR (DMSO- d_6 , δ =39.52 ppm, 100 MHz):

δ 153.10, 150.70, 142.40, 138.33, 132.30, 118.02, 117.76, 116.26, 116.07, 111.83, 78.15, 55.30, 46.25, 33.25, 31.81, 27.84, 25.42, 23.73, 23.06, 18.01, -4.82; ^{19}F NMR (DMSO- d_6 , 376 MHz): δ -134.91, -136.21; HRMS (ESI) m/z : Anal. calcd. for $[\text{M}+\text{H}]^+$ $\text{C}_{24}\text{H}_{37}\text{FN}_3\text{O}_3\text{Si}$: 462.2583; found 462.2585.

***tert*-Butyl (S)-2-((4-((*tert*-butyldimethylsilyl)oxy)phenyl)-carbamoyl)-pyrrolidine-1-carboxylate (11f).** Yield (63.0 mg, 92%); ^1H NMR (DMSO- d_6 , δ =2.5 ppm, 500 MHz): δ 9.83-9.81 (d, 1H), 7.47-7.44 (m, 2H), 6.79-6.78 (d, 2H), 4.22-4.13 (m, 1H), 3.43-3.40 (m, 1H), 3.32-3.30 (m, 1H), 2.20-2.13 (m, 1H), 1.91-1.75 (m, 3H), 1.39-1.27 (app s, 9H), 0.94 (s, 9H), 0.16 (s, 6H); ^{13}C NMR (DMSO- d_6 , δ =39.52 ppm, 126 MHz): δ 170.98, 153.16, 150.73, 132.92, 120.77, 119.73, 78.40, 60.29, 46.55, 31.02, 27.95, 25.58, 23.96, 23.37, 17.93; HRMS (ESI) m/z : Anal. calcd. for $[\text{M}+\text{Na}]^+$ $\text{C}_{22}\text{H}_{36}\text{N}_2\text{NaO}_4\text{Si}$: 443.2337; found 443.2340.

***tert*-Butyl (S)-2-(5-(3-((*tert*-butyldimethylsilyl)oxy)phenyl)-1*H*-imidazol-2-yl)pyrrolidine-1-carboxylate (11g).** Yield (545 mg, 81%); ^1H NMR (DMSO- d_6 , δ =2.5 ppm, 500 MHz): δ 11.88-11.82 (app s, 1H), 7.44-7.18 (m, 4H), 6.63 (s, 1H), 4.83-4.77 (d, 1H), 3.54 (s, 1H), 3.36 (s, 1H), 2.22-2.14 (d, 1H), 2.07 (s, 1H), 1.97-1.83 (m, 2H), 1.39-1.16 (app s, 9H), 0.96 (s, 9H), 0.19 (s, 6H); ^{13}C NMR (DMSO- d_6 , δ =39.52 ppm, 126 MHz): δ 155.26, 153.39, 139.10, 129.35, 117.52, 115.55, 112.01, 78.10, 55.27, 46.26, 33.27, 31.79, 30.63, 27.84, 25.57, 23.74, 23.08, 17.93; HRMS (ESI) m/z : Anal. calcd. for $[\text{M}+\text{H}]^+$ $\text{C}_{24}\text{H}_{38}\text{N}_3\text{O}_3\text{Si}$: 444.2677; found 444.2681.

General procedure for SuFEx reaction

A mixture of silylated monomer (0.408 mmol), fosylated monomer (0.272 mmol) and DBU (0.05 mmol) in DMF (10 mL) was stirred at 50 °C for 12 h. The mixture was then poured in 1 N aq HCl solution and extracted with CH_2Cl_2 . The organic layer dried over magnesium sulfate,

and then was purified by the column chromatography (n-hexane / ethyl acetate). The residue was obtained as solid.

Di-tert-butyl 2,2'-((((sulfonylbis(oxy))bis(4,1-phenylene))bis(azane-diyl))bis(carbonyl))(2S,2'S)-bis(pyrrolidine-1-carboxylate) (12a).

Yield (76.1 mg, 90%); ¹H NMR (DMSO-d₆, δ=2.5 ppm, 400 MHz): δ 10.28 (s, 1H), 7.72-7.70 (d, 4H), 7.39-7.37 (d, 4H), 4.23-4.16 (m, 2H), 3.39-3.32 (m, 4H), 2.21-2.16 (t, 2H), 1.86-1.78 (m, 6H), 1.38-1.25 (app br s, 18H); ¹³C NMR (DMSO-d₆, δ= 39.52 ppm, 100 MHz): δ 172.2, 153.5, 145.2, 138.8, 121.9, 120.9, 79.0, 63.0, 60.7, 46.8, 31.2, 28.2, 23.7; HRMS (ESI) m/z: Anal. calcd. for [M+Na]⁺ C₃₂H₄₂N₄NaO₁₀S: 697.2514; found 697.2515.

Di-tert-butyl 2,2'-((((sulfonylbis(oxy))bis(3,1-phenylene))-bis(azane-diyl))bis(carbonyl))(2S,2'S)-bis(pyrrolidine-1-carboxylate) (12b).

Yield (1.84 g, 69%); ¹H NMR (DMSO-d₆, δ=2.5 ppm, 400 MHz): δ 10.32 (s, 1H), 8.21-7.77 (m, 3H), 7.59-7.57 (d, 2H), 7.47 (s, 1H), 7.40-7.22 (m, 1H), 7.12-7.08 (t, 1H), 4.24-4.18 (d, 2H), 3.41 (br s, 4H), 2.20 (s, 2H), 1.88-1.80 (m, 6H), 1.39-1.24 (app br s, 18H); ¹³C NMR (DMSO-d₆, δ= 39.52 ppm, 100 MHz): δ 172.0, 153.1, 149.9, 140.8, 130.6, 118.4, 115.3, 111.4, 78.6, 60.5, 46.6, 30.9, 27.9, 23.4; HRMS (ESI) m/z: Anal. calcd. for [M+Na]⁺ C₃₂H₄₂N₄NaO₁₀S: 697.2514; found 697.2514.

tert-Butyl (S)-2-((3-(((4-((S)-1-(tert-butoxycarbonyl)pyrrolidine-2-carboxamido)phenoxy)-sulfonyl)oxy)phenyl)carbamoyl)pyrrolidine-1-carboxylate (12c).

Yield (170 mg, 93%); ¹H NMR (DMSO-d₆, δ=2.5 ppm, 500 MHz): δ 10.34-10.23 (d, 2H), 7.96-7.88 (m, 1H), 7.75-7.73 (d, 2H), 7.58-7.55 (t, 1H), 7.49-7.37 (m, 3H), 7.11-7.10 (d, 1H), 4.26-4.16 (m, 2H), 3.45-3.40 (m, 2H), 3.36-3.31 (m, 2H), 2.23-2.15 (m, 2H), 1.93-1.77 (m, 6H), 1.39-1.24 (app br s, 18H); ¹³C NMR (DMSO-d₆, δ=39.52 ppm, 126 MHz): δ 171.80, 153.08, 149.91, 144.95, 144.91, 140.75,

138.75, 130.59, 121.56, 120.58, 118.31, 115.45, 111.39, 78.54, 60.41, 46.58, 30.95, 30.14, 27.90, 23.99, 23.40; HRMS (ESI) m/z: Anal. calcd. for $[M+Na]^+$ $C_{32}H_{42}N_4NaO_{10}S$: 697.2514; found 697.2515.

Di-tert-butyl 2,2'-((((sulfonylbis(oxy))bis(4-fluoro-3,1-phe-nylene))bis(azanediyl))bis(carbonyl))(2S,2'S)-bis(pyrolidine-1-carboxylate) (12d).

Yield (217 mg, 78%); 1H NMR (DMSO- d_6 , δ =2.5 ppm, 400 MHz): δ 10.33 (s, 2H), 8.11-8.08 (t, 2H), 7.60-7.58 (d, 2H), 7.53-7.48 (t, 2H), 4.23-4.13 (m, 2H), 3.42-3.40 (m, 2H), 3.35-3.32 (m, 2H), 2.21-2.18 (m, 2H), 1.91-1.78 (m, 6H), 1.38-1.23 (app br s, 18H); ^{13}C NMR (DMSO- d_6 , δ =39.52 ppm, 100 MHz): δ 171.92, 153.60, 153.04, 149.87, 147.41, 136.27, 119.94, 117.90, 113.55, 78.60, 60.45, 46.57, 30.92, 30.11, 27.86, 23.99, 23.40; ^{19}F NMR (DMSO- d_6 , 376 MHz): δ -135.44; HRMS (ESI) m/z: Anal. calcd. for $[M+Na]^+$ $C_{32}H_{40}F_2N_4NaO_{10}S$: 733.2325; found 733.2324.

Di-tert-butyl 2,2'-((((sulfonylbis(oxy))bis(2-fluoro-3,1-phe-nylene))bis(azanediyl))bis(carbonyl))(2S,2'S)-bis(pyrolidine-1-carboxylate) (12e).

Yield (231 mg, 98%); 1H NMR (DMSO- d_6 , δ =2.5 ppm, 400 MHz): δ 10.12 (s, 2H), 8.00-7.97 (t, 1H), 7.90-7.87 (t, 1H), 7.43-7.40 (t, 2H), 7.35-7.31 (t, 2H), 4.43-4.34 (m, 2H), 3.44-3.39 (m, 2H), 3.30 (m, 2H), 2.32-2.11 (m, 2H), 1.91-1.76 (m, 6H), 1.40- 1.29. (br s, 18H); ^{13}C NMR (DMSO- d_6 , δ =39.52 ppm, 100 MHz): δ 172.17, 153.07, 137.06, 128.08, 124.67, 124.04, 118.49, 78.61, 59.83, 46.55, 31.04, 29.98, 27.90, 23.95, 23.31; ^{19}F NMR (DMSO- d_6 , 376 MHz): δ -138.71, -139.67; HRMS (ESI) m/z: Anal. calcd. for $[M+Na]^+$ $C_{32}H_{40}F_2N_4NaO_{10}S$: 733.2325; found 733.2321.

tert-Butyl (S)-2-((3-(((5-((S)-1-(tert-butoxycarbonyl)pyrrole-dine-2-carbox-amido)-2-fluorophenoxy)sulfonyl)oxy)-2-fluoro-phenyl)carbonyl)pyrrolidine-1-carboxylate (12f). Yield (112 mg, 58%); 1H NMR (DMSO- d_6 , δ =2.5

ppm, 400 MHz): δ 10.33 (s, 1H), 10.11 (s, 1H), 8.12-7.90 (m, 2H), 7.61 (s, 1H), 7.54-7.49 (t, 1H), 7.40-7.31 (m, 2H), 4.43-4.36 (m, 1H), 4.23-4.13 (m, 1H), 3.40 (s, 2H), 3.30 (s, 2H), 2.21 (s, 2H), 1.88-1.79 (m, 6H), 1.39-1.23 (app br s, 18H); ^{13}C NMR (DMSO- d_6 , δ =39.52 ppm, 100 MHz): δ 171.95, 153.61, 153.04, 149.87, 147.41, 137.09, 136.21, 128.05, 124.70, 124.01, 119.90, 117.92, 113.55, 78.61, 60.45, 46.56, 30.92, 30.12, 27.88, 23.99, 23.39; ^{19}F NMR (DMSO- d_6 , 376 MHz): δ -135.48, -138.91, -139.77; HRMS (ESI) m/z : Anal. calcd. for $[\text{M}+\text{Na}]^+$ $\text{C}_{32}\text{H}_{40}\text{F}_2\text{N}_4\text{NaO}_{10}\text{S}$: 733.2325; found 733.2325.

Di-tert-butyl 2,2'-(((sulfonylbis(oxy))bis(4,1-phenylene))bis-(1H-imidazole-5,2-diyl))(2S,2'S)-bis(pyrrolidine-1-carboxylate) (12g). Yield (32.2 mg, 69%); ^1H NMR (DMSO- d_6 , δ =2.5 ppm, 400 MHz): δ 11.99 (s, 2H), 7.88-7.85 (d, 3H), 7.53 (s, 2H), 7.39-7.38 (d, 3H), 7.30-7.27 (d, 1H), 6.91-6.87 (d, 1H), 4.84-4.77 (d, 2H), 4.03-3.98 (t, 1H), 3.53 (s, 2H), 3.29-3.25 (m, 1H), 2.22-2.14 (m, 2H), 2.05-1.93 (m, 2H), 1.85-1.71 (m, 4H), 1.39-1.15 (app br s, 18H); ^{13}C NMR (DMSO- d_6 , δ =39.52 ppm, 100 MHz): δ 174.6, 153.4, 147.9, 125.7, 121.1, 78.3, 59.6, 55.2, 46.4, 33.3, 31.0, 30.0, 28.0, 23.9, 23.2; HRMS (ESI) m/z : Anal. calcd. for $[\text{M}+\text{Na}]^+$ $\text{C}_{36}\text{H}_{45}\text{N}_6\text{O}_8\text{S}$: 721.3014; found 721.3014.

Di-tert-butyl 2,2'-(((sulfonylbis(oxy))bis(3,1-phenylene))bis-(1H-imidazole-5,2-diyl))(2S,2'S)-bis(pyrrolidine-1-carboxylate) (12h). Yield (54.4 mg, 67%); ^1H NMR (DMSO- d_6 , δ =2.5 ppm, 400 MHz): δ 12.04-11.97 (br d, 2H), 8.21-7.76 (t, 4H), 7.64-7.61 (d, 1H), 7.52-7.44 (q, 2H), 7.37-7.20 (m, 2H), 6.93-6.74 (q, 1H), 4.83-4.77 (d, 2H), 3.53 (s, 2H), 3.39-3.36 (m, 2H), 2.22-2.15 (m, 2H), 1.98-1.79 (m, 6H), 1.38-1.14 (app br s, 18H); ^{13}C NMR (DMSO- d_6 , δ =39.52 ppm, 100 MHz): δ 153.4, 150.4, 138.1, 131.3, 130.5, 123.5, 119.2, 117.8, 116.4, 116.2, 78.2, 55.2, 46.3, 33.3, 27.9, 23.1; HRMS (ESI) m/z : Anal. calcd. for $[\text{M}+\text{Na}]^+$ $\text{C}_{36}\text{H}_{45}\text{N}_6\text{O}_8\text{S}$: 721.3014; found 721.3014.

***tert*-Butyl (S)-2-(5-(3-(((4-(2-((S)-1-(*tert*-butoxycarbonyl)-pyrrolidin-2-yl)-1*H*-imidazol-5-yl)phenoxy)sulfonyl)oxy)-phenyl)-1*H*-imidazol-2-yl)pyrrolidine-1-carboxylate (12i).** Yield (721 mg, 52%); ¹H NMR (DMSO-*d*₆, δ=2.5 ppm, 400 MHz): δ 8.25-8.04 (m, 6H), 7.66-7.51 (d, 4H), 5.12 (s, 2H), 3.63 (s, 2H), 3.41 (s, 2H), 2.38 (s, 2H), 2.07-1.91 (m, 6H), 1.38-1.15. (app br s, 18H); ¹³C NMR (DMSO-*d*₆, δ=39.52 ppm, 100 MHz): δ 153.71, 152.45, 150.67, 150.56, 150.22, 149.56, 131.39, 127.37, 124.78, 122.07, 117.89, 116.19, 115.71, 79.19, 52.97, 46.45, 32.89, 31.98, 27.70, 23.92, 23.38; HRMS (ESI) *m/z*: Anal. calcd. for [M+H]⁺ C₃₆H₄₅N₆O₈S: 721.3014; found 721.3016.

Di-tert-butyl 2,2'-(((sulfonylbis(oxy))bis(4-fluoro-3,1-phe-nylene))bis(1*H*-imidazole-5,2-diyl))(2*S*,2'*S*)-bis(pyrolidine-1-carboxylate) (12j). Yield (305 mg, 63%); ¹H NMR (DMSO-*d*₆, δ=2.5 ppm, 400 MHz): δ 12.01 (s, 2H), 7.92-7.91 (d, 2H), 7.82 (s, 2H), 7.58 (s, 2H), 7.52-7.47 (t, 2H), 4.82-4.76 (d, 2H), 3.52 (s, 2H), 3.37-3.17 (m, 2H), 2.22-2.13 (m, 2H), 1.95-1.84 (t, 2H), 1.37-1.14(app br s, 18H); ¹³C NMR (DMSO-*d*₆, δ=39.52 ppm, 100 MHz): δ 153.35, 152.22, 150.24, 136.98, 136.87, 133.21, 125.00, 118.39, 117.68, 113.11, 78.24, 55.22, 46.29, 33.23, 31.78, 27.83, 23.77, 23.07; ¹⁹F NMR (DMSO-*d*₆, 376 MHz): δ -133.22; HRMS (ESI) *m/z*: Anal. calcd. for [M+H]⁺ C₃₆H₄₃F₂N₆O₈S: 757.2826; found 757.2828.

Di-tert-butyl 2,2'-(((sulfonylbis(oxy))bis(2-methyl-3,1-phenyl-ene))bis(azanediy))bis(carbonyl))(2*S*,2'*S*)-bis(pyrrolidine-1-carboxylate) (12k). Yield 321 mg (75%); ¹H NMR (DMSO-*d*₆, δ=2.5 ppm, 400 MHz): 9.66-9.61 (d, 2H), 7.41 (s, 2H), 7.37-7.33 (t, 2H), 7.26-7.24 (d, 2H), 4.31-4.29 (t, 2H), 3.42 (s, 2H), 3.34 (s, 2H), 2.25-2.23 (br d, 2H), 2.11 (s, 6H), 1.97-1.82 (m, 6H), 1.41-1.35 (app br s, 18H). ¹³C NMR (DMSO-*d*₆, δ=39.52 ppm, 100 MHz): 171.7, 153.8, 153.2, 148.6, 138.3, 126.8, 125.9, 125.1, 118.1, 78.6, 59.9, 46.6, 31.3, 30.0,

28.1, 24.1, 23.2, 11.4. HRMS (ESI) m/z : Anal. calcd. for $[M+Na]^+$ $C_{34}H_{46}N_4NaO_{10}S$: 725.2827; found 725.2826.

Di-tert-butyl 2,2'-((((sulfonylbis(oxy))bis(4-methyl-3,1-phenyl-ene))bis(azanediyl))bis(carbonyl))(2S,2'S)-bis(pyrrolidine-1-carboxylate) (121). Yield 229 mg (72%); 1H NMR (DMSO- d_6 , δ =2.5 ppm, 400 MHz): 10.22 (s, 2H), 7.95 (s, 2H), 7.54-7.48 (q, 2H), 7.34-7.32 (d, 2H), 4.24-4.13 (m, 2H), 3.42-3.31 (m, 4H), 2.20-2.17 (d, 8H), 1.91-1.77 (m, 6H), 1.38-1.23 (app br s, 18H). ^{13}C NMR (DMSO- d_6 , δ =39.52 ppm, 100 MHz): 171.8, 153.1, 148.2, 138.4, 131.9, 124.5, 118.5, 111.6, 78.5, 60.4, 46.5, 30.9, 27.9, 23.4, 15.1. HRMS (ESI) m/z : Anal. calcd. for $[M+Na]^+$ $C_{34}H_{46}N_4NaO_{10}S$: 725.2827; found 725.2827.

General procedure for synthesis of inhibitors

A mixture of precursor (0.151 mmol) in CF_3CO_2H (3 mL) / CH_2Cl_2 (3 mL) was stirred at room temperature for 30 m. The volatile component was removed in vacuo, 1-Ethyl-3-(3-dimethylaminopropyl)carbodiimide (0.392 mmol), Hydroxy-benzotriazole hydrate (0.392 mmol), Capping group (0.362 mmol) were added in batches over 4 min to a solution of *N,N*-Diisopropylethylamine (0.754 mmol) in CH_2Cl_2 (10 mL) and the reaction mixture stirred at room temperature for overnight. The mixture was then poured in 1 N aq HCl solution and extracted with CH_2Cl_2 . The organic layer dried over magnesium sulfate, and then was purified by the column chromatography (CH_2Cl_2 / MeOH). The residue was obtained as solid.

Bis(4-((S)-1-((methoxycarbonyl)-L-valyl)pyrrolidine-2-carbox-amido)phenyl) sulfate (16, BMK-21057). Yield 85.5 mg (69%); 1H NMR (DMSO- d_6 , δ =2.5 ppm, 400 MHz): 10.30 (s, 2H), 7.72-7.71 (d, 4H), 7.39-7.32 (m, 6H), 4.44 (s, 2H), 4.05-4.02 (t, 2H), 3.81 (s, 2H), 3.63 (s, 2H), 3.52 (s, 6H), 2.19-2.08 (m, 2H), 1.99-1.89 (m, 8H), 1.26-1.23 (m, 2H), 0.94-0.88 (m, 12H). ^{13}C NMR (DMSO- d_6 , δ =39.52 ppm, 125 MHz): 170.7, 170.3, 156.8, 144.8, 138.7, 121.5,

120.3, 60.2, 57.9, 51.4, 47.2, 29.9, 29.4, 24.6, 18.9, 18.6. HRMS (ESI) m/z : Anal. calcd. for $[M+H]^+$ $C_{36}H_{49}N_6O_{12}S$: 789.3124; found 789.3129.

Bis(4-((S)-1-((methoxycarbonyl)-D-valyl)pyrrolidine-2-carbox-amido)phenyl sulfate (17, BMK-21013). Yield (58.0 mg, 86 %); 1H NMR (DMSO- d_6 , δ =2.5 ppm, 400 MHz): 10.00 (s, 2H), 7.74-7.72 (d, 4H), 7.42-7.34 (q, 6H), 4.42-4.40 (d, 2H), 4.11-4.07 (t, 2H), 3.79 (s, 2H), 3.63-3.60 (d, 2H), 3.54 (s, 6H), 2.13-1.91 (m, 10H), 0.89-0.86 (t, 10H), 0.80-0.78 (d, 1H), 0.72-0.70 (d, 1H). ^{13}C NMR (DMSO- d_6 , δ =39.52 ppm, 100 MHz): 170.69, 170.2, 156.9, 145.0, 138.6, 121.5, 120.5, 60.3, 58.0, 54.9, 51.6, 47.1, 29.7, 29.4, 24.3, 19.1, 18.3. HRMS (ESI) m/z : Anal. calcd. for $[M+Na]^+$ $C_{36}H_{48}N_6NaO_{12}S$: 811.2943; found 811.2941.

Bis(4-((S)-1-((R)-2-((methoxycarbonyl)amino)-2-phenylacetyl)-pyrrolidine-2-carboxamido)phenyl sulfate (18, BMK-21007). Yield 37.6 mg (59%); 1H NMR (DMSO- d_6 , δ =2.5 ppm, 400 MHz): 10.14 (s, 1H), 7.76-7.52 (m, 7H), 7.42-7.32 (m, 12H), 7.23-7.09 (m, 1H), 5.51-5.49 (d, 2H), 4.40-4.38 (d, 2H), 3.82 (br s, 2H), 3.54 (s, 6H), 3.20-3.18 (d, 2H), 2.04-1.80 (m, 8H). ^{13}C NMR (DMSO- d_6 , δ =39.52 ppm, 100 MHz): 170.6, 168.2, 156.4, 144.9, 138.7, 136.9, 128.6, 128.5, 128.1, 121.6, 120.5, 62.8, 62.8, 60.8, 56.7, 51.6, 46.9, 29.3, 29.1, 24.7. HRMS (ESI) m/z : Anal. calcd. for $[M+Na]^+$ $C_{42}H_{44}N_6NaO_{12}S$: 879.2630; found 879.2630.

Bis(4-(2-((S)-1-((R)-2-((methoxycarbonyl)amino)-2-phenylacetyl)-pyrrolidin-2-yl)-1H-imidazol-5-yl)phenyl sulfate (19, BMK-21016). Yield (56.1 mg, 43%); 1H NMR (DMSO- d_6 , δ =2.5 ppm, 400 MHz): 8.14 (s, 1H), 8.07 (s, 1H), 7.98-7.96 (d, 2H), 7.92-7.85 (q, 2H), 7.80-7.78 (d, 1H), 7.71-7.60 (m, 5H), 7.39 (s, 4H), 7.35-7.34 (d, 1H), 7.30-7.29 (d, 4H), 7.04 (s, 1H), 5.54-5.50 (t, 2H), 5.21-5.19 (m, 2H), 3.96-3.77 (m, 2H), 3.51 (s, 6H), 3.39-3.14 (m, 2H), 2.38-2.23 (m, 2H), 2.09-1.86 (m, 6H). ^{13}C NMR (DMSO- d_6 , δ =39.52 ppm, 100 MHz): 169.0, 158.6, 156.3, 149.2, 149.4, 136.8, 131.43, 128.68, 128.32, 128.12,

127.45, 127.25, 122.10, 115.93, 57.00, 53.48, 51.62, 47.00, 30.81, 24.14. HRMS (ESI) m/z : Anal. calcd. for $[M+H]^+$ $C_{46}H_{47}N_8O_{10}S$: 903.3130; found 903.3133.

Bis(4-(2-((S)-1-((methoxycarbonyl)-D-valyl)pyrrolidin-2-yl)-1H-imidazol-5-yl)phenyl) sulfate (20, BMK-21015). Yield 76.9 mg (74%); 1H NMR (DMSO- d_6 , δ =2.5 ppm, 400 MHz): 8.09 (s, 2H), 7.96-7.94 (d, 4H), 7.65-7.62 (d, 3H), 7.58-7.52 (m, 1H), 7.25-7.23 (d, 2H), 5.19-5.16 (q, 2H), 4.19-4.15 (t, 2H), 3.91-3.83 (m, 2H), 3.70-3.61 (m, 2H), 3.53 (s, 6H), 2.38-2.36 (t, 2H), 2.08-1.94 (m, 8H), 0.90-0.85 (q, 10H), 0.71-0.70 (d, 1H), 0.35-0.34 (d, 1H). ^{13}C NMR (DMSO- d_6 , δ =39.52 ppm, 100 MHz): 170.8, 156.8, 149.6, 149.6, 127.3, 122.0, 115.8, 57.8, 53.2, 51.6, 47.0, 30.9, 29.7, 24.4, 19.3, 17.8. HRMS (ESI) m/z : Anal. calcd. for $[M+H]^+$ $C_{40}H_{51}N_8O_{10}S$: 835.3443; found 835.3444.

Bis(4-(2-((S)-1-((methoxycarbonyl)-L-valyl)pyrrolidin-2-yl)-1H-imidazol-5-yl)phenyl) sulfate (21, BMK-21030). Yield 25 mg, (13%); 1H NMR (DMSO- d_6 , δ =2.5 ppm, 400 MHz): 11.88 (s, 2H), 7.88-7.81 (m, 4H), 7.52 (s, 2H), 7.39-7.37 (d, 4H), 7.29-7.27 (d, 2H), 5.07 (s, 2H), 4.08-3.99 (m, 2H), 3.80-3.74 (m, 4H), 3.54 (s, 6H), 2.14 (s, 2H), 1.99-1.91 (m, 6H), 1.86-1.76 (m, 2H), 0.89-0.83 (q, 12H). ^{13}C NMR (DMSO- d_6 , δ =39.52 ppm, 100 MHz): 173.5, 170.4, 170.2, 156.8, 147.9, 125.7, 121.2, 59.2, 58.0, 54.2, 51.5, 46.8, 30.9, 29.9, 24.3, 19.0, 18.5. HRMS (ESI) m/z : Anal. calcd. for $[M+H]^+$ $C_{40}H_{51}N_8O_{10}S$: 835.3443; found 835.3445.

Bis(3-((S)-1-((R)-2-((methoxycarbonyl)amino)-2-phenylacetyl)-pyrrolidine-2-carboxamido)phenyl) sulfate (22, BMK-21014). Yield 1.08 g (70%); 1H NMR (DMSO- d_6 , δ =2.5 ppm, 400 MHz): 10.25 (s, 1H), 7.88-7.85 (d, 3H), 7.72-7.70 (d, 2H), 7.63-7.61 (d, 2H), 7.50-7.47 (t, 2H), 7.40-7.30 (m, 8H), 7.16-7.10 (q, 2H), 5.50-5.48 (d, 2H), 4.38-4.36 (m, 2H), 3.81-3.73 (d, 2H), 3.52 (s, 6H), 3.20-3.17 (m, 2H), 2.02-1.79 (m, 8H). ^{13}C NMR (DMSO- d_6 , δ =39.52 ppm, 100 MHz): 170.8, 168.4, 149.9, 140.7, 137.2, 130.7, 128.6, 128.4, 128.0, 118.4,

115.5, 111.3, 60.7, 56.7, 51.6, 47.0, 29.2, 24.3. HRMS (ESI) m/z : Anal. calcd. for $[M+Na]^+$ $C_{42}H_{44}N_6NaO_{12}S$: 879.2630; found 879.2629.

Bis(3-((S)-1-((S)-2-((methoxycarbonyl)amino)-3,3-dimethyl-butanoyl)-pyrrolidine-2-carboxamido)phenyl) sulfate (23, BMK-21042). Yield 29.7 mg (22%); 1H NMR (DMSO- d_6 , δ =2.5 ppm, 400 MHz): 10.41-10.16 (d, 2H), 7.88-7.82 (d, 2H), 7.62-7.60 (d, 2H), 7.48-7.44 (t, 2H), 7.27-7.10 (q, 4H), 4.45-4.41 (t, 2H), 4.23-4.20 (d, 2H), 3.79-3.76 (m, 2H), 3.65-3.62 (m, 2H), 3.54 (s, 6H), 2.20-2.14 (m, 2H), 2.02-1.84 (m, 6H), 0.96 (s, 18H). ^{13}C NMR (DMSO- d_6 , δ =39.52 ppm, 125 MHz): 170.9, 169.6, 156.9, 149.9, 140.9, 130.7, 118.2, 115.2, 111.1, 60.3, 59.1, 51.5, 47.9, 34.7, 29.5, 26.4, 26.2, 24.8. HRMS (ESI) m/z : Anal. calcd. for $[M+Na]^+$ $C_{38}H_{52}N_6NaO_{12}S$: 839.3256; found 839.3255.

Bis(3-(2-((S)-1-((R)-2-((methoxycarbonyl)amino)-2-phenylacetyl)-pyrrolidin-2-yl)-1H-imidazol-5-yl)phenyl) sulfate (24, BMK-21019). Yield 97.2 mg (67%). 1H NMR (DMSO- d_6 , δ =2.5 ppm, 400 MHz): 12.05 (br s, 1H), 7.96 (s, 1H), 7.94-7.64 (m, 5H), 7.50 (s, 1H), 7.39-7.25 (m, 13H), 7.00-6.93 (d, 1H), 5.49-5.40 (m, 2H), 5.14-5.05 (d, 2H), 4.18-3.67 (m, 2H), 3.55 (s, 6H), 3.43-3.41 (t, 1H), 3.11 (s, 1H), 1.98-1.72 (m, 8H). ^{13}C NMR (DMSO- d_6 , δ =39.52 ppm, 100 MHz): 173.4, 172.1, 168.4, 156.0, 150.5, 149.6, 137.2, 130.6, 128.4, 127.7, 124.2, 123.6, 119.0, 116.3, 109.8, 72.3, 60.3, 58.1, 57.0, 55.2, 51.6, 46.7, 31.1, 29.2, 24.0. HRMS (ESI) m/z : Anal. calcd. for $[M+H]^+$ $C_{46}H_{47}N_8O_{10}S$: 903.3130; found 903.3133.

Bis(3-(2-((S)-1-((S)-2-((methoxycarbonyl)amino)-3,3-dimethyl-butanoyl)-pyrrolidin-2-yl)-1H-imidazol-5-yl)phenyl) sulfate (25, BMK-21032). Yield 43.8 mg (73%); 1H NMR (DMSO- d_6 , δ =2.5 ppm, 400 MHz): 8.07-7.83 (m, 1H), 7.78-7.71 (m, 4H), 7.66-7.63 (t, 1H), 7.57-7.40 (m, 3H), 7.29-7.21 (m, 2H), 7.08-7.06 (d, 1H), 5.42-5.05 (m, 2H), 4.21-4.19 (d, 2H), 3.81-3.68 (m, 4H), 3.54 (s, 6H), 2.18-2.08 (m, 3H), 2.02-1.66 (m, 5H), 0.94-0.88 (app br s, 18H).

^{13}C NMR (DMSO- d_6 , δ =39.52 ppm, 125 MHz): 172.7, 169.7, 156.9, 150.4, 130.5, 128.6, 127.4, 125.1, 124.5, 123.5, 119.6, 119.1, 116.4, 109.9, 83.4, 62.8, 59.2, 53.8, 52.5, 51.5, 47.5, 34.6, 30.9, 26.3, 24.4, 16.5. HRMS (ESI) m/z : Anal. calcd. for $[\text{M}+\text{H}]^+$ $\text{C}_{42}\text{H}_{55}\text{N}_8\text{O}_{10}\text{S}$: 863.3756; found 863.3757.

Bis(3-(2-((S)-1-((methoxycarbonyl)-L-valyl)pyrrolidin-2-yl)-1H-imidazol-5-yl)phenyl) sulfate (26, BMK-21025). Yield 60.8 mg (44%); ^1H NMR (DMSO- d_6 , δ =2.5 ppm, 400 MHz): 11.98 (br s, 1H), 7.98-7.96 (d, 1H), 7.77-7.75 (d, 3H), 7.71-7.69 (d, 1H), 7.59 (s, 1H), 7.53-7.45 (q, 3H), 7.42-7.38 (t, 1H), 7.28-7.26 (d, 1H), 7.21-7.18 (d, 1H), 5.06 (s, 2H), 4.05-4.01 (t, 2H), 3.86-3.76 (m, 4H), 3.53 (s, 6H), 2.12-2.07 (m, 4H), 1.94-1.87 (m, 6H), 0.91-0.84 (m, 8H), 0.81-0.80 (d, 4H). ^{13}C NMR (DMSO- d_6 , δ =39.52 ppm, 125 MHz): 170.4, 156.8, 150.4, 149.8, 131.1, 129.9, 127.8, 126.6, 123.9, 118.8, 116.8, 110.3, 57.7, 57.2, 54.7, 53.6, 51.3, 29.9. HRMS (ESI) m/z : Anal. calcd. for $[\text{M}+\text{H}]^+$ $\text{C}_{40}\text{H}_{51}\text{N}_8\text{O}_{10}\text{S}$: 835.3443; found 835.3442.

Bis(3-((S)-1-((R)-2-((methoxycarbonyl)amino)-2-phenylacetyl)-pyrrolidine-2-carboxamido)-2-methylphenyl) sulfate (27, BMK-21028). Yield 84.5 mg (85%); ^1H NMR (DMSO- d_6 , δ =2.5 ppm, 500 MHz): 9.73-9.56 (d, 2H), 7.76-7.58 (m, 2H), 7.48-7.21 (m, 15H), 7.12-6.67 (m, 1H), 5.52-5.43 (m, 2H), 4.65-4.47 (m, 2H), 3.85 (s, 1H), 3.75-3.62 (m, 1H), 3.55-3.50 (app br s, 6H), 3.17 (s, 2H), 2.16 (s, 6H), 2.00-1.73 (m, 8H). ^{13}C NMR (DMSO- d_6 , δ =39.52 ppm, 125 MHz): 170.4, 168.8, 156.1, 148.6, 138.2, 137.1, 128.6, 128.1, 126.8, 126.0, 125.3, 118.3, 60.6, 56.8, 51.6, 47.0, 29.1, 24.3, 11.3. HRMS (ESI) m/z : Anal. calcd. for $[\text{M}+\text{Na}]^+$ $\text{C}_{44}\text{H}_{48}\text{N}_6\text{NaO}_{12}\text{S}$: 907.2943; found 907.2940.

Bis(5-((S)-1-((R)-2-((methoxycarbonyl)amino)-2-phenylacetyl)-pyrrolidine-2-carboxamido)-2-methylphenyl) sulfate (28, BMK-21020). Yield 105 mg (74%). ^1H NMR (DMSO- d_6 , δ =2.5 ppm, 400 MHz): 10.36-10.19 (d, 2H), 7.94-7.89 (d, 2H), 7.75-7.67 (q, 2H), 7.58 (s, 2H), 7.42-7.41 (d, 3H), 7.36-7.07 (m,

9H), 5.52-5.47 (t, 2H), 4.47-4.38 (d, 2H), 3.82-3.66 (d, 2H), 3.53 (s, 6H), 3.18-3.09 (d, 2H), 2.22 (s, 6H), 1.99-1.78 (m, 8H). ¹³C NMR (DMSO-d₆, δ=39.52 ppm, 100 MHz): 170.6, 168.4, 156.1, 148.3, 138.5, 136.9, 132.0, 128.6, 128.1, 124.6, 118.5, 111.4, 60.7, 56.7, 51.6, 47.0, 29.3, 24.3, 15.3. HRMS (ESI) *m/z*: Anal. calcd. for [M+Na]⁺ C₄₄H₄₈N₆NaO₁₂S: 907.2943; found 907.2943.

3-((S)-1-((R)-2-((Methoxycarbonyl)amino)-2-phenylacetyl)-pyrrolidine-2-carboxamido)phenyl (4-((S)-1-((R)-2-((methoxy-carbonyl)-amino)-2-phenylacetyl)pyrrolidine-2-carboxamido)-phenyl) sulfate (29, BMK-21022). Yield (106.7 mg, 83 %); ¹H NMR (DMSO-d₆, δ=2.5 ppm, 400 MHz): δ 10.63-10.31/10.27/10.17 (m/s/s, 0.87H+0.5H+0.57H), 7.91-7.89 (d, 1H), 7.80-7.72 (m, 3H), 7.68-7.56 (m, 2H), 7.50-7.26 (m, 12H), 7.17-7.05 (m, 2H), 5.53-5.42/5.37-5.34/4.94-4.90 (m/t/t, 1.61H+0.19H+0.18H), 4.61-4.39 (m, 2H), 3.86-3.81 (qui, 1H), 3.73-3.66 (m, 1H), 3.54 (s, 6H), 3.22-3.17 (q, 1H), 3.13-3.09 (t, 1H), 2.32-2.14 (m, 1H), 2.07-1.76 (m, 8H), 1.23/0.85 (2 s, 0.30H+0.10H); ¹³C NMR (DMSO-d₆, δ=39.52 ppm, 100 MHz): δ 170.59, 168.40, 156.09, 149.89, 145.03, 140.74, 138.70, 137.21, 130.65, 128.62, 128.06, 121.61, 120.65, 118.31, 115.50, 111.35, 60.71, 56.71, 51.65, 46.98, 29.25, 24.30; HRMS (ESI) *m/z*: Anal. calcd. for [M+Na]⁺ C₄₂H₄₄N₆NaO₁₂S: 879.2630; found 879.2631.

3-((S)-1-((Methoxycarbonyl)-D-valyl)pyrrolidine-2-carboxamido)-phenyl (4-((S)-1-((methoxycarbonyl)-D-valyl)-pyrrolidine-2-carboxamido)phenyl) sulfate (30, BMK-21023). Yield (46.7 mg, 71 %); ¹H NMR (DMSO-d₆, δ=2.5 ppm, 400 MHz): δ 10.64/10.54/10.13/10.02 (4 s, 0.2H+0.2H+0.86H+0.82H), 7.87 (s, 1H), 7.76-7.73 (d, 2H), 7.61-7.59 (d, 2H), 7.51-7.36 (m, 5H), 7.14-7.08 (m, 1H), 4.43-4.39 (q, 2H), 4.12-4.07 (t, 2H), 3.79(s, 2H), 3.64-3.58 (q, 2H), 3.55-3.53 (app s, 6H), 3.48-3.45 (m, 1H), 2.16-2.08 (m, 2H), 2.04-1.92 (m, 8H), 0.89-0.86 (t, 10H), 0.80-0.77 (t, 1H), 0.72-0.68 (m, 1H); ¹³C NMR (DMSO-d₆, δ=39.52 ppm, 100

MHz): δ 171.01, 170.71, 170.24, 156.92, 149.85, 144.94, 140.71, 138.67, 130.61, 121.57, 120.50, 118.19, 115.42, 111.22, 60.32, 60.27, 58.01, 51.56, 47.11, 29.76, 29.41, 29.37, 24.39, 24.35, 19.09, 18.32; HRMS (ESI) m/z : Anal. calcd. for $[M+Na]^+$ $C_{36}H_{48}N_6NaO_{12}S$: 811.2943; found 811.2913.

Bis(2-fluoro-3-((S)-1-((R)-2-((methoxycarbonyl)amino)-2-phenyl-acetyl)pyrrolidine-2-carboxamido)phenyl) sulfate (31, BMK-21036).

Yield (41.0 mg, 49%); 1H NMR (DMSO- d_6 , δ =2.5 ppm, 400 MHz): δ 10.21 (s, 1H), 10.10 (s, 1H), 8.02-7.97 (q, 2H), 7.72-7.66 (q, 2H), 7.41-7.40 (m, 6H), 7.37-7.29 (m, 7H), 7.27-7.25/7.12-7.10 (2 d, 0.48H+0.35H), 5.51-5.45 (q, 2H), 4.69-4.67 (m, 1H), 4.57-4.55 (m, 1H), 3.81 (s, 1H), 3.71-3.65 (m, 1H), 3.53 (s, 6H), 3.20-3.14 (q, 1H), 3.10-3.08 (d, 1H), 2.18-2.16 (d, 1H), 2.03-1.78 (m, 7H), 1.23/0.85 (2 s, 2.02H+0.62H); ^{13}C NMR (DMSO- d_6 , δ =39.52 ppm, 126 MHz): δ 170.92, 168.45, 168.25, 156.33, 155.97, 136.74, 128.60, 128.38, 128.35, 127.99, 124.76, 123.15, 118.26, 118.03, 60.26, 56.65, 51.55, 46.85, 29.14, 24.69, 24.27; ^{19}F NMR (DMSO- d_6 , 376 MHz): δ -74.67, -139.84, -139.84; HRMS (ESI) m/z : Anal. calcd. for $[M+Na]^+$ $C_{42}H_{42}F_2N_6NaO_{12}S$: 915.2442; found 915.2445.

Bis(2-fluoro-5-((S)-1-((R)-2-((methoxycarbonyl)amino)-2-phenyl-acetyl)pyrrolidine-2-carboxamido)phenyl) sulfate (32, BMK-21024).

Yield (63.4 mg, 52 %); 1H NMR (DMSO- d_6 , δ =2.5 ppm, 400 MHz): δ 10.64/10.47/10.32/10.28 (4 s, 0.06H+0.3H+0.33H+1.19H), 8.13-8.01 (m, 2H), 7.87-7.72 (m, 2H), 7.65 (s, 2H), 7.55-7.50 (t, 2H), 7.42-7.29 (m, 8H), 7.25-7.23/7.06-7.03 (2 m, 0.52H+0.74H) 7.06-7.04 (t, 1H), 5.52-5.47/5.35-5.33/4.87-4.85 (m/d/d, 1.56H+0.26H+0.20H), 4.48-4.35 (m, 2H), 3.84-3.81 (m, 2H), 3.53 (s, 6H), 3.20-3.09 (m, 2H), 2.04-1.77 (m, 8H), 1.23/0.85 (2 s, 0.35H+0.07H); ^{13}C NMR (DMSO- d_6 , δ =39.52 ppm, 100 MHz): δ 170.71, 168.39, 156.07, 149.70, 147.73, 137.20, 136.26, 128.59, 128.03, 119.96, 117.92, 113.47, 60.69, 56.67, 51.63, 46.96, 29.21,

24.31; ^{19}F NMR (DMSO- d_6 , 376 MHz): δ -135.20; HRMS (ESI) m/z : Anal. calcd. for $[\text{M}+\text{Na}]^+ \text{C}_{42}\text{H}_{42}\text{F}_2\text{N}_6\text{NaO}_{12}\text{S}$: 915.2442; found 915.2443.

2-Fluoro-3-((S)-1-((R)-2-((methoxycarbonyl)amino)-2-phenylacetyl)-pyrrolidine-2-carboxamido)phenyl (2-fluoro-5-((S)-1-((R)-2-((methoxycarbonyl)amino)-2-phenylacetyl)-pyrrolidine-2-carboxamido)-phenyl) sulfate (33, BMK-21047). Yield (112 mg, 58%); ^1H NMR (DMSO- d_6 , $\delta=2.5$ ppm, 400 MHz): δ 10.46/10.27/10.21/10.11 (4 s, 0.57H+0.53H+0.32H+0.36H), 8.11-7.80 (m, 2H), 7.74-7.64 (m, 3H), 7.55-7.50 (t, 1H), 7.39-7.21 (m, 11H), 7.09-7.04 (d, 2H), 5.51-5.20/5.10-5.08/4.86-4.84 (m/d/d, 1.96H+0.06H+0.08H), 4.68/4.57-4.55/4.46-4.43/4.36-4.34 (4 m, 0.28H+0.40H+0.46H+0.62H), 3.81-3.67 (m, 2H), 3.52 (s, 6H), 3.17-3.08 (m, 2H), 2.27-2.16 (m, 1H), 1.99-1.80 (m, 7H), 1.23/0.85 (2 s, 0.31H+0.10H); ^{13}C NMR (DMSO- d_6 , $\delta=39.52$ ppm, 100 MHz): δ 170.92, 168.38, 156.30, 156.05, 149.85, 147.40, 137.16, 136.77, 136.25, 136.08, 128.58, 128.35, 128.01, 124.81, 123.48, 123.06, 119.72, 117.96, 117.78, 113.31, 60.67, 56.65, 51.54, 46.94, 29.18, 24.30; ^{19}F NMR (DMSO- d_6 , 376 MHz): δ -73.82, -135.52, -139.50, -139.97; HRMS (ESI) m/z : Anal. calcd. for $[\text{M}+\text{Na}]^+ \text{C}_{42}\text{H}_{42}\text{F}_2\text{N}_6\text{NaO}_{12}\text{S}$: 915.2442; found 915.2441.

Bis(2-fluoro-5-((S)-1-((methoxycarbonyl)-D-valyl)pyrrolidine-2-carboxamido)phenyl) sulfate (34, BMK-21027). Yield (77.7 mg, 80 %); ^1H NMR (DMSO- d_6 , $\delta=2.5$ ppm, 500 MHz): δ 10.63/10.15 (2 s, 0.35H+1.62H), 8.04 (s, 2H), 7.63-7.61 (d, 2H), 7.52-7.48 (t, 2H), 7.36-7.35 (d, 2H), 4.38-4.36 (d, 2H), 4.11-4.07 (t, 2H), 3.78-3.74 (m, 2H), 3.63-3.57 (m, 2H), 3.53 (s, 6H), 2.15-2.08 (m, 2H), 2.08-1.84 (m, 8H), 0.88-0.86 (t, 10H), 0.77-0.76 (d, 1H), 0.67-0.67 (d, 1H); ^{13}C NMR (DMSO- d_6 , $\delta=39.52$ ppm, 126 MHz): δ 170.87, 170.22, 156.93, 149.64, 147.66, 136.25, 120.42, 119.35, 117.33, 113.56, 113.09, 60.63, 59.92, 57.96, 51.42, 29.95, 24.44, 19.09, 18.29; ^{19}F NMR (DMSO- d_6 , 376 MHz):

δ -135.35; HRMS (ESI) m/z : Anal. calcd. for $[M+Na]^+$ $C_{36}H_{46}F_2N_6NaO_{12}S$: 847.2755; found 847.2752.

2-Fluoro-3-((S)-1-((methoxycarbonyl)-D-valyl)pyrrolidine-2-carboxamido)phenyl (2-fluoro-5-((S)-1-((methoxycarbonyl)-D-valyl)pyrrolidine-2-carboxamido)phenyl) sulfate (35, BMK-21048).

Yield (40.3 mg, 39%); 1H NMR (DMSO- d_6 , δ =2.5 ppm, 400 MHz): δ 10.64/10.45/10.16/9.97 (4 s, 0.16H+0.22H+0.81H+0.71H), 8.08-8.07 (d, 1H), 7.99-7.82 (m, 1H), 7.64-7.60 (m, 1H), 7.53-7.48 (t, 1H), 7.44-7.28 (m, 4H), 5.17-5.15/5.03-5.01/4.60-4.58 (3 d, 0.14H+0.16H+0.77H), 4.38-4.37 (d, 1H), 4.12-4.07 (t, 2H), 3.87-3.71 (m, 2H), 3.64-3.58 (m, 1H), 3.53-3.50 (app s, 6H), 3.46-3.45 (m, 1H), 2.21-2.09 (m, 2H), 1.99-1.81 (m, 8H), 1.23 (s, 0.32H), 0.89-0.66 (m, 12H); ^{13}C NMR (DMSO- d_6 , δ =39.52 ppm, 100 MHz): δ 170.90, 170.22, 156.84, 149.90, 147.44, 146.40, 143.89, 137.12, 136.06, 128.18, 124.71, 123.31, 119.81, 117.89, 113.39, 60.28, 58.00, 51.54, 47.09, 29.75, 24.38, 19.07, 18.30; ^{19}F NMR (DMSO- d_6 , 376 MHz): δ -134.98, -135.41, -138.11, -139.92; HRMS (ESI) m/z : Anal. calcd. for $[M+Na]^+$ $C_{36}H_{46}F_2N_6NaO_{12}S$: 847.2755; found 847.2754.

Bis(2-fluoro-3-((S)-1-((methoxycarbonyl)-D-valyl)pyrrolidine-2-carboxamido)phenyl) sulfate (36, BMK-21038). Yield (97.9 mg, 74%); 1H NMR (DMSO- d_6 , δ =2.5 ppm, 400 MHz): δ 10.45/10.14/9.97 (3 s, 0.33H+0.20H+1.44H), 7.98-7.81 (m, 2H), 7.48-7.29 (m, 6H), 5.17-5.15/4.60-4.58 (2 d, 0.27H+1.48H), 4.12-4.07 (t, 1H), 3.87-3.79 (m, 2H), 3.66-3.60 (m, 4H), 3.50 (s, 6H), 2.25-2.11 (m, 2H), 1.98-1.85 (m, 8H), 1.23 (s, 0.15H), 0.89-0.71 (m, 12H); ^{13}C NMR (DMSO- d_6 , δ =39.52 ppm, 100 MHz): δ 170.53, 156.87, 146.52, 144.01, 137.14, 128.15, 124.70, 123.42, 118.19, 59.91, 58.04, 51.45, 48.64, 47.13, 29.75, 29.16, 24.37, 19.08, 18.32; ^{19}F NMR (DMSO- d_6 , 376 MHz): δ -78.40, -142.54, -144.44; HRMS (ESI) m/z : Anal. calcd. for $[M+Na]^+$ $C_{36}H_{46}F_2N_6NaO_{12}S$: 847.2755; found 847.2757.

Bis(2-fluoro-5-(2-((S)-1-((methoxycarbonyl)-D-valyl)pyrro-lidin-2-yl)-1H-imidazol-5-yl)phenyl) sulfate (37, BMK-21046). Yield (34.5 mg, 52%); ¹H NMR (DMSO-d₆, δ=2.5 ppm, 400 MHz): δ 8.08-8.06 (d, 2H), 8.01 (s, 2H), 7.92-7.91 (d, 2H), 7.80 (s, 1H), 7.73-7.68 (t, 1H), 7.59-7.46 (m, 1H), 7.25-7.23 (d, 1H), 5.69-5.67/5.14-5.12 (2 d, 0.35H+1.32H), 4.17-4.13 (t, 2H), 3.87-3.86 (d, 2H), 3.68-3.62 (q, 2H), 3.53 (s, 6H), 2.32 (s, 2H), 2.08-1.67 (m, 8H), 1.23 (s, 0.47H), 0.90-0.29 (m, 12H); ¹³C NMR (DMSO-d₆, δ=39.52 ppm, 100 MHz): δ 170.71, 156.88, 149.66, 137.07, 136.94, 126.54, 120.06, 118.57, 115.78, 57.87, 53.48, 51.58, 46.95, 30.88, 29.69, 24.28, 19.25, 18.57, 18.41, 17.93; ¹⁹F NMR (DMSO-d₆, 376 MHz): δ -74.27; HRMS (ESI) m/z: Anal. calcd. for [M+H]⁺ C₄₀H₄₉F₂N₈O₁₀S: 871.3255; found 871.3256.

Bis(2-fluoro-5-(2-((S)-1-((methoxycarbonyl)-L-valyl)pyrro-lidin-2-yl)-1H-imidazol-5-yl)phenyl) sulfate (38, BMK-21044). Yield (90.1 mg, 48%); ¹H NMR (DMSO-d₆, δ=2.5 ppm, 400 MHz): δ 8.06-8.05 (d, 2H), 7.99 (s, 2H), 7.90-7.88 (d, 2H), 7.71-7.67 (t, 2H), 7.30-7.28 (d, 2H), 5.45/5.11-5.08 (m/t, 0.13H+1.99H), 4.10-4.06 (t, 2H), 3.86-3.76 (m, 4H), 3.53 (s, 6H), 2.32-2.28 (t, 2H), 2.14-2.10 (m, 2H), 2.07-1.94 (m, 6H), 1.23 (s, 0.46H), 0.81-0.75 (q, 12H); ¹³C NMR (DMSO-d₆, δ=39.52 ppm, 100 MHz): δ 170.95, 158.36, 158.03, 156.88, 149.87, 137.07, 136.93, 126.37, 119.84, 118.72, 118.55, 57.93, 53.34, 51.52, 47.05, 31.00, 29.30, 24.58, 19.13, 17.99; ¹⁹F NMR (DMSO-d₆, 376 MHz): δ -78.32, -138.05; HRMS (ESI) m/z: Anal. calcd. for [M+H]⁺ C₄₀H₄₉F₂N₈O₁₀S: 871.3255; found 871.3254.

Bis(2-fluoro-5-(2-((S)-1-((R)-2-((methoxycarbonyl)amino)-2-phenylacetyl)pyrrolidin-2-yl)-1H-imidazol-5-yl)phenyl) sulfate (39, BMK-21045). Yield (34.5 mg, 73%); ¹H NMR (DMSO-d₆, δ=2.5 ppm, 400 MHz): δ 8.11-8.03 (m, 4H), 7.98-7.93 (m, 2H), 7.79-7.71 (m, 2H),

7.68-7.64 (t, 2H), 7.39-7.34 (m, 6H), 7.29 (s, 2H), 6.99 (s, 2H), 5.65-5.63/5.50-5.49/5.40-5.38 (3 d, 0.51H+1.37H+0.49H), 5.17-5.16 (d, 2H), 3.93-3.82 (m, 2H), 3.53-3.51 (app s, 6H), 3.18-3.12 (q, 2H), 2.22-2.15 (m, 2H), 2.02-2.00 (d, 4H), 1.87 (s, 2H), 1.23 (s, 0.72H); ¹³C NMR (DMSO-d₆, δ=39.52 ppm, 100 MHz): δ 168.88, 155.95, 151.56, 149.53, 137.11, 136.95, 128.67, 128.27, 128.11, 127.78, 126.70, 120.27, 118.82, 118.63, 115.87, 56.99, 53.80, 51.61, 46.94, 30.91, 24.10; ¹⁹F NMR (DMSO-d₆, 376 MHz): δ -78.97, -133.12; HRMS (ESI) m/z: Anal. calcd. for [M+H]⁺ C₄₆H₄₅F₂N₈O₁₀S: 939.2942; found 939.2939.

3-(2-((S)-1-((R)-2-((Methoxycarbonyl)amino)-2-phenylacetyl)pyrrolidin-2-yl)-1H-imidazol-5-yl)phenyl (4-(2-((S)-1-((R)-2-((methoxycarbonyl)amino)-2-phenylacetyl)pyrrolidin-2-yl)-1H-imidazol-5-yl)phenyl) sulfate (40, BMK-21040). Yield (53.3 mg, 35%); ¹H NMR (DMSO-d₆, δ=2.5 ppm, 400 MHz): δ 8.19-8.06 (m, 2H), 7.98-7.96 (d, 2H), 7.91-7.83 (m, 2H), 7.73-7.64 (m, 5H), 7.39-7.25 (m, 10H), 7.03 (s, 1H), 5.53-5.49/5.45-5.43/5.40-5.38 (t/d/d, 1.51H+0.25H+0.18H), 5.18 (m, 2H), 3.91-3.85 (d, 1H), 3.80-3.71 (m, 1H), 3.54-3.51 (app br s, 6H), 3.46-3.38 (d, 1H), 3.17-3.15 (d, 1H), 2.37-2.22 (m, 2H), 2.08-1.89 (m, 6H), 1.23 (s, 0.20H); ¹³C NMR (DMSO-d₆, δ=39.52 ppm, 126 MHz): δ 168.99, 156.34, 155.97, 150.33, 149.40, 136.86, 131.50, 128.69, 128.62, 128.31, 128.12, 127.79, 127.44, 127.23, 124.83, 122.11, 122.06, 117.94, 115.90, 57.00, 56.73, 53.48, 51.62, 47.01, 30.88, 24.14; HRMS (ESI) m/z: Anal. calcd. for [M+H]⁺ C₄₆H₄₇N₈O₁₀S: 903.3130; found 903.3130.

3-(2-((S)-1-((Methoxycarbonyl)-D-valyl)pyrrolidin-2-yl)-1H-imidazol-5-yl)phenyl (4-(2-((S)-1-((methoxycarbonyl)-D-valyl)-pyrrolidin-2-yl)-1H-imidazol-5-yl)phenyl) sulfate (41, BMK-21043). Yield (107 mg, 86%); ¹H NMR (DMSO-d₆, δ=2.5 ppm, 400 MHz): δ 8.13-8.08 (d, 2H), 7.95-7.87 (m, 4H), 7.78-7.63 (m, 3H), 7.54-7.48 (m, 1H), 7.30-7.23 (m, 2H), 5.80-5.74/5.19-5.10 (d/m, 0.25H+1.73H), 4.18-4.07 (m, 2H), 3.88-

3.78 (m, 2H), 3.68-3.66 (d, 2H), 3.53 (s, 6H), 2.36 (s, 2H), 2.08-1.96 (m, 8H), 1.23 (s, 0.39H), 0.90-0.68 (m, 12H), 0.33 (s, 1H); ¹³C NMR (DMSO-d₆, δ=39.52 ppm, 100 MHz): δ 170.80, 158.49, 158.15, 156.87, 150.32, 149.57, 131.43, 127.33, 124.70, 122.08, 120.79, 117.78, 116.21, 115.85, 57.84, 53.19, 51.59, 47.00, 30.89, 29.70, 24.34, 19.28, 17.89; HRMS (ESI) m/z: Anal. calcd. for [M+H]⁺ C₄₀H₅₁N₈O₁₀S: 835.3443; found 835.3446.

3-(2-((S)-1-((Methoxycarbonyl)-L-valyl)pyrrolidin-2-yl)-1H-imidazol-5-yl)phenyl 4-(2-((S)-1-((methoxycarbonyl)-L-valyl)-pyrrolidin-2-yl)-1H-imidazol-5-yl)phenyl sulfate (42, BMK-21039). Yield (110 mg, 54%); ¹H NMR (DMSO-d₆, δ=2.5 ppm, 400 MHz): δ 12.37-12.39/12.16-12.13/11.92-11.86 (3 d, 0.14H+0.18H+1.51H), 7.85-7.83 (d, 2H), 7.76-7.73 (m, 2H), 7.61 (s, 1H), 7.54 (s, 1H), 7.48-7.44 (t, 1H), 7.39-7.36 (d, 2H), 7.31-7.26 (t, 2H), 7.19-7.16 (q, 1H), 5.22/5.08-5.03 (2 m, 0.14H+1.86H), 4.11-4.00 (m, 2H), 3.78 (s, 2H), 3.53 (s, 6H), 3.17-3.16 (d, 1H), 2.13 (s, 4H), 1.94-1.87 (m, 6H), 0.89-0.80 (m, 12H); ¹³C NMR (DMSO-d₆, δ=39.52 ppm, 126 MHz): δ 170.35, 156.77, 150.39, 149.67, 147.82, 137.76, 135.00, 130.43, 125.64, 123.38, 121.04, 117.89, 116.19, 113.71, 113.19, 57.99, 54.18, 51.44, 48.61, 46.79, 30.96, 30.87, 29.84, 24.26, 18.51; HRMS (ESI) m/z: Anal. calcd. for [M+H]⁺ C₄₀H₅₁N₈O₁₀S: 835.3443; found 835.3445.

Methyl ((R)-2-((S)-2-((3-hydroxyphenyl)carbamoyl)pyrrolidin-1-yl)-2-oxo-1-phenylethyl)carbamate (43a). Yield (839 mg, 79%); ¹H NMR (DMSO-d₆, δ=2.5 ppm, 400 MHz): δ 10.00/9.86/9.73 (3 s, 0.20H+0.14H+0.72H), 9.37 (s, 1H), 7.98-7.97/7.71-7.69/7.55-7.52 (d/d/m, 0.34H+0.86H+0.41H), 7.42-7.30 (m, 4H), 7.20/7.15-7.13 (s/t, 0.70H+0.39H), 7.09-7.05 (t, 1H), 7.00-6.85/6.87-6.85 (2 d, 0.73H+0.19H), 6.47-6.45 (d, 1H), 5.51-5.49/5.33-5.31/4.92-4.89 (3 d, 0.74H+0.21H+0.19H), 4.39-4.37 (t, 1H), 3.81 (s, 1H), 3.54 (s, 3H), 3.21-3.15 (q, 1H), 2.33-1.77 (m, 4H); ¹³C NMR (DMSO-d₆, δ=39.52 ppm, 126

MHz): δ 170.09, 168.34, 157.61, 156.07, 140.03, 137.20, 129.31, 128.61, 128.04, 110.42, 110.04, 106.48, 60.69, 56.71, 51.64, 46.95, 29.34, 24.25; HRMS (ESI) m/z : Anal. calcd. for $[M+Na]^+$ $C_{21}H_{23}N_3NaO_5$: 420.1530; found 420.1531.

Methyl ((S)-1-((S)-2-(5-(3-hydroxyphenyl)-1H-imidazol-2-yl)pyrrolidin-1-yl)-3-methyl-1-oxobutan-2-yl)carbamate (43b). Yield (455 mg, 64 %); 1H NMR (DMSO- d_6 , δ =2.5 ppm, 500 MHz): δ 11.67 (app br s, 1H), 9.44 (app br s, 1H), 7.36-7.25 (m, 2H), 7.17-6.86 (m, 3H), 6.56 (s, 1H), 5.24-5.23/5.08-5.07 (2 d, 0.13H+0.81H), 4.08-4.05 (t, 1H), 3.80-3.76 (d, 2H), 3.54-3.44 (app s, 3H), 2.27-2.08 (m, 2H), 2.01-1.86 (m, 3H), 0.89-0.84 (q, 6H); ^{13}C NMR (DMSO- d_6 , δ =39.52 ppm, 126 MHz): δ 170.43, 157.61, 156.85, 129.33, 115.06, 113.06, 111.10, 58.05, 57.54, 55.19, 54.25, 51.47, 46.87, 30.92, 29.88, 24.31, 19.04, 18.53; HRMS (ESI) m/z : Anal. calcd. for $[M+H]^+$ $C_{20}H_{27}N_4O_4$: 387.2027; found 387.2029.

3-((S)-1-((R)-2-((Methoxycarbonyl)amino)-2-phenylacetyl)-pyrrolidine-2-carboxamido)phenyl sulfurofluoridate (43c). A mixture of Methyl ((R)-2-((S)-2-((3-hydroxyphenyl)carbamoyl)-pyrrolidin-1-yl)-2-oxo-1-phenylethyl)carbamate (276 mg, 0.695 mmol) and *N,N*-Diisopropylethylamine (363 μ L, 2.09 mmol) in CH_2Cl_2 (10 mL) was stirred under sulfuryl fluoride at room temperature for 5 h. The mixture was then poured in 1 N aq HCl solution and extracted with CH_2Cl_2 . The organic layer dried over magnesium sulfate, filtered, and concentrated in vacuo. Without any purification, the residue was obtained as a white oil; Yield (255 mg, 76%); 1H NMR (DMSO- d_6 , δ =2.5 ppm, 400 MHz): δ 10.58/10.51/10.41/10.34 (4 s, 0.02H+0.23H+0.11H+0.53H), 7.99-7.86 (m, 1H), 7.74-7.66 (m, 1H), 7.63-7.59 (t, 1H), 7.56-7.52 (t, 1H), 7.42-7.41 (d, 2H), 7.38-7.35 (t, 2H), 7.34-7.32 (m, 1H), 7.29-7.24/7.06-7.05/6.72-6.70 (m/d/d, 0.88H+0.28H+0.06H), 5.52-5.47/5.35-5.33/4.90-4.88 (m/d/d, 0.88H+0.08H+0.08H), 4.50-4.38 (m, 1H), 3.83-3.62 (m, 1H),

3.54 (s, 3H), 3.20-3.10 (m, 1H), 2.29-1.78 (m, 4H); ^{13}C NMR (DMSO- d_6 , δ =39.52 ppm, 100 MHz): δ 170.95, 168.40, 156.06, 149.63, 140.92, 137.15, 130.98, 128.58, 128.39, 128.02, 119.34, 115.34, 111.06, 60.69, 56.66, 51.59, 46.94, 29.17, 24.28; ^{19}F NMR (DMSO- d_6 , 376 MHz): 38.64; HRMS (ESI) m/z : Anal. calcd. for $[\text{M}+\text{Na}]^+$ $\text{C}_{21}\text{H}_{22}\text{FN}_3\text{NaO}_7\text{S}$: 502.1055; found 502.1054.

Methyl ((S)-1-((S)-2-(5-(3-((tert-butyldimethylsilyl)oxy)-phe-nyl)-1H-imidazol-2-yl)pyrrolidin-1-yl)-3-methyl-1-oxobutan-2-yl)carbamate

(43d). A mixture of Methyl ((S)-1-((S)-2-(5-(3-hydroxyphenyl)-1H-imidazol-2-yl)pyrrolidin-1-yl)-3-methyl-1-oxobutan-2-yl)carbamate (158 mg, 0.409 mmol), *tert*-Butyldimethylsilyl chloride (123 mg, 0.817 mmol), Imidazole (139 mg, 2.04 mmol) in CH_2Cl_2 (10 mL) was stirred at room temperature for 4 h. The mixture was then poured in H_2O and extracted with CH_2Cl_2 . The organic layer dried over magnesium sulfate, and then was purified by the column chromatography (n-hexane / ethyl acetate). The residue was obtained as sticky white oil; Yield (187 mg, 91%); ^1H NMR (DMSO- d_6 , δ =2.5 ppm, 400 MHz): δ 12.12/12.03/11.77 (3 s, 0.16H+0.09H+0.68H), 7.44-7.06 (m, 5H), 6.69-6.60 (m, 1H), 5.06-5.05 (d, 1H), 4.08-4.04 (t, 1H), 3.79 (s, 2H), 3.53 (s, 3H), 2.16-2.07 (m, 2H), 1.96-1.89 (m, 3H), 0.96 (s, 9H), 0.92-0.90 (d, 2H), 0.88-0.82 (q, 4H), 0.18 (s, 6H); ^{13}C NMR (DMSO- d_6 , δ =39.52 ppm, 126 MHz): δ 170.30, 156.78, 155.24, 149.15, 138.83, 136.71, 129.36, 117.49, 117.08, 115.60, 112.41, 57.96, 54.21, 51.42, 46.80, 31.01, 29.84, 25.61, 24.13, 19.01, 18.56, 17.96; HRMS (ESI) m/z : Anal. calcd. For $[\text{M}+\text{H}]^+$ $\text{C}_{26}\text{H}_{41}\text{N}_4\text{O}_4\text{Si}$: 501.2892; found 501.2894.

3-(2-((S)-1-((Methoxycarbonyl)-L-valyl)pyrrolidin-2-yl)-1H-imidazol-5-yl)phenyl (3-((S)-1-((R)-2-((methoxycarbonyl)-amino)-2-phenyl-acetyl)pyrrolidine-2-carboxamido)phenyl) sulfate (43, BMK-21060). A mixture of 3-((S)-1-((R)-2-((Methoxycarbonyl)-amino)-2-

phenylacetyl)pyrrolidine-2-carboxamido)phenyl sulfurofluoridate (88.9 mg, 0.178 mmol), Methyl ((*S*)-1-((*S*)-2-(5-(3-((*tert*-butyldimethylsilyl)oxy)phenyl)-1H-imidazol-2-yl)pyrrolidin-1-yl)-3-methyl-1-oxobutan-2-yl)carbamate (102 mg, 0.213 mmol) and DBU (34.5 μ L, 0.230 mmol) in DMF (10 mL) was stirred at 50°C for 12 h. The mixture was then poured in water and extracted with CH₂Cl₂. The organic layer dried over magnesium sulfate, and then crude product was purified by the column chromatography (n-hexane / ethyl acetate). The residue was obtained as white solid; Yield (97.1 mg, 65%); ¹H NMR (DMSO-d₆, δ =2.5 ppm, 500 MHz): δ 11.95 (s, 1H), 10.46/10.28 (2 s, 0.56H+0.31H), 7.92-7.88 (d, 1H), 7.82-7.72 (m, 2H), 7.66-7.63 (m, 1H), 7.61-7.58 (t, 1H), 7.49-7.46 (t, 1H), 7.41-7.40 (d, 2H), 7.38-7.35 (t, 1H), 7.33-7.25 (m, 3H), 7.22-7.20 (d, 1H), 7.12-7.08 (t, 1H), 7.03-6.63 (m, 1H), 5.51-5.46/5.32-5.31/5.22-5.20 (m/d/d, 0.76H+0.06H+0.11H), 5.07-5.04/4.90-4.88 (m/d, 0.80H+0.05H), 4.49-4.37 (m, 1H), 4.06-4.03 (t, 1H), 3.79-3.65 (m, 2H), 3.53 (s, 6H), 3.45-3.39 (m, 1H), 3.23-3.08 (m, 1H), 2.19-2.08 (m, 2H), 1.95-1.94 (d, 2H), 1.92-1.85 (m, 2H), 1.65-1.55 (m, 3H), 1.23 (s, 0.81H) 0.87-0.81 (m, 6H); ¹³C NMR (DMSO-d₆, δ =39.52 ppm, 126 MHz): δ 170.76, 170.34, 168.34, 168.15, 156.77, 156.29, 150.38, 149.89, 140.83, 136.78, 130.62, 130.49, 128.56, 128.33, 128.00, 127.75, 123.42, 118.12, 116.18, 115.30, 111.13, 60.59, 57.96, 56.60, 54.15, 51.41, 46.79, 30.96, 29.83, 29.20, 24.69, 24.19, 18.83, 18.48; HRMS (ESI) m/z: Anal. calcd. for [M+H]⁺ C₄₁H₄₈N₇O₁₁S: 846.3127; found 846.3129.

Methyl ((*R*)-2-((*S*)-2-((3-((*tert*-butyldimethylsilyl)oxy)-*phe-nyl*)carbamoyl)pyrrolidin-1-yl)-2-oxo-1-phenylethyl)-carbamate (44a). A mixture of methyl ((*R*)-2-((*S*)-2-((3-Hydroxyphenyl)carbamoyl)pyrrolidin-1-yl)-2-oxo-1-phenyl-ethyl)carbamate (51.1 mg, 0.129 mmol), *tert*-Butyldimethylsilyl chloride (29.1 mg, 0.193 mmol), imidazole (26.3 mg, 0.0263 mmol) in CH₂Cl₂ (10 mL) was stirred at room temperature for 4 h. The mixture was then poured in H₂O and extracted with CH₂Cl₂. The

organic layer dried over magnesium sulfate, and then was purified by the column chromatography (n-hexane / ethyl acetate). The residue was obtained as sticky white oil; Yield (53.5 mg, 81%); ^1H NMR (DMSO- d_6 , $\delta=2.5$ ppm, 500 MHz): δ 10.08/9.82 (2 s, 0.18H+0.81H), 7.97-7.96/7.71-7.69 (2 d, 0.13H+0.81H), 7.41-7.31 (m, 4H), 7.26 (s, 1H), 7.17-6.97 (m, 2H), 6.54 (s, 1H), 5.50-5.48/5.32-5.30/4.90-4.88 (3 d, 0.84H+0.14H+0.13H), 4.37 (s, 1H), 3.81 (s, 1H), 3.53 (s, 3H), 3.18-3.16 (d, 1H), 1.98-1.77 (m, 4H), 0.96-0.95 (app s, 9H), 0.20-0.19 (app s, 6H); ^{13}C NMR (DMSO- d_6 , $\delta=39.52$ ppm, 126 MHz): δ 170.21, 168.29, 156.01, 155.28, 140.18, 137.15, 129.46, 128.56, 128.00, 127.70, 114.58, 112.27, 110.74, 60.67, 56.66, 51.58, 46.90, 29.26, 25.54, 24.22, 17.89, -4.50; HRMS (ESI) m/z : Anal. calcd. for $[\text{M}+\text{Na}]^+ \text{C}_{27}\text{H}_{37}\text{N}_3\text{NaO}_5\text{Si}$: 534.2395; found 534.2396.

***tert*-Butyl (S)-2-((3-(((3-((S)-1-((R)-2-((methoxycarbonyl)-amino)-2-phenyl-acetyl)pyrrolidine-2-carboxamido)phenoxy)-sulfonyl)oxy)phenyl)carbamoyl)pyrrolidine-1-carboxylate (44b).** A mixture of Methyl ((R)-2-((S)-2-((3-((*tert*-butyldimethylsilyl)-oxy)phenyl)carbamoyl)pyrrolidin-1-yl)-2-oxo-1-phenylethyl)-carbamate (602 mg, 1.18 mmol), *tert*-Butyl (S)-2-((3-((fluorosulfonyl)oxy)phenyl)carbamoyl)pyrrolidine-1-carboxylate (914 mg, 0.235 mmol) and DBU (35.2 μL , 0.235 mmol) in DMF (10 mL) was stirred at 50°C for 12 h. The mixture was then poured in 1 N aq HCl solution and extracted with CH_2Cl_2 . The organic layer dried over magnesium sulfate, and then was purified by the column chromatography (n-hexane / ethyl acetate). The residue was obtained as white solid; Yield (676 mg, 75%); ^1H NMR (DMSO- d_6 , $\delta=2.5$ ppm, 500 MHz): δ 10.44-10.25 (m, 2H), 7.94-7.90 (t, 2H), 7.73-7.71 (d, 1H), 7.66-7.57 (m, 2H), 7.49-7.45 (m, 2H), 7.42-7.40 (d, 2H), 7.38-7.24 (m, 3H), 7.14-7.04 (m, 2H), 5.52-5.47/5.35-5.33/4.91-4.89 (m/d/d, 0.83H+0.10H+0.09H), 4.51-4.38 (m, 1H), 4.27-4.25/4.20-4.17 (d/q, 0.35H+0.64H), 4.14-4.10 (q, 1H), 3.82 (s, 1H), 3.53 (s, 3H), 3.46-3.42 (m, 1H), 3.37-3.34 (m, 1H) 3.19-3.17 (d, 3H), 2.24-2.13 (m, 1H), 2.05-1.78 (m, 7H),

1.39-1.24 (app s, 9H); ^{13}C NMR (DMSO- d_6 , δ =39.52 ppm, 126 MHz): δ 172.03, 170.78, 168.35, 153.06, 149.85, 140.74, 130.66, 128.57, 128.34, 128.00, 118.40, 115.34, 111.40, 78.60, 60.46, 56.64, 51.61, 46.56, 30.91, 29.19, 27.89, 24.27, 23.39; HRMS (ESI) m/z : Anal. calcd. for $[\text{M}+\text{Na}]^+ \text{C}_{37}\text{H}_{43}\text{N}_5\text{NaO}_{11}\text{S}$: 788.2572; found 788.2575.

3-((*S*)-1-((*R*)-2-((Methoxycarbonyl)amino)-2-phenylacetyl)-pyrrolidine-2-carboxamido)phenyl (3-((*S*)-1-(5-((3*aS*,4*S*,6*aR*)-2-oxohexahydro-1*H*-thieno[3,4-*d*]imidazol-4-yl)pentanoyl)-pyrrolidine-2-carboxamido)phenyl) sulfate (44, BMK-21057). A mixture of *tert*-Butyl (*S*)-2-((3-(((3-((*S*)-1-((*R*)-2-((methoxycarbonyl)amino)-2-phenylacetyl)pyrrolidine-2-carboxamido)phenoxy)sulfonyl)-oxy)phenyl)carbamoyl)pyrrolidine-1-carboxylate (426 mg, 0.557 mmol) in $\text{CF}_3\text{CO}_2\text{H}$ (5 mL) / CH_2Cl_2 (5 mL) was stirred at room temperature for 30 m. The volatile component was removed in vacuo, 1-Ethyl-3-(3-dimethylaminopropyl)-carbodiimide (139 mg, 0.724 mmol), Hydroxybenzotriazole hydrate (97.8 mg, 0.724 mmol), 5-[(3*aS*,4*S*,6*aR*)-2-Oxohexahydro-1*H*-thieno[3,4-*d*]imidazol-4-yl]pentanoic acid (163 mg, 0.668 mmol) were added in batches over 4 min to a solution of *N,N*-Diisopropylethylamine (485 μL , 2.78 mmol) in CH_2Cl_2 (10 mL) and the reaction mixture stirred at room temperature for overnight. The mixture was then poured in 1 N aq HCl solution and extracted with CH_2Cl_2 . The organic layer dried over magnesium sulfate, and then was purified by the column chromatography (n-Hexane / EA). The residue was obtained as white solid; Yield (479 mg, 96 %); ^1H NMR (DMSO- d_6 , δ =2.5 ppm, 500 MHz): δ 10.52/10.45/10.36/10.27 (4 s, 0.38H+0.53H+0.89H+0.31H), 7.91-7.84 (m, 2H), 7.75-7.58 (m, 3H), 7.50-7.44 (m, 2H), 7.41-7.29 (m, 5H), 7.23-7.04 (m, 2H), 6.44 (s, 1H), 6.39-6.34 (t, 1H), 5.50-5.45/5.32-5.30/5.21-5.19/5.09/4.88-4.87 (q/d/d/s/d, 0.84H+0.07H+0.05H+0.03H+0.10H), 4.54-4.25 (m, 4H), 4.13-4.07 (m, 1H), 3.81-3.56 (m, 3H), 3.53 (s, 3H), 3.20-3.00 (m, 2H), 2.82-2.74 (m,

1H), 2.58-2.56 (d, 1H), 2.33-2.26 (m, 2H), 2.17-2.12 (m, 1H), 2.17-1.96 (m, 2H), 1.91-1.81 (m, 5H), 1.64-1.58 (m, 1H), 1.51-1.44 (m, 3H), 1.40-1.33 (m, 2H), 1.23 (s, 1H); ¹³C NMR (DMSO-d₆, δ=39.52 ppm, 126 MHz): δ 171.41, 170.81, 168.35, 162.71, 156.31, 149.87, 140.88, 136.79, 130.62, 128.57, 128.33, 128.00, 118.22, 115.23, 113.71, 111.17, 61.05, 60.61, 60.01, 59.19, 56.61, 55.47, 51.53, 46.93, 33.35, 29.47, 29.20, 28.20, 24.46, 24.24; HRMS (ESI) m/z: Anal. calcd. for [M+Na]⁺ C₄₂H₄₉N₇NaO₁₁S₂: 915.0012; found 914.2826.

Biological Studies

Measurement of the anti-HCV activities of compounds using HCVcc

Cell line and cell culture

Huh 7.5.1 cells were grown in Dulbecco's Modified Eagle's medium (DMEM; Gibco) containing antibiotics (100 U/mL penicillin, 10 µg/mL streptomycin) and 10% heat-inactivated fetal bovine serum (ΔFBS; Hyclone) at 37°C in a humidified 6.0% CO₂ incubator.

Virus production

In vitro transcribed RNA of JFH5a-Rluc-ad34, which is a derivative of JFH1 with adaptive mutations in the E2 and p7 regions,^[74] was transfected into Huh7.5.1 cells by electroporation. JFH5a-Rluc-ad34 virus contains a reporter *Renilla* luciferase (Rluc) for convenient virus proliferation assay.^[74] HCV-containing cell culture media were collected 3~5 days after electroporation and filtered through a 0.45 µM pore size filter.

Antiviral activity test with infectious HCV particles

Huh 7.5.1 cells were inoculated with a JFH5a-Rluc-ad34 virus stock and cultivated for 3 h. At 3 h after the virus inoculation, HCV-infected Huh7.5.1 cells were cultured with media containing serially diluted compounds. At 3 days after the chemical treatment, the cells were harvested and their luciferase activities were measured using a *Renilla* luciferase assay system (Promega) according to the manufacturer's direction. Finally, the luciferase activities were normalized to those obtained from mock-treated cells.

Measurement of anti-HCV activities of compounds using HCV replicon

Cell line and cell culture

Huh 7.5.1 cells containing a bicistronic HCV replicon NK5.1-Gluc cell line (genotype 1b) were employed for the interrogation of the anti-HCV activities of the compounds (Figure 7). The first open reading frame (ORF) of the replicon contains the Gaussia luciferase gene fused with foot-and-mouth disease virus (FMDV) 2a gene and the neomycin phosphotransferase gene, and the second ORF contains HCV nonstructural genes NS3-5. The replicon-containing cells were cultivated under the same conditions as described above in presence of an additional antibiotic G418 (0.5 mg/ml, Calbiochem).

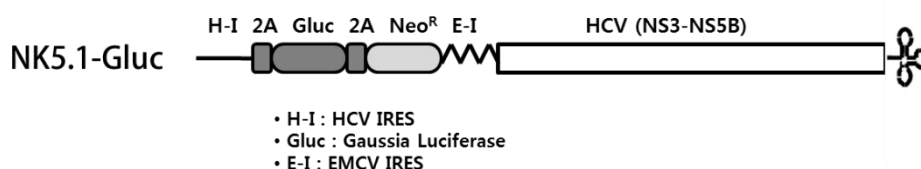


Figure 7. The structure of replicon NK5.1-Gluc.

Antiviral activity assay test with HCV replicon

Huh 7.5.1 cells containing HCV replicon (NK5.1-Gluc) were planted on a 12-well plate (Figure 7). At 16 h after cultivation, the replicon containing NK/R2AN-containing cells were incubated with media containing serially diluted compounds for 3 days. After the chemical treatment, the cell culture media were collected and luciferase activities were measured through the use of the *Renilla* luciferase assay system (Promega) according to manufacturer's direction, and then normalized to those obtained from mock-treated cells.

hERG ligand binding assay^[75]

The hERG ligand binding assay was performed by using the hERG Fluorescence Polarization Assay Kit (Cat No. PV5365), containing predictorTM hERG tracer red, predictorTM hERG membrane, and predictorTM hERG FP assay buffer. Test compounds (10 μ M) and positive control (Astemizole) were added to the 384-well plate (5 μ L each; low-volume polystyrene plate, corning #3677). Then, membrane (10 μ L) and tracer (5 μ L) were added to each plate through the use of a multi-pipette (Multi 16 channel pipette type 5–50 μ L, Thermo). The plate was then covered with aluminum foil and was kept for 2–3 h at room temperature. Lastly, the fluorescence polarization of the hERG red tracer was measured using a microplate reader (molecular devices, SpectraMax M5e, excitation (540 nm) emission (585 nm) filters).

Plasma stability measurement

Rat plasma (297 μ L) was pre-incubated for 5 min at 37°C in a water bath. The plasma and 100 μ M test compounds (3.0 μ L) were agitated through the use of a vortex, and incubated for 37°C in a water bath. Then the mixture was sampled multiple times (0, 15, 30, 60, and 120 min). A mixture of crude sample (50 μ L) and acetonitrile (100 μ L) was then treated by centrifugation at 10,000 rpm for 10 min at 25°C. Finally, the supernatant was isolated and analyzed using a LC-MS/MS.

Ames test^[61]

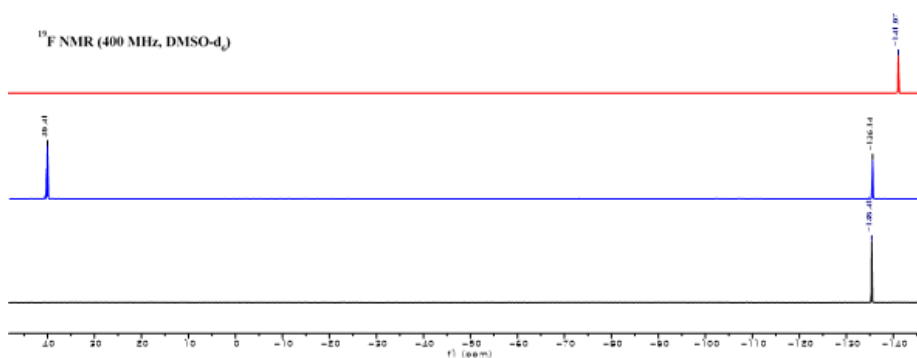
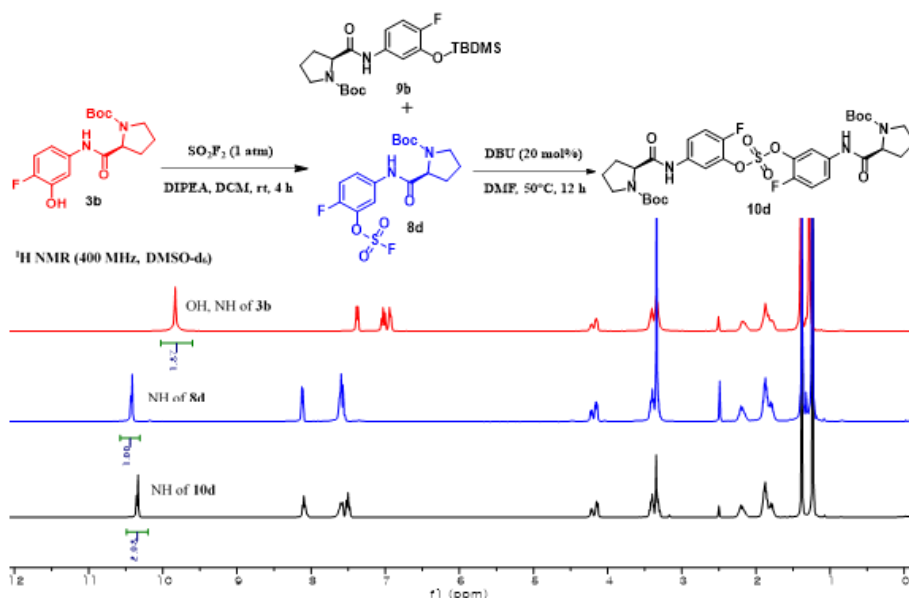
The Ames test was carried out with the Maron's method using Ames MPF™ 98/100 Mutagenicity Assay kit. Histidine-dependent strains (TA98, and TA100) of *Salmonella typhimurium* were treated with inhibitors **BMK-21014** and **BMK-21025** at 1,000 µg/plate and bis(4-aminophenyl) sulfate at 5,000 µg/plate and with positive controls (2-nitrofluorene, sodium azide, and benzo[a]pyrene). The number of colonies was counted three times for each medium to provide acceptable data for statistical analysis.

Observation of the effects of co-treatment of two compounds

Huh 7.5.1 cells containing the HCV replicon (NK5.1-Gluc) were plated on a 12-well plate (5×10^4 cells per well). At 16 h after cultivation, the replicon containing cells were treated with inhibitors alone or with mixtures of inhibitors and sofosbuvir at serially diluted concentrations. At 3 days after treatment, Gaussia luciferase activities were measured using the Renilla luciferase assay system (Promega) according to the manufacturer's direction, and then normalized to those obtained from mock-treated cells. Combination index was calculated by using Compusyn Freeware Program (ComboSyn, Inc).

Molecular docking

The X-ray structure of 3FQQ and NMR structure of 1R7G were retrieved from the protein data bank (PDB) and prepared via homology modeling with Discovery Studio Client. The default ligand settings were used to prepare all tautomers, and further energy minimized. The inhibitors were then docked into each of the NS5A dimer models using the CDOCKER



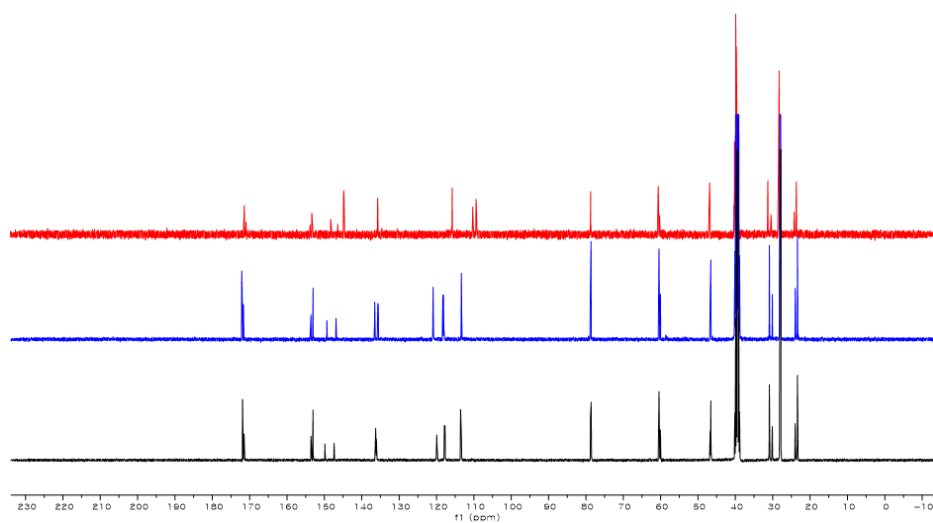
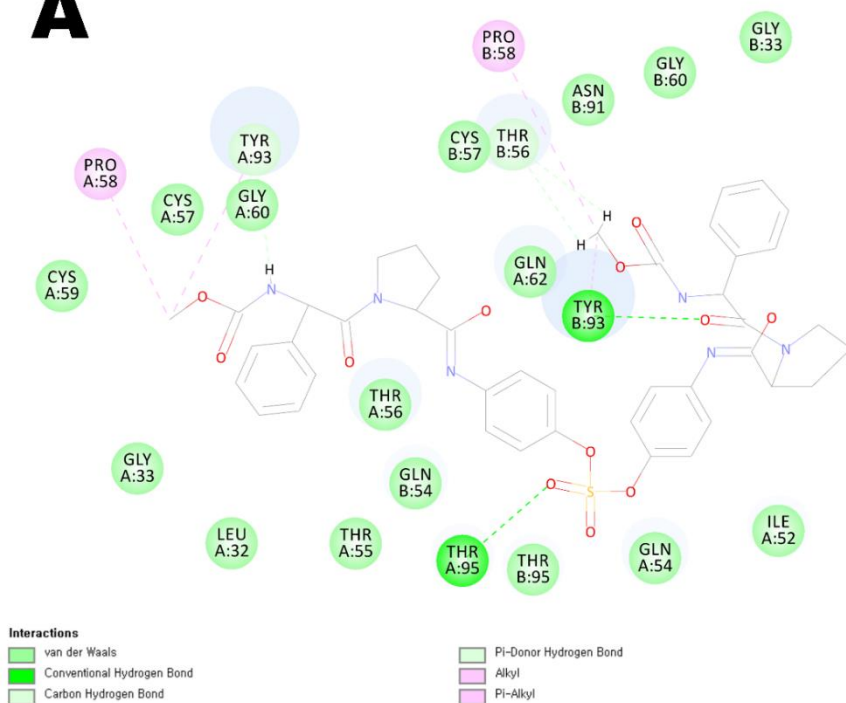
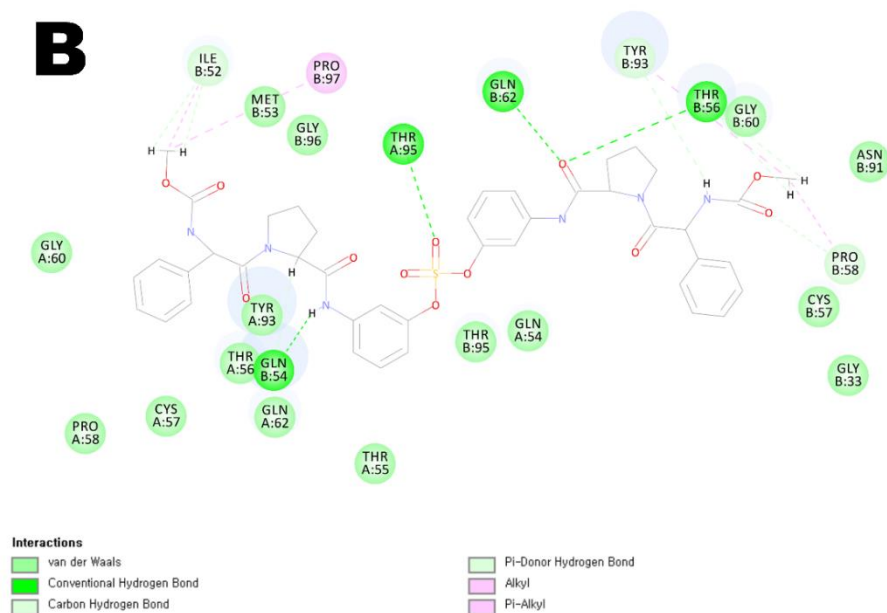


Figure 10. Representative ^{13}C NMR (400 MHz, DMSO-d_6) Analysis of Fosylation and SuFEx. Reaction illustrated a Starting Material (red) and fosylated compound (blue) and SuFEx product (black).

A



B



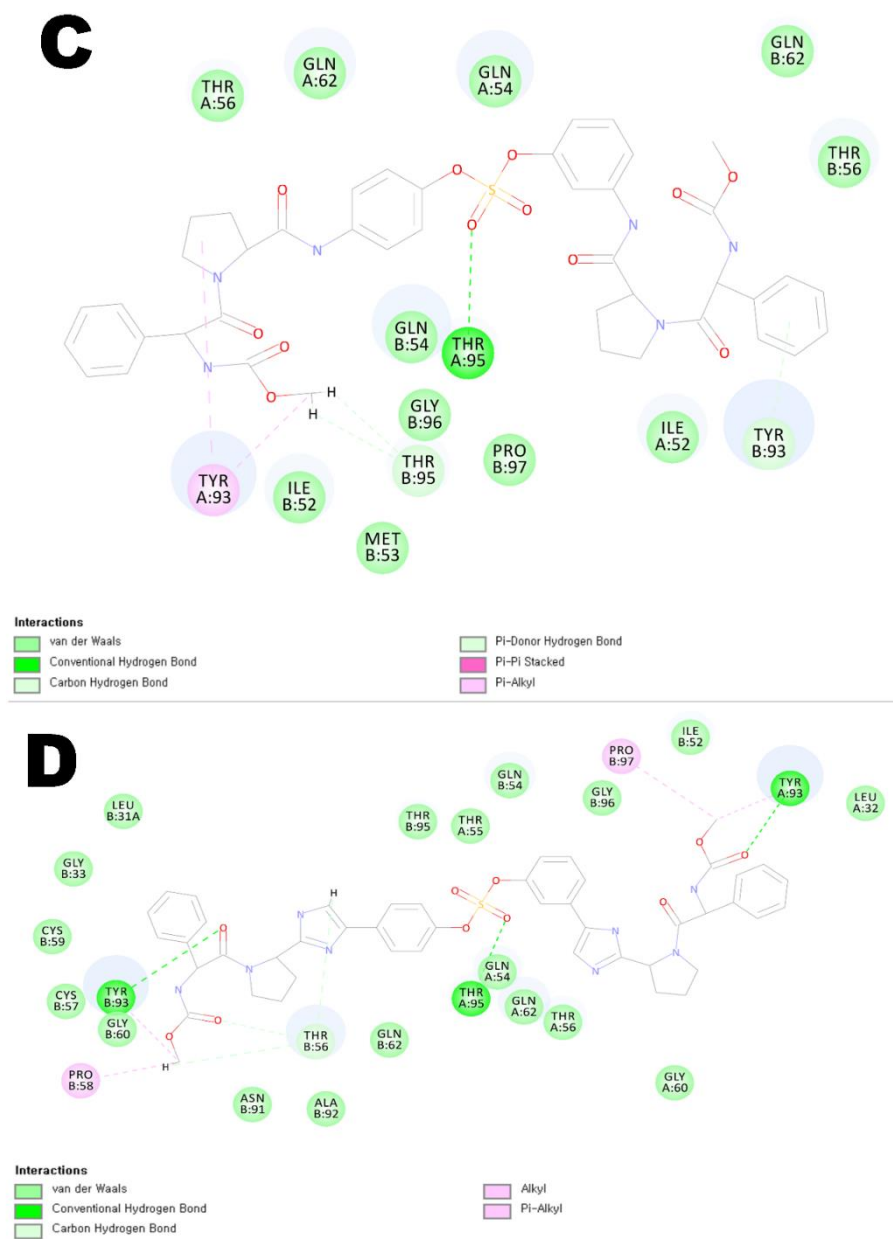


Figure 11. 2D-interaction docking model of compounds in an NS5A dimer model. (A) **BMK-21007**, (B) **BMK-21014**, (C) **BMK-21022**, and (D) **BMK-21040** inside NS5A dimer model (3FQQ). Various interactions are depicted by different color legends. Inhibitors are shown by line, interacting residues by colored sphere, and interactions by dash lines.

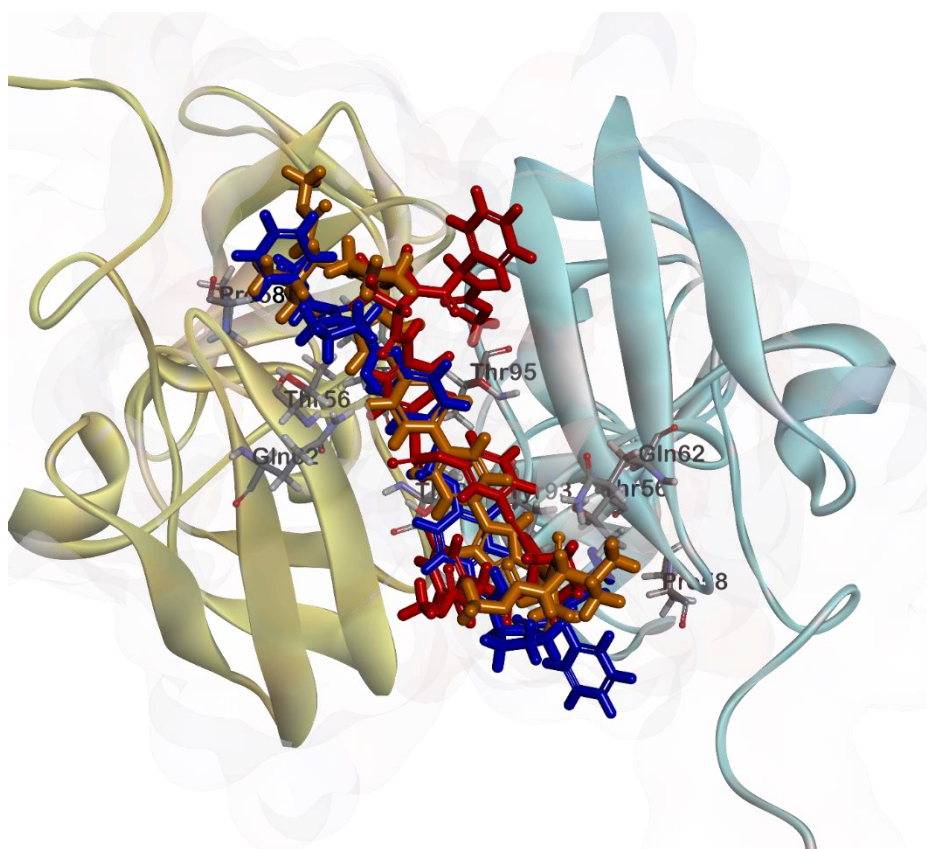


Figure 12. Superposed model of inhibitors inside NS5A dimer model (3FQQ). Daclatasvir, **BMK-21007**, and **BMK-21022** shown by orange, blue, and red, respectively.

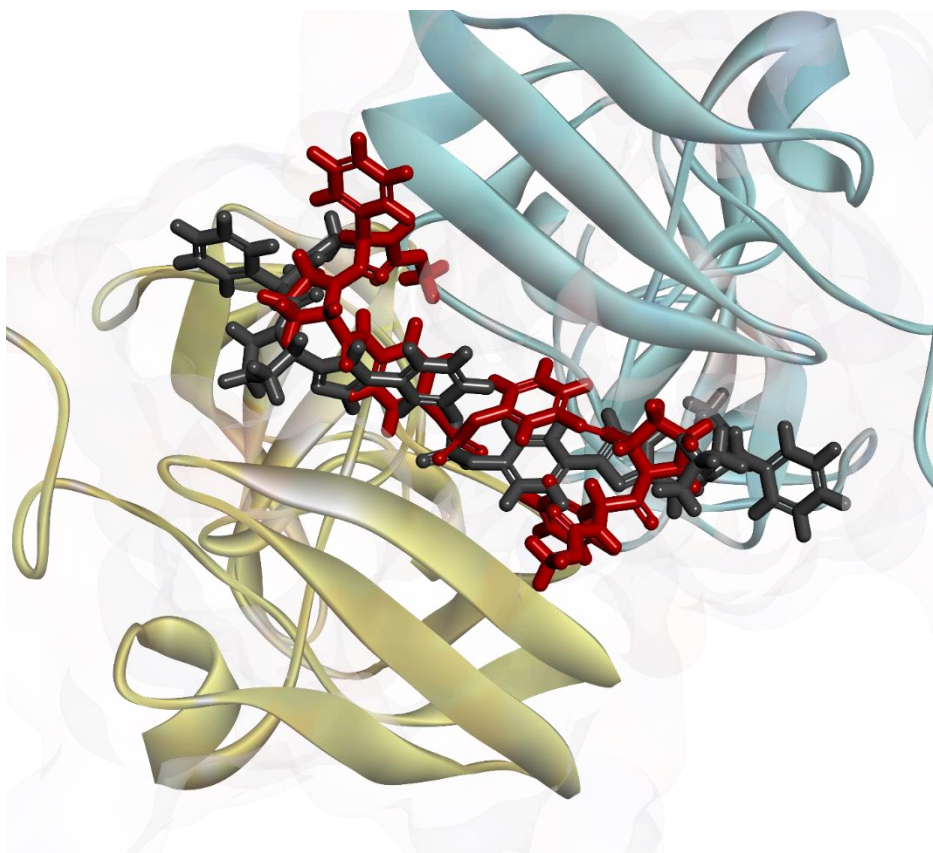


Figure 13. Superposed model of inhibitors inside NS5A dimer model (3FQQ). Compounds **BMK-21022** and **BMK-21040** shown by red and grey, respectively.

Chapter 3.

Development of effective treatments for hepatitis C genetic mutations based on fluorene structures

1. Introduction

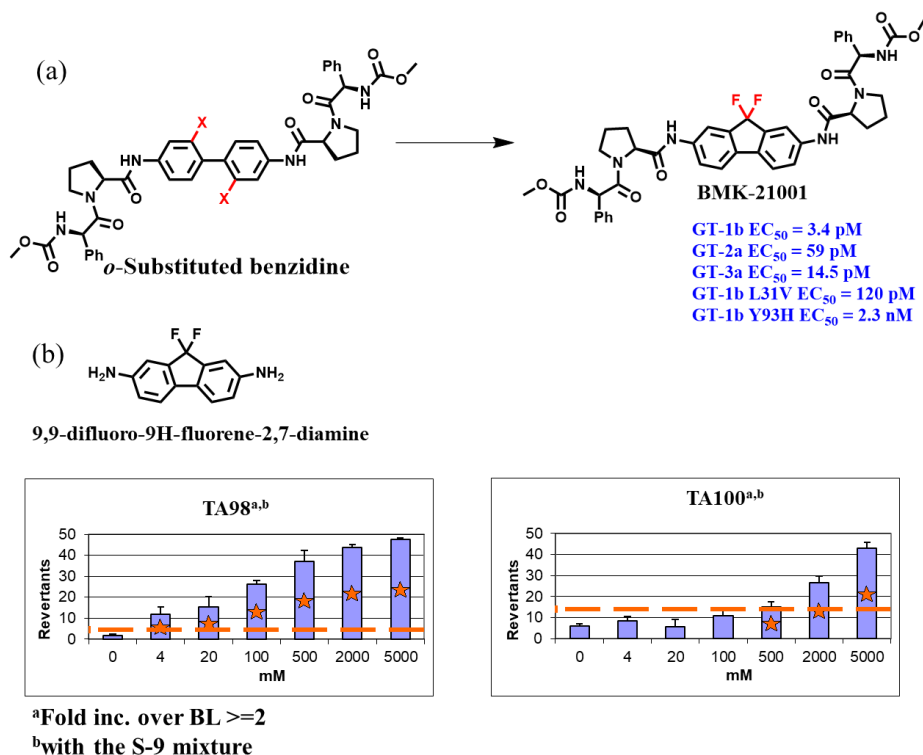


Figure 14. Structure of **BMK-21001** and Ames results of metabolite. (a) Structure of **BMK-21001** and EC₅₀ for genotypes of HCV. (b) Ames test results of metabolite of **BMK-21001**. Orange line means fold induction over the baseline. If fold induction value is more than 3, it is regarded as mutagen.

Based on chemical structure of the **BMK-20113**, we had optimized the NS5A inhibitor by introducing the substituted benzidine derivatives. When we tested the anti-viral activities of compounds, meta-substitution of the benzidine prolinamides made the inhibitors highly potent HCV inhibitors. In addition, previously reported NS5A inhibitors containing a fluorenyl core structure have the positive results of various genotypes for HCV. Therefore, we envisioned that the activity of *m,m*-connected benzidine like fluorene derivatives would exhibit high potency in the antiviral assays. Among them, **BMK-21001** which

has 9,9-difluorofluorene and prolinamide skeleton structure has picomolar range of EC_{50} value at wild type and L31V resistance mutant as shown in the figure 14. However, that inhibitor could not fully overcome major daclatasvir resistance mutant such as Y93H and double mutant (L31V+Y93H).^[19, 53] Moreover, the 9,9-difluoro-9H-fluorene-2,7-diamine, which is metabolite compound of **BMK-21001**, showed a positive result in the Ames test. the fluorene structures have generally genotoxicity like 2-nitrofluorene, which are used for Ames positive control. However, we were convinced that fluorene must have been good pharmacophore as the NS5A inhibitor. So, we screened the 2,7-diaminofluorene derivatives to find the Ames negative fluorene structure. Among the fluorene derivatives, the compounds containing an alkyl chain that has 4 or 5 carbon atoms at the 9-position in fluorene were shown the Ames positive only at 5 mM or more (data not shown).

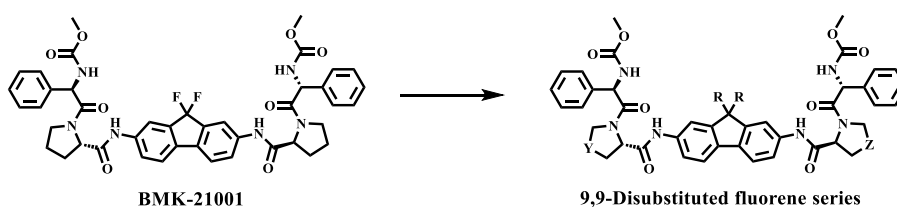


Figure 15. Design strategy of new NS5A inhibitors. We tested inhibition effect by modifying X, Y and Z site in **BMK-21001**.

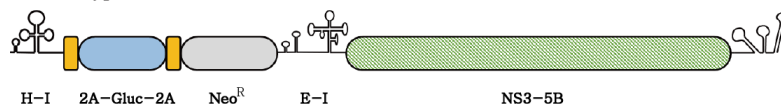
Based on these results, we further developed NS5A inhibitors based upon a 9,9-dibutyl or 9,9-dipentyl fluorene prolinamide skeleton that have high inhibition effect on pan-genotype HCV and genotype 1b daclatasvir resistance mutant (figure 15).

2. Results and Discussion

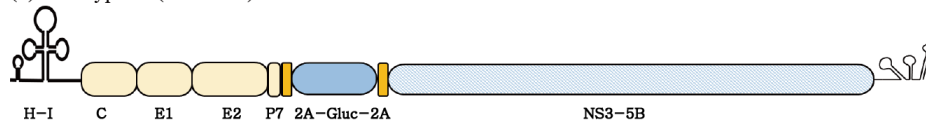
NS5A inhibitory activities of new inhibitors depending upon the substituted fluorine core structure

To determine structure activity relationship (SAR) of new anti-NS5A inhibitors, we sequentially modified the NS5A inhibitor structure at the 9 position of fluorenyl core structure as can be seen in Figure 14. We modified the length of the 9,9-dialkyl substitution of the fluorene core (R) to determine the replication inhibitory activities on pan-genotype and daclatasvir resistant mutant HCV such as L31V, Y93H and L31V+Y93H. To evaluate the 50% of effective concentration (EC₅₀) of modified compounds, we used HCV cell culture system (HCVcc) and HCV replicon system.^[76, 77] For measuring EC₅₀ in HCVcc system (GT 2a), we made a modified JC1 clone (JC1-Gluc) containing *Gaussia* Luciferase gene (Gluc) between P7 and NS2 region as previously reported.^[77] Using the JC1-Gluc system, we infected this virus to Huh 7.5.1 cells for 4 hrs. After 4 hrs, huh 7.5.1 cells were incubated with Dulbecco's Modified Eagle Medium (DMEM) containing serially diluted inhibitor and waited until 72 hrs. After 72 hrs, the cell supernatant was harvested for measuring the *Gaussia* luciferase activity. To determine the inhibitory effect of the compounds on HCV 1b and 3a replication, we used HCV replicon system.

(a) Genotype 1b (NK 5.1-Gluc)



(b) Genotype 2a (JC1-Gluc)



(c) Genotype 3a (S52-Feo)

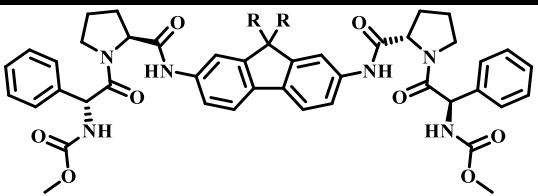


- H-I : HCV IRES
- E-I : EMCV IRES
- 2A : FMDV 2A protease
- Gluc : *Gaussia* luciferase
- Fluc : Firefly luciferase

Figure 16. Schematic structure of replicons. (a) genotype 1b (NK5.1-Gluc) (b) genotype 2a (JC1-Gluc) (c) genotype 3a (S52-Feo)

The replicon system contains the HCV non-structured proteins (NS3-NS5B) which are bicistronically co-translated with luciferase gene fused with neomycin phosphotransferase as described in material and method (Figure 15). The replicon system is capable of viral RNA replication in the cell. Procedure for making the replicon cell line is described in material and methods. HCV bicistronic RNA-containing cell lines were incubated in the presence of inhibitors for 72 hrs. After 72hrs later, cultivated cells or supernatants were harvested for measuring the luciferase activity in genotypes 1b and 3a, respectively. 0.1% DMSO treated cells were used to normalize the luciferase activity.

Table 11. The EC₅₀ values of inhibitors containing a fluorene core.^a

							
compd	R	GT-1b (pM)	GT-2a (nM)	GT-3a (pM)	L31V ^b (pM)	Y93H ^b (nM)	D.M. ^b (nM)
45 (BMK-21077)	Ethyl	71.3	0.700	366	200	18.3	> 100
46 (BMK-21053)	<i>n</i> -Pr	139	14.5	311	144	4.60	> 100
47 (BMK-21054)	<i>n</i> -Bu	1.57	1.20	16.4	3.63	0.880	41.4
48 (BMK-21065)	<i>n</i> -Pent	3.30	5.90	7.30	2.70	2.30	47.8

^aResults from three independent experiments with duplicate. EC₅₀, Effective concentration 50%.

^bDaclatasvir resistance mutant for genotype 1b, D.M., Double mutant (L31V+Y93H).

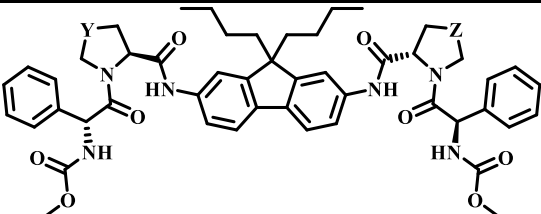

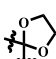

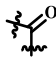

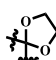
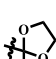
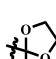
Based on Figure 15 structure, we fixed the linker and cap region in compounds as phenylglycine and carbamate moiety, respectively, and changed only the carbon length of the substituents on the fluorene core (R at Figure 15) as described in Table 11. The compound **45**, which has ethyl residue substituent in fluorene core, showed EC₅₀ of 0.071 nM and 0.336 nM in genotype 1b and 3a, respectively. However, the compound **48**, which has a longer fluorene core length than compound **45**, showed single digit pM range EC₅₀ values in genotype 1b and 3a HCV. The assay result indicated that inhibition effect was related to fluorene core length on genotype 1 and 3 HCV. Also increasing the

alkyl length of fluorene core has a role for inhibition against 1b and 3a HCV, not 2a.

Next, to determine the inhibition effect of the above-mentioned compounds on resistance mutant HCV, we transfected resistance mutant HCV RNA to Huh7.5.1 as described in Experimental section. Table 11 indicates the EC_{50} value of the compounds against daclatasvir resistance mutant HCV. By comparing compounds **45** to **48**, we found that length of the alkyl group on the fluorene core plays a key role for inhibiting the L31V resistance mutant. As a result, these data suggest that we not only developed compounds having a good inhibitory effect on wild type HCV by modifying the fluorene core, but also confirmed the role of the alkyl group length on the fluorene core for the inhibition of L31V resistance mutant.

Proline structure dependent Y93H resistance mutant effect in genotype 1b HCV

Table 12. The EC₅₀ values of inhibitors containing 9,9-dibutylfluorene and pyrrolidine derivatives (pM)^a

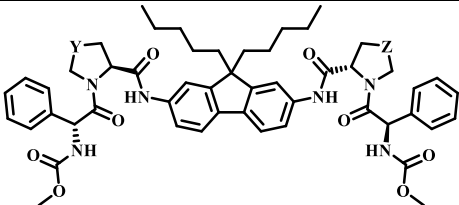

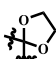

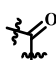

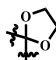
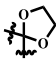
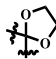
								
compd	Y	Z	GT-1b (pM)	GT-2a (nM)	GT-3a	L31 V ^b	Y93 H ^b	D.M. ^b (nM)
47 (BMK-21054)	-CH ₂	-CH ₂	1.57	1.20	16.4	3.60	882	41.4
49 (BMK-21064)		-CH ₂	4.00	0.700	29.6	3.70	780	14.8
50 (BMK-21070)		-CH ₂	6.10	1.60	30.2	6.90	75.3	1.04
51 (BMK-21058)			13.5	0.600	81.7	4.40	153	2.20
52 (BMK-21059)			21.6	1.40	78.7	2.90	24.6	0.438
53 (BMK-21069)			5.40	5.60	354	6.90	45.5	0.033
54 (BMK-21075)	(R)-OH	(R)-OH	29.6	3.50	133	25.2	29.0	0.058

^aResults from three independent experiments with duplicate. EC₅₀, Effective concentration 50%

^bDaclatasvir resistance mutant for genotype 1b, D.M., Double mutant (L31V+Y93H)

Among our candidate compounds, compounds containing 9,9-dibutylfluorene or 9,9-dipentylfluorene core structure (compound **47** and **48**, respectively) showed remarkable inhibitory effects against L31V resistance mutant. In this regard, we fixed core residue with 9,9-dibutylfluorene or 9,9-dipentylfluorene structure to determine the effect of the modification on the L-proline residue (Y, Z at Figure 15) against daclatasvir resistance mutant HCV.

Table 13. The EC₅₀ values of inhibitors containing 9,9-dipentylfluorene and pyrrolidine derivatives (pM)^a

								
compd	Y	Z	GT-1b	GT-2a	GT-3a	L31 V ^b	Y93H ^b	D.M. ^b (nM)
48 (BMK-21065)	-CH ₂	-CH ₂	3.00	5,900	59.0	3.00	2,030	47.8
55 (BMK-21083)		-CH ₂	13.0	6,100	44.0	7.00	1,570	58.5
56 (BMK-21066)		-CH ₂	3.00	19,700	37.0	1.40	116	2.80
57 (BMK-21082)			8.00	1,900	79.0	6.00	637	14.3
58 (BMK-21084)			31.0	58,700	452	19.0	348	3.10
59 (BMK-21067)			3.00	19,400	435	0.60	4.60	0.051
Daclatasvir (reference)			7.00	28.0	1,000	410	620	0.781

^aResults from three independent experiments with duplicate. EC₅₀, Effective concentration 50%

^bDaclatasvir resistance mutant for genotype 1b, D.M., Double mutant (L31V+Y93H)

Prior to observing the inhibition effect of the compounds on daclatasvir resistance mutant HCV, we first ascertained whether the inhibitors possessing

the modified L-proline structure have anti-HCV effect against wild type HCV and they exhibited picomolar EC₅₀ values in genotype 1b and 3a HCV, but not 2a HCV (Table 12 and 13).

Next, we measured the inhibition effect of proline modified compounds against daclatasvir resistance mutant HCV. Interestingly, when we compared the compound series from compound **47** to **59**, it was observed that the inhibitory effect on Y93H resistance mutant varied depending on the proline structure. In particular, by comparing EC₅₀ values between proline modified compounds and non-modified compounds (**47** and **48**, respectively), we learned that compounds with 4-oxo-L-proline, 4-spiro cyclic ketal-L-proline or 4-hydroxyl-L-proline structure are related to the inhibition of Y93H and double mutant, L31V and Y93H (Table 12 and 13). Particularly, 4-spiro cyclic ketal-L-proline (**53** and **59**) or 4-hydroxyl-L-proline **54** showed single or double digit EC₅₀ values at Y93H or double mutant resistance mutant HCV. Consequently, these results suggest that L-Proline (Y and Z in Figure 15) residue of compound served to inhibit HCV replication by binding of NS5A Y93 or H93 residue together with fluorene core residue.

Structure dependent colony formation assay on replicon HCV

HCV RNA encodes an error-prone RNA dependent RNA polymerase (RdRp) NS5B, which has low fidelity in RNA proofreading process.^[14] For this reason, the media containing NS5A inhibitor can eliminate HCV in the cell since generating mutation by NS5A inhibitor cannot be revised during replication, which results in the selection of HCV RNA resistance cells against the NS5A inhibitors. As described before, HCV replicon system has two IRES elements that allow the co-translation of non-structural protein and Neomycin phosphotransferase bicistronically. If the HCV RNA survive by accruing resistance mutant, it will translate neomycin phosphotransferase and as results, cells with mutant RNA can grow media containing G418 condition. Thus, cell containing HCV RNA, which get resistance mutation, can grow by compound treatment condition and eventually can be observed through colony forming.

Moreover, by comparing rate of colony formation, we can infer the compound resistance barrier on the level of mutant colony formation or elimination of HCV replicon cell.^[21]

To compare the rate of colony formation caused by compound structure, each of compounds was treated with the same concentration for 5 days to genotype 1b or 3a replicon cell in the absence of G418. After 5 days, the compounds inoculated cells were split with two plate, one plate kept treating compounds without G418 and the other plate maintained in presence of 1mg/ml G418 without treating compounds for 14 days for colony forming. This procedure was repeated every 5 days and proceeded for 15 days. The selected cells by G418 can display a change in the colony formation rate depending on the treatment time, compound concentration and structure, so these results indicated the population of HCV resistance replicon cells against NS5A inhibitor.

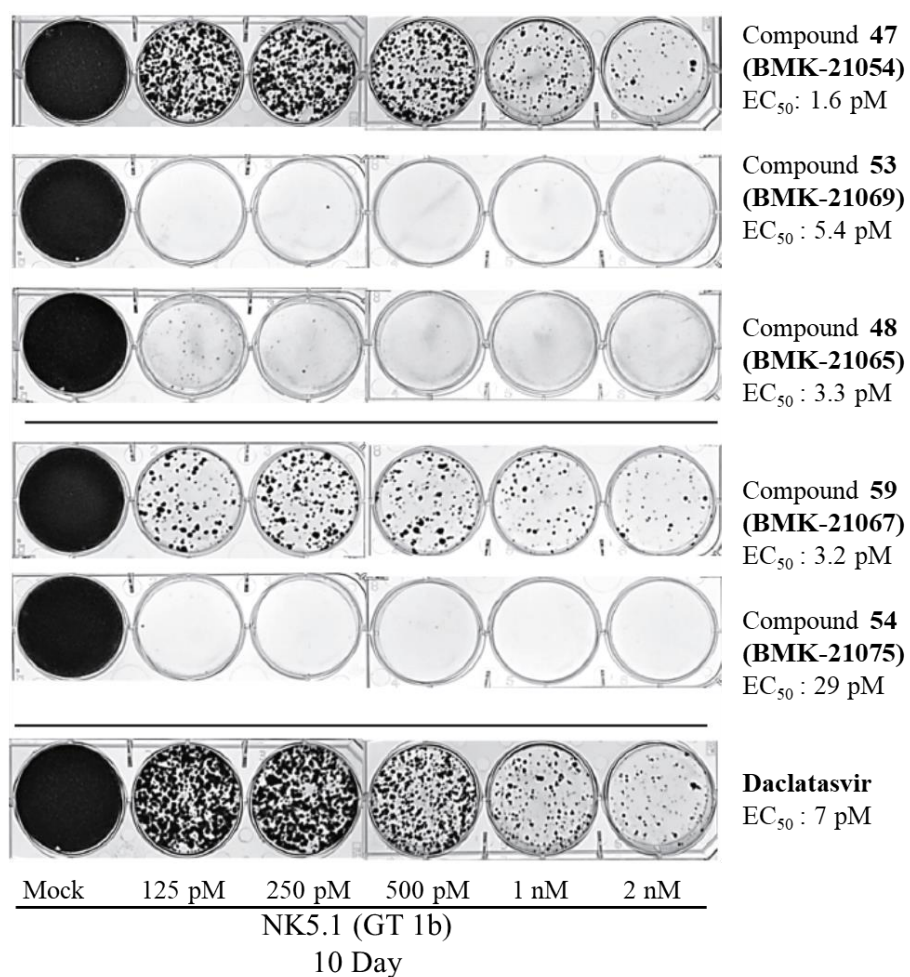


Figure 17. Colony formation assay on NK5.1 replicon HCV (GT-1b)

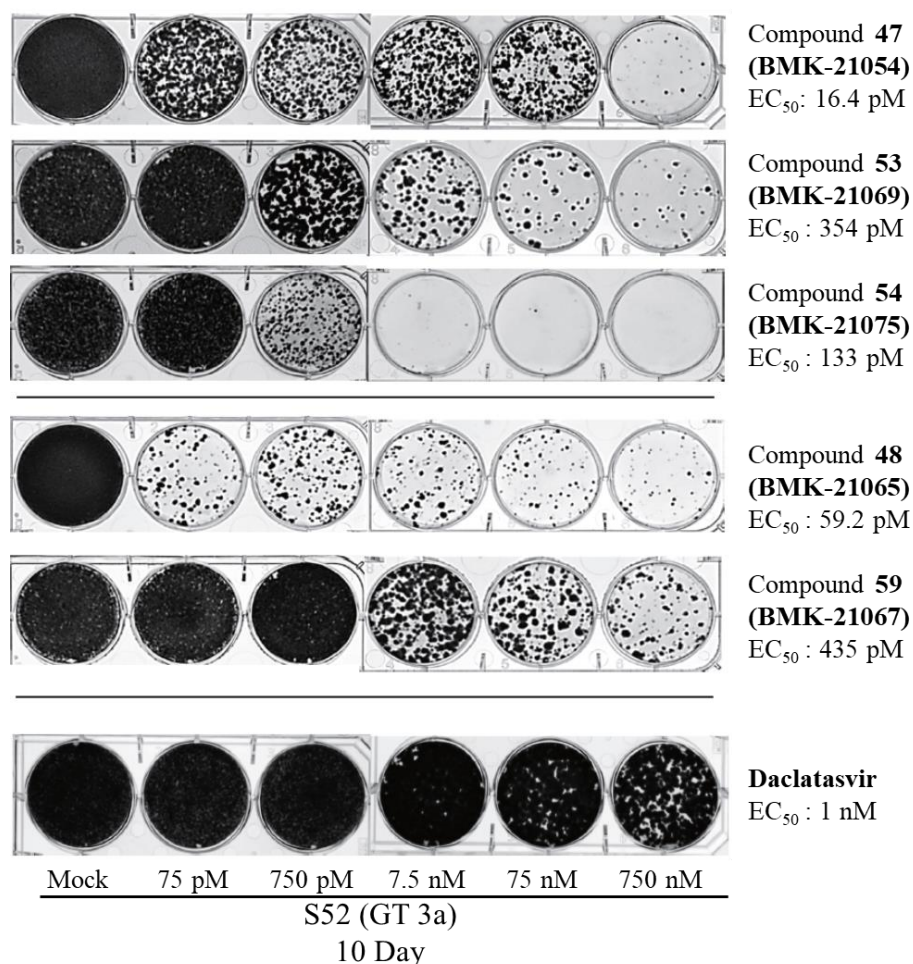


Figure 18. Colony formation assay on S52 replicon HCV (GT-3a)

Using this procedure, we incubated compounds on replicon cell for long periods to see the resistance barrier depending on compound structure. The colony formation results showed that compound **47** and **48**, which have L-proline residue, have low inhibition effect for emergency of colony formation. And also, **53**, **54** and **59**, which modified L-proline residue as 4-spiro-ketal proline or 4-hydroxyl-L-proline, more efficiently inhibited generating resistance colony on genotype 1b replicon (Figure 17). Especially, **54** showed high elimination level for forming resistance colony than **47** or **48** in spite of the high EC_{50} value on genotype 3a replicon cell. So, the **54** has a high

resistance barrier on both HCV genotype (Figure 17 and 18). As a result, this experiment indicated that the resistance barriers for each compound and also modification of L-proline moiety well inhibit the production of colonies containing resistance mutants.

Humanized mice liver test in Genotype 3a HCV

In-vitro assay results indicated that modified compounds have high inhibition effect on 1b and 3a replicon cell. Even though genotype 1b is most prevalent genotype, many of commercial drugs including daclatasvir already targeted 1b HCV and those have high SVR rated.^[78] In this regard, we chose genotype 3a HCV for *in-vivo* efficacy test since occurring of genotype 3a resistance mutant still has a problem to decrease SVR rate by DAA's.^[23] To observe genotype 3a HCV inhibition effect in *in-vivo* system, we used humanized liver mice that human hepatocytes (h-heps) transplanted into the spleen of urokinase-type plasminogen activator (uPA) / severe combined immunodeficient (SCID)-mice.^[24, 32] By transplanting, the level of Human-Albumin (h-Alb) was monitored for 8 weeks to confirm the regeneration of human hepatocytes (h-heps) with mice liver. After 8 weeks, mice well expressed the h-Alb were inoculated with genotype 3a HCV. Then HCV RNA level was confirmed by using RT-PCR after 10 weeks.

Table 14. Pharmacokinetics results about compounds **47** and **54** at CD-1 mice.^{a,b}

NO.	Adminis- tration route	Dose (mg/kg)	AUC _{last} (hr*ng/mL)	C _{max} (ng/ml)	t _{1/2} (h)	F(%)
47	P.O.	8	21893.8	1374.5	4.6	39.3
(BMK-21054)^c	I.V.	1.5	9654.36	2735.37	6.2	
54	P.O.	20	256.5	142.0	2.9	0.6
(BMK-21075)^d	I.V.	5	10873.8	16400	4.4	

^aValues are mean and standard deviation; p.o., oral; i.v., intravenous; AUC_{last}, Area under the plasma semi logarithmic concentration versus time curve from the time of dosing to the last measurable concentration; C_{max}, maximum concentration of the drug; t_{1/2}, half-life; F(%), oral bioavailability.

^bPK experiments were conducted using male mice (*n* = 3).

^cVehicle: 5% DMSO, 10% Solutol, 85% HPBCD (20%, w/v).

^dVehicle: 10% Dimethylacetamide, 10% Polysorbate 80, 80% HPBCD (20%, w/v)

Even though compound **54** has highest resistance barrier, but it showed poor pharmacokinetics profile on oral administration (Table 14). On the other hand, compound **47** showed good pharmacokinetics profile on oral administration. So, we chose compound **47** to determine the inhibition effect against genotype 3a HCV for infection to humanized liver mice.

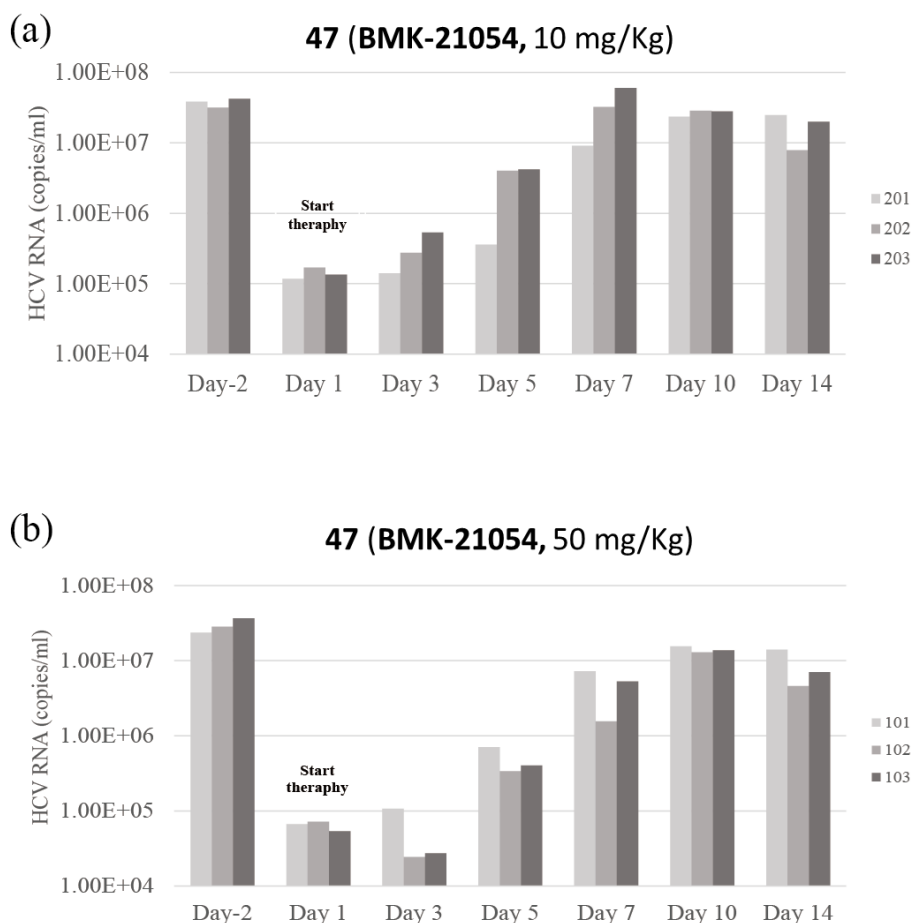


Figure 19. Genotype 3a HCV inoculated to humanized mice. HCV RNA was determined through RT-PCR in mouse serum after inoculated with HCV genotype 3a. (a) compound **47** was treated for 2 weeks with 10 mg/kg. (b) 50 mg/kg.

The compound **47** had well inhibited HCV replication for 3 days at 10 mg/kg or 50 mg/kg treatment concentration, but HCV RNA level rebounded after 3 day despite of continuation of the compound treatment (Figure 19). Previous reports already noted that mono-administration of daclatasvir resulted in virus recovery due to low resistance barrier of NS5A inhibitor in genotype 1a or 1b HCV infected patient serum.^[79] So these results suggests that mono-treatment of NS5A inhibitor has a limitation to inhibit HCV completely since the

resistance mutants of genotype 3a HCV could be generated. In spite of having some limitation, our results suggests a possibility that compound **47** can inhibit genotype 3a HCV well in human liver.

Combination test with NS3-4A protease inhibitor

The structure modification of anti-NS5A compound brought high inhibition effect on wild type HCV and daclatasvir resistance mutant HCV. Among them, the compound **47** has a good inhibition effect on humanized liver mice infected with genotype 3a HCV. However, the results of humanized liver mice additionally indicated the limitation of NS5A mono-treatment since HCV RNA level was rebounded after 3 days in mice serum. To overcome the limitation of mono-treatment, we referred to guideline of HCV therapy that NS5A inhibitors should be co-treated with other DAA's such as NS3/4A protease inhibitors or NS5B inhibitors.^[79, 80] To determine the combination effect, we selected several NS5A inhibitors (compound **47**, **53**, **59** and **54**), which called key compounds, showing high inhibition effect on genotype 1b and 3a and daclatasvir resistance mutant HCV. To evaluate combination effect of key compounds with representative DAA's, such as grazoprevir (NS3-4A inhibitor), we used the *Chou-Talalay* method.^[73] Compound **47**, **53**, **59** and **54** were co-treated with constant ratio of grazoprevir to genotype 1b or 3a replicon cell, respectively. And then, we calculated relative inhibition ratio by 0.1% DMSO treated cell. To calculate combination index value, we used Compusyn freeware program (Compusyn, Inc.).^[60]

Table 15. Combination index of NS5A inhibitors and grazoprevir.^{a,b}

Compound	Genotype 1b (NK5.1)		Genotype 3a (S52)	
	EC ₅₀	EC ₇₅	EC ₅₀	EC ₇₅
	CI value ^c	CI value ^d	CI value	CI value
47 (BMK-21054)	0.8	1.1	0.65	0.76
53 (BMK-21069)	0.9	1.13	0.54	0.65
59 (BMK-21067)	0.6	1.0	0.91	0.93
54 (BMK-21075)	0.7	0.8	1.0	0.82

^aCI > 1, antagonism effect; CI < 1, synergistic effect; CI ~ 1, additive effect

^bNS3-4A Inhibitor

^cEC₅₀ CI value, Effective Concentration 50 percent Combination Index value

^dEC₇₀ CI value, Effective Concentration 75 percent Combination Index value

Combination index value of key compounds was below 1 point at 50% and 75% effective concentration. That combination index value suggests that key compounds have synergic or additive effect with other DAA's at each effective concentration (Table 15).

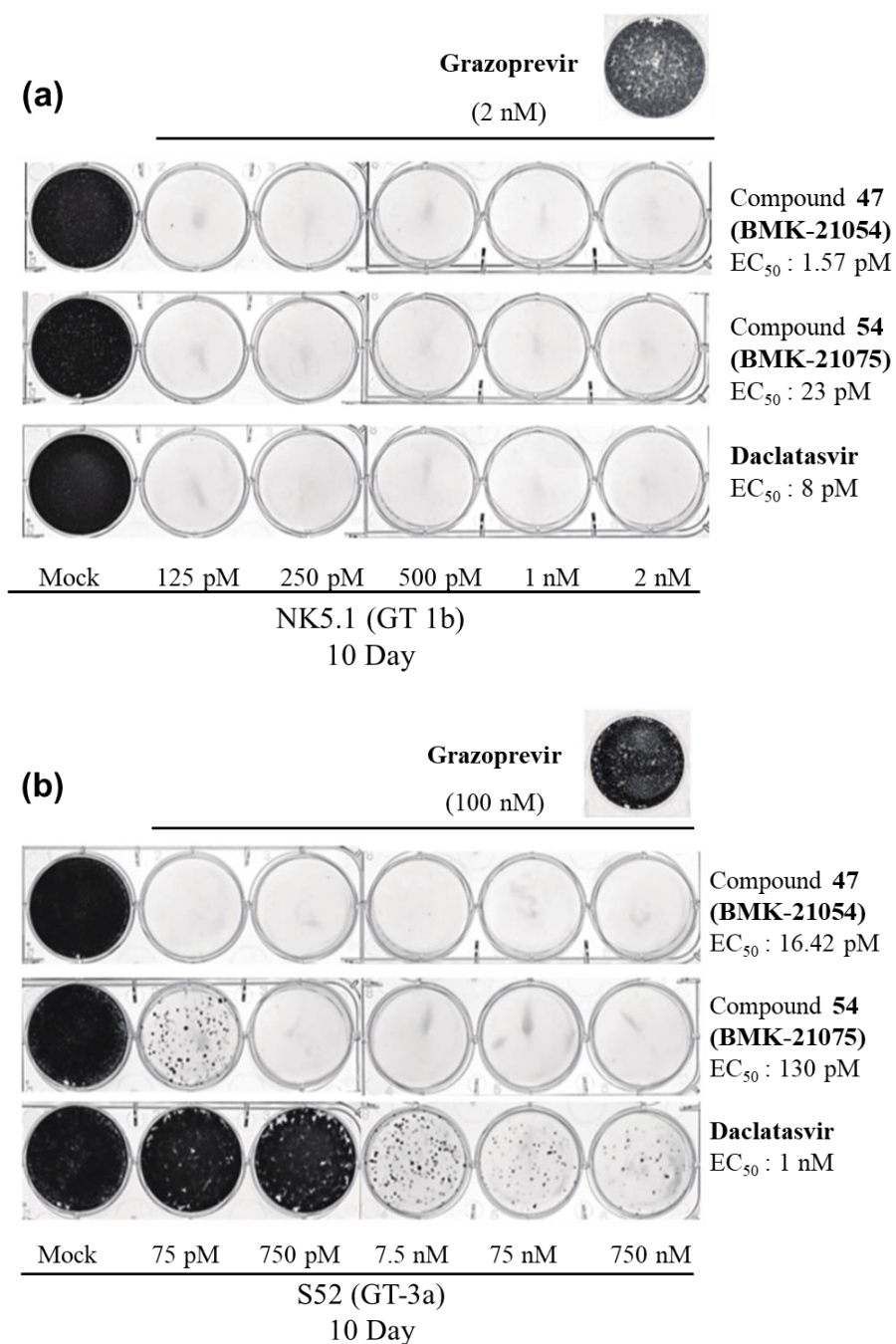


Figure 20. Colony formation assay for combination with grazoprevir. (a) NK5.1 replicon HCV (GT-1b) (b) S52 replicon HCV (GT-3a)

Previously, we showed the resistance barrier of key compounds as a colony formation assay in genotype 1b or 3a HCV replicon cell. Using this method, compound **47** or **54** was treated with grazoprevir (about EC₉₀ concentration) to detect the combination effect on the development of resistance mutant and we observed that resistance colonies were virtually eliminated by concomitant treatment with grazoprevir, which mean that the limitation of NS5A inhibitor mono-therapy could be overcome by concomitant with other DAA's (Figure 20). We also wondered whether the low concentration of grazoprevir was effective or not in removing HCV when co-administered with the NS5A inhibitor. Previous reports showed grazoprevir concentration in the blood to be approximately 8.8-15.2 nM after 24 hours of administration (C24) of 200 mg of grazoprevir, we used 15 nM concentration of grazoprevir to see the combination effect at colony formation assay.^[81]

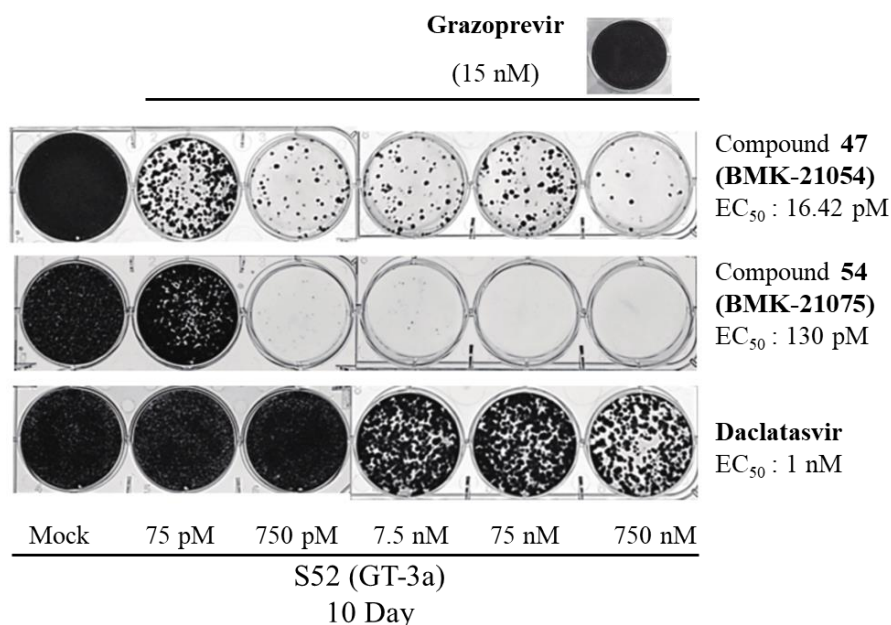


Figure 21. Colony formation assay for combination with grazoprevir on S52 replicon HCV (GT-3a)

We treated the major compounds with C24 concentration of grazoprevir, about 15 nM, resulting in a synergistic effect of colony elimination levels (Figure 21).^[81] Those results suggest that the occurring of resistance mutant caused by the single administration of the NS5A inhibitor can be got over by the combined administration of other DAA's.

(CI > 1: antagonism effect. CI=1: additive effect, CI <1: synergistic effect).

Docking study

Through our investigation, we have seen that proline and fluorene moieties play an important role in inhibiting wild type HCV and resistance mutant HCV. Additionally, in order to relate *in-vitro* study results with *in-silico* docking study, we computationally performed the docking analysis for association between our compound and NS5A domain 1.

(a)

Compound	EC ₅₀ (nM)		Docking score (Kcal/mol)	
	WT	D.M.	WT	D.M.
47 (BMK-21054)	0.0016	41.4	-8.22	-6.26
54 (BMK-21075)	0.0296	0.058	-9.48	-7.04

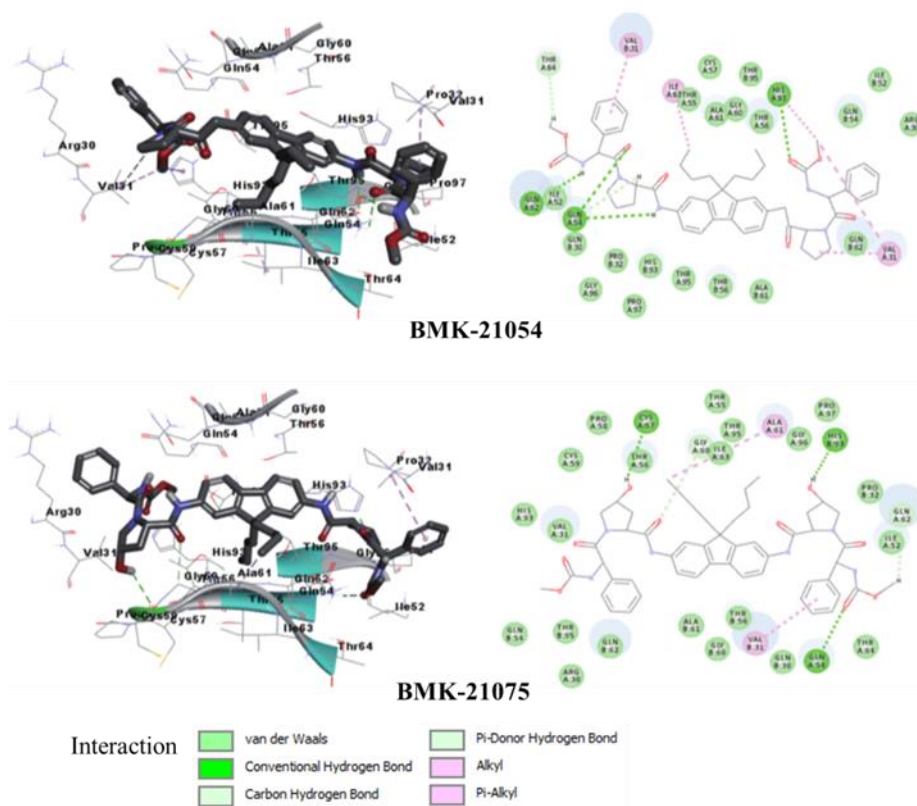


Figure 22. Docking studies of an inhibitor compound and NS5A dimer model (NS5A domain 1 PDB ID: 3FQQ, 1ZH1; AH helix NMR structure PDB ID: 1R7G) (a) docking score for compound **47** and **54** (b) compound **47** and NS5A dimer interaction (c) compound **54** and NS5A dimer interaction

We used two kinds of NS5A domain 1 structures and AH region for docking analysis (NS5A Domain 1 PDB ID: 3FQQ, 1ZH1; AH helix NMR structure PDB ID: 1R7G). The docking score proposes that 3FQQ model was well fitted with NS5A inhibitor than 1ZH1 model (Figure 22a). Also, the docking analysis could predict the possible interaction residues between NS5A inhibitor and NS5A protein which are likely to bind to each of inhibitors with hydrophobic or hydrophilic interactions. We used NS5A with a daclatasvir resistance mutant and expected that V31 residue would interact with fluorene core region since alkylchain of 9-position in fluorene core region inhibited L31V resistance mutant in assay results, but unlike our expectation, the V31 residue was observed to be located on the phenyl glycine region at docking results. Although these results were different with our expectations, it had a part of consensus with the previously reported by Michael W. Parker group report.^[80] The other daclatasvir resistance mutation, the H93 residue, was well in agreement with our conjecture because the 4-hydrosyl-L-proline of compound **54** interacts with H93 of the NS5A protein via hydrogen bond (Figure 22b and 21c). Taken together, through the docking analysis, we suggest a possibility that *in-vitro* assay results could be proved as docking score. Also, we could infer that docking score might in part reflect the assay results in terms of efficacy of compounds on resistance mutant HCV. Furthermore, it should be noted that, it was beyond our scope to do docking analysis for NS5A inhibitor and genotype 3a NS5A structure because of the lacking of structural information for the protein.

3. Conclusion

In conclusion, we developed novel structure of NS5A inhibitors based on a fluorene derivatives and proline-amide skeleton. Additionally, we could observe the relationship between the specific part such as fluorene moiety or L-proline of our inhibitors and NS5A protein for inhibiting HCV replication.

Finally, among variously designed inhibitors, we found a few inhibitors to be shown highly effective response on genotype 1b and 3a HCV as well as on daclatasvir resistance mutants.

4. Experimental

Materials and Method

Without additional notes, all reagents were commercially available and used without further purification. THF was distilled over sodium and benzophenone, and degassed by argon bubbling for 10 minutes before using on polymerization. Toluene, 1,4-dioxane, methanol, DMF were purified by solvent purification system using alumina column, and degassed by argon bubbling. *N,N'*-dimethylacetamide (DMA) was purchased from Junsei and degassed by argon for 10 minutes before using on polymerization without further purification.

DNA constructs and *in-vitro* transcription of RNA

NK5.1-Gluc

For inserting the *Gaussia* luciferase gene to NK5.1 clone, we used site direct mutagenesis (SDM) PCR to generate restriction enzyme site (*AscI*) between HCV IRES and Neomycin phosphotransferase region. The FMDV (Foot and Mouth disease virus) 2A protease fused *Gaussia* luciferase gene was amplified using PCR. This amplified 2A-Gluc-2A PCR product containing *AscI* site was digested with restriction enzyme and ligated with NK5.1 (Figure 16). To synthesize the replicon RNA, it was linearized by *ScaI* and *in-vitro* transcribed RNA using T7 polymerase.

JC1-Gluc

For inserting the 2A-Gluc-2A between P7 and NS2 region of JC1 clone, we used Site direct mutagenesis (SDM) PCR to generate restriction enzyme site (*AscI*) between P7 and NS2 region. The FMDV (Foot and Mouth disease virus) 2A protease fused *Gaussia* luciferase gene was amplified using PCR. This amplified 2A-Gluc-2A PCR product containing *AscI* site was digested with

restriction enzyme and ligated with JC1 (Figure 16). To synthesize the RNA, it was linearized by *Xba*I and *in-vitro* transcribed RNA using T7 polymerase.

S52-Feo

Dr. Charles M. Rice kindly provided the S52-Feo (genotype 3a). To synthesize the RNA, it was linearized by *Xba*I and *in-vitro* transcribed RNA using T7 polymerase.

Measurement of the anti-HCV activities of inhibitors using HCVcc

Cell line and cell culture

Huh 7.5.1 cells were grown in Dulbecco's Modified Eagle's medium (DMEM; Gibco) supplemented with antibiotics (100 U/mL penicillin, 10 µg/mL streptomycin) and 10% fetal bovine serum (FBS; PEAK) at 37°C in a humidified 6.0% CO₂ incubator.

Virus production

In vitro transcribed HCV RNA were electrophoresed in Huh 7.5.1 cell as described previously. Briefly, the transfected cells were maintained with culture media for three days and then the culture media containing HCV were collected for 7 days and then filtered through a 0.45 µm pore size filter.

Antiviral activity test with infectious HCV particles

Huh 7.5.1 cells were inoculated with a JC1-Gluc virus for 4h. At 4h after the virus inoculation, HCV-infected Huh7.5.1 cells were cultivated with media containing serially diluted inhibitors. At 3 days post chemical treatment, the culture media was harvested and *Gaussia* luciferase activities were measured using a *Renilla* luciferase assay system (Promega) according to the manufacturer's direction. The luciferase activities were normalized to those

obtained from mock-treated cells. A four parameter Logistic of the SigmaPlot Program was used for calculating the EC₅₀ value and Statistics Value.

Measurement of anti-HCV activities of inhibitors using HCV replicon

Cell line and cell culture

Huh 7.5.1 cells containing a bicistronic HCV replicon NK5.1-Gluc (genotype 1b) and S52-Feo (genotype 3a) were used to test the anti-HCV activities of the inhibitors (Figure 16). *In-vitro* transcribed replicon RNA (30 µg) was transfected to Huh7.5.1 cell and then inoculated with G418 (0.5 mg/ml, Calbiochem) containing DMEM media for selecting HCV RNA replicating cell. After this selection process, the selected replicon-containing cells were cultivated under DMEM media supplemented with antibiotics (100 U/mL penicillin, 10 µg/mL streptomycin) and 10% fetal bovine serum (FBS; PEAK) and additional antibiotic G418 (0.5 mg/ml, Calbiochem).

Antiviral activity assay test with HCV replicon

HCV replicating cells were seeded on a 12-well plate (5 x 10⁴ cells per well). One day later, the replicon cells were replaced with fresh media containing serially diluted inhibitors and incubated for three days. To measure the luciferase activity of NK5.1-Gluc replicon cell, 3 day post treatment cell culture media were collected and *Gaussia* luciferase activities were measured using *Renilla* luciferase assay system (Promega).

In the case of 3a replicon cell (S52-Feo), Luciferase activities were measured using cell lysate by *firefly* luciferase assay system (Promega) according to the manufacturer's direction, and then normalized to those obtained from mock-treated (0.1% DMSO) cells. A four parameter logistic of the SigmaPlot Program was used for calculating the EC₅₀ value and Statistics Value.

Observation of the effects of co-treatment of two inhibitors

The HCV replicating cells were treated with each of inhibitors alone or with mixtures of grazoprevir at serially diluted concentrations. At 3 days after treatment, luciferase activities were measured using the luciferase assay system (Promega) according to the manufacturer's direction, and then normalized to those obtained from mock-treated (0.1% DMSO) cells. Combination index was calculated by using Compusyn Freeware Program (Compusyn, Inc.).

Colony formation assay

Huh 7.5.1 cells containing HCV replicon (NK5.1-Gluc or S52-Feo) were used for colony formation assay. HCV replicon cells were seeded on a 6 well plates (5×10^4 cells per well). At 16hr after plating, culture media was replaced with fresh media containing serially diluted compound without G418 for 5 days. When cell confluence reaches ~95% after 5 days, the cells were split into two 6 well plates. About 20% confluence cells were plated with inhibitor containing DMEM media without G418. About 25% confluence cell was maintained in the other plate with DMEM media containing 1mg/ml G418. Cell culture media was changed with fresh one in every two or three days. Two weeks after, the cells, which were selected by G418, was fixed with a solution of 1% formaldehyde and 1% methanol and 0.5g crystal violet solution for 20 min and washed with PBS. After drying the plate, we took a picture using Amersham™ Imager 600 (GE healthcare).

Antiviral assay test using resistance mutant HCV

We substituted amino acid codon to L31V, Y93H and L31V+Y93H of NS5A protein of NK5.1-Gluc genome using site direct mutagenesis PCR. It was linearized with *Scal* restriction enzyme and used as *in-vitro* transcription. *In-vitro* transcribed mutant RNA were electrophoresed to Huh 7.5.1 cells individually and seeded in a 12 well plate. One day later, the transfected cells were replaced with fresh culture media containing serially diluted compounds and incubated for 3 days. 3 days post treatment, cell culture media was collected

and *Gaussia* luciferase activities were measured using *Renilla* luciferase assay system (Promega). Luciferase activities were normalized to those obtained from mock-treated (0.1% DMSO) cell. A four parameter Logistic of the SigmaPlot Program was used for calculating the EC₅₀ value and Statistics Value.

Cytotoxicity test

To determine the cytotoxicity effect of tested inhibitors, Huh 7.5.1 cells were seeded on 24 wells plate (2×10^4 cells per well). One day later, culture media was replaced with DMEM media containing serially diluted inhibitors and inoculated for three days. Post treatment, the culture supernatant harvested from each well and centrifuged to remove cell debris (12,000 rpm, 4°C, 10 min). Using cell supernatant, the cytotoxicity level was measured using ToxiLight™(Lonza) kit according to manufacturer's directions.

Docking analysis

All experiments of docking analysis were performed by Korea Institute of Science and Technology (KIST)

Humanized liver mice test

All experiments of Humanize liver mice test were performed by PhoenixBio. Co.

References

1. A. M. Di Bisceglie, *The Lancet*, **1998**, 351, 351-355.
2. A. U. Neumann, N. P. Lam, H. Dahari, D. R. Gretch, T. E. Wiley, T. J. Layden and A. S. Perelson, *Science*, **1998**, 282, 103-107.
3. T. L. Tellinghuisen, J. Marcotrigiano and C. M. Rice, *Nature*, **2005**, 435, 374-379.
4. G. L. Davis, M. J. Alter, H. El-Serag, T. Poynard and L. W. Jennings, *Gastroenterology*, **2010**, 138, 513-521, 521 e511-516.
5. D. Lavanchy, *Liver Int.*, **2009**, 29 Suppl 1, 74-81.
6. M. Zajac, I. Muszalska, A. Sobczak, A. Dadej, S. Tomczak and A. Jelinska, *Eur. J. Med. Chem.*, **2019**, 165, 225-249.
7. N. Arima, C. Y. Kao, T. Licht, R. Padmanabhan, Y. Sasaguri and R. Padmanabhan, *J. Biol. Chem.*, **2001**, 276, 12675-12684.
8. H. R. Rosen, *N. Engl. J. Med.*, **2011**, 364, 2429-2438.
9. G. M. Lauer and B. D. Walker, *N. Engl. J. Med.*, **2001**, 345, 41-52.
10. Y. Huang, K. Staschke, R. De Francesco and S.-L. Tan, *Virology*, **2007**, 364, 1-9.
11. K.-H. Lan, M.-L. Sheu, S.-J. Hwang, S.-H. Yen, S.-Y. Chen, J.-C. Wu, Y.-J. Wang, N. Kato, M. Omata, F.-Y. Chang and S.-D. Lee, *Oncogene*, **2002**, 21, 4801-4811.
12. R. Bartenschlager, V. Lohmann and F. Penin, *Nat. Rev. Microbiol.*, **2013**, 11, 482-496.
13. S. A. Qureshi, *Med. Res. Rev.*, **2007**, 27, 353-373.
14. M. U. Ashraf, K. Iman, M. F. Khalid, H. M. Salman, T. Shafi, M. Rafi, N. Javaid, R. Hussain, F. Ahmad, S. Shahzad-Ul-Hussan, S. Mirza, M. Shafiq, S. Afzal, S. Hamera, S. Anwar, R. Qazi, M. Idrees, S. A. Qureshi and S. U. Chaudhary, *Med. Res. Rev.*, **2019**, 39, 1091-1136.
15. I. H. Bae, J. K. Choi, C. Chough, S. J. Keum, H. Kim, S. K. Jang and B. M. Kim, *ACS Med. Chem. Lett.*, **2014**, 5, 255-258.
16. N. Horscroft, V. C. H. Lai, W. Cheney, N. Yao, J. Z. Wu, Z. Hong and W.

- Zhong, *Antiviral Chem. Chemother.*, **2005**, *16*, 1-12.
17. T. L. Tellinghuisen, M. J. Evans, T. von Hahn, S. You and C. M. Rice, *J. Virol.*, **2007**, *81*, 8853-8867.
 18. A. Aghemo and R. De Francesco, *Hepatology*, **2013**, *58*, 428-438.
 19. R. A. Fridell, D. Qiu, C. Wang, L. Valera and M. Gao, *Antimicrob. Agents Chemother.*, **2010**, *54*, 3641-3650.
 20. M. Gao, R. E. Nettles, M. Belema, L. B. Snyder, V. N. Nguyen, R. A. Fridell, M. H. Serrano-Wu, D. R. Langley, J. H. Sun, D. R. O'Boyle, 2nd, J. A. Lemm, C. Wang, J. O. Knipe, C. Chien, R. J. Colonno, D. M. Grasela, N. A. Meanwell and L. G. Hamann, *Nature*, **2010**, *465*, 96-100.
 21. C. Wang, H. Huang, L. Valera, J.-H. Sun, D. R. O'Boyle, II, P. T. Nower, L. Jia, D. Qiu, X. Huang, A. Altaf, M. Gao and R. A. Fridell, *Antimicrob. Agents Chemother.*, **2012**, *56*, 1350-1358.
 22. R. A. Love, O. Brodsky, M. J. Hickey, P. A. Wells and C. N. Cronin, *J. Virol.*, **2009**, *83*, 4395-4403.
 23. A. Chan, K. Patel and S. Naggie, *Drugs*, **2017**, *77*, 131-144.
 24. C. Tateno, Y. Kawase, Y. Tobita, S. Hamamura, H. Ohshita, H. Yokomichi, H. Sanada, M. Kakuni, A. Shiota, Y. Kojima, Y. Ishida, H. Shitara, N. A. Wada, H. Tateishi, M. Sudoh, S. Nagatsuka, K. Jishage and M. Kohara, *PloS one*, **2015**, *10*, e0142145.
 25. V. K. Rustgi, *Expert Opin. Drug Saf.*, **2010**, *9*, 883-892.
 26. M. Belema, V. N. Nguyen, D. R. St. Laurent, O. D. Lopez, Y. Qiu, A. C. Good, P. T. Nower, L. Valera, D. R. O'Boyle, J.-H. Sun, M. Liu, R. A. Fridell, J. A. Lemm, M. Gao, J. O. Knipe, N. A. Meanwell and L. B. Snyder, *Bioorg. Med. Chem. Lett.*, **2013**, *23*, 4428-4435.
 27. R. A. Fridell, C. Wang, J. H. Sun, D. R. O'Boyle, 2nd, P. Nower, L. Valera, D. Qiu, S. Roberts, X. Huang, B. Kienzle, M. Bifano, R. E. Nettles and M. Gao, *Hepatology*, **2011**, *54*, 1924-1935.
 28. S. Pol, R. H. Ghalib, V. K. Rustgi, C. Martorell, G. T. Everson, H. A. Tatum, C. Hezode, J. K. Lim, J.-P. Bronowicki, G. A. Abrams, N. Braeu, D. W. Morris, P. J. Thuluvath, R. W. Reindollar, P. D. Yin, U. Diva, R. Hindes, F.

- McPhee, D. Hernandez, M. Wind-Rotolo, E. A. Hughes and S. Schnittman, *Lancet Infect. Dis.*, **2012**, *12*, 671-677.
29. S. Zeuzem, M. Mizokami, S. Pianko, A. Mangia, K.-H. Han, R. Martin, E. Svarovskaia, H. Dvory-Sobol, B. Doehle, C. Hedskog, C. Yun, D. M. Brainard, S. Knox, J. G. McHutchison, M. D. Miller, H. Mo, W.-L. Chuang, I. Jacobson, G. J. Dore and M. Sulkowski, *J. Hepatol.*, **2017**, *66*, 910-918.
 30. M. C. Sorbo, V. Cento, V. C. Di Maio, A. Y. M. Howe, F. Garcia, C. F. Perno and F. Ceccherini-Silberstein, *Drug Resistance Updates*, **2018**, *37*, 17-39.
 31. D. R. O'Boyle Ii, J. H. Sun, P. T. Nower, J. A. Lemm, R. A. Fridell, C. Wang, J. L. Romine, M. Belema, V. N. Nguyen, D. R. Laurent, M. Serrano-Wu, L. B. Snyder, N. A. Meanwell, D. R. Langley and M. Gao, *Virology*, **2013**, *444*, 343-354.
 32. K. Vercauteren, Y. P. de Jong and P. Meuleman, *Curr. Opin. Virol.*, **2015**, *13*, 67-74.
 33. D. R. St. Laurent, M. Belema, M. Gao, J. Goodrich, R. Kakarla, J. O. Knipe, J. A. Lemm, M. Liu, O. D. Lopez, V. N. Nguyen, P. T. Nower, D. O'Boyle, Y. Qiu, J. L. Romine, M. H. Serrano-Wu, J.-H. Sun, L. Valera, F. Yang, X. Yang, N. A. Meanwell and L. B. Snyder, *Bioorg. Med. Chem. Lett.*, **2012**, *22*, 6063-6066.
 34. D. J. Cada, J. Leonard, T. L. Levien and D. E. Baker, *Hosp. Pharm.*, **2015**, *50*, 396-412.
 35. A. M. Bell, J. L. Wagner, K. E. Barber and K. R. Stover, *Int. J. Hepatol.*, **2016**, *2016*, 3852126.
 36. E. B. Chahine, D. Kelley and L. M. Childs-Kean, *Ann Pharmacother.*, **2018**, *52*, 352-363.
 37. P. McCormack, *Drugs*, **2015**, *75*, 515-524.
 38. D. Ross-Thriepeland and M. Harris, *J. Gen. Virol.*, **2015**, *96*, 727-738.
 39. S. Giroux, J. Xu, T. J. Reddy, M. Morris, K. M. Cottrell, C. Cadilhac, J. A. Henderson, O. Nicolas, D. Bilimoria, F. Denis, N. Mani, N. Ewing, R. Shawgo, L. L'Heureux, S. Selliah, L. Chan, N. Chauret, F. Berlioz-Seux,

- M. N. Namchuk, A. L. Grillot, Y. L. Bennani, S. K. Das and J. P. Maxwell, *ACS Med. Chem. Lett.*, **2014**, 5, 240-243.
40. M. Zhong, E. Peng, N. Huang, Q. Huang, A. Huq, M. Lau, R. Colonno and L. Li, *Bioorg. Med. Chem. Lett.*, **2014**, 24, 5731-5737.
 41. M. Issur and M. Götte, *Viruses*, **2014**, 6, 4227-4241.
 42. A. V. Ivachtchenko, O. D. Mitkin, P. M. Yamanushkin, I. V. Kuznetsova, E. A. Bulanova, N. A. Shevkun, A. G. Koryakova, R. N. Karapetian, V. V. Bichko, A. S. Trifelenkov, D. V. Kravchenko, N. V. Vostokova, M. S. Veselov, N. V. Chufarova and Y. A. Ivanenkov, *J. Med. Chem.*, **2014**, 57, 7716-7730.
 43. Y. You, H. S. Kim, J. W. Park, G. Keum, S. K. Jang and B. M. Kim, *RSC Advances*, **2018**, 8, 31803-31821.
 44. J. J. Kohler, J. H. Nettles, F. Amblard, S. J. Hurwitz, L. Bassit, R. A. Stanton, M. Ehteshami and R. F. Schinazi, *Infect. Drug. Resist.*, **2014**, 7, 41-56.
 45. D. B. Ascher, J. Wielens, T. L. Nero, L. Doughty, C. J. Morton and M. W. Parker, *Sci. Rep.*, **2014**, 4, 4765.
 46. E. P. Gillis, K. J. Eastman, M. D. Hill, D. J. Donnelly and N. A. Meanwell, *J. Med. Chem.*, **2015**, 58, 8315-8359.
 47. J. Dong, K. B. Sharpless, L. Kwisnek, J. S. Oakdale and V. V. Fokin, *Angewandte Chemie*, **2014**, 53, 9466-9470.
 48. J. Dong, L. Krasnova, M. G. Finn and K. B. Sharpless, *Angewandte Chemie*, **2014**, 53, 9430-9448.
 49. S. Li, L. T. Beringer, S. Chen and S. Averick, *Polymer*, **2015**, 78, 37-41.
 50. A. Narayanan and L. H. Jones, *Chem. Sci.*, **2015**, 6, 2650-2659.
 51. J. Yatvin, K. Brooks and J. Locklin, *Chemistry*, **2016**, 22, 16348-16354.
 52. A. Dondoni and A. Marra, *Org. Biomol. Chem.*, **2017**, 15, 1549-1553.
 53. I. H. Bae, H. S. Kim, Y. You, C. Chough, W. Choe, M. K. Seon, S. G. Lee, G. Keum, S. K. Jang and B. Moon Kim, *Eur. J. Med. Chem.*, **2015**, 101, 163-178.
 54. D. R. St Laurent, M. H. Serrano-Wu, M. Belema, M. Ding, H. Fang, M.

- Gao, J. T. Goodrich, R. G. Krause, J. A. Lemm, M. Liu, O. D. Lopez, V. N. Nguyen, P. T. Nower, D. R. O'Boyle, 2nd, B. C. Pearce, J. L. Romine, L. Valera, J. H. Sun, Y. K. Wang, F. Yang, X. Yang, N. A. Meanwell and L. B. Snyder, *J. Med. Chem.*, **2014**, *57*, 1976-1994.
55. T. R. Webb and C. Eigenbrot, *J. Org. Chem.*, **1991**, *56*, 3009-3016.
 56. K. S. Lim, D. W. Kang, Y. S. Kim, M. S. Kim, S. G. Park, S. Choi, L. V. Pearce, P. M. Blumberg and J. Lee, *Bioorg Med Chem Lett*, **2011**, *21*, 299-302.
 57. L. C. King and G. K. Ostrum, *J. Org. Chem.*, **1964**, *29*, 3459-3461.
 58. S. D. Schimler, M. A. Cismesia, P. S. Hanley, R. D. Froese, M. J. Jansma, D. C. Bland and M. S. Sanford, *J. Am. Chem. Soc.*, **2017**, *139*, 1452-1455.
 59. R. Zelli, S. Tommasone, P. Dumy, A. Marra and A. Dondoni, *Euro. J. Org. Chem.*, **2016**, DOI: 10.1002/ejoc.201600732, 5102-5116.
 60. Y. You, H. S. Kim, I. H. Bae, S. G. Lee, M. H. Jee, G. Keum, S. K. Jang and B. M. Kim, *Eur. J. Med. Chem.*, **2017**, *125*, 87-100.
 61. C. S. Kim, S. J. Keum and S. K. Jang, *PloS one*, **2011**, *6*, e22808.
 62. B. D. Lindenbach, M. J. Evans, A. J. Syder, B. Woelk, T. L. Tellinghuisen, C. C. Liu, T. Maruyama, R. O. Hynes, D. R. Burton, J. A. McKeating and C. M. Rice, *Science*, **2005**, *309*, 623-626.
 63. C. Wang, L. Jia, H. Huang, D. Qiu, L. Valera, X. Huang, J. H. Sun, P. T. Nower, D. R. O'Boyle, 2nd, M. Gao and R. A. Fridell, *Antimicrob. Agents Chemother.*, **2012**, *56*, 1588-1590.
 64. M. Belema, O. D. Lopez, J. A. Bender, J. L. Romine, D. R. St Laurent, D. R. Langley, J. A. Lemm, D. R. O'Boyle, 2nd, J. H. Sun, C. Wang, R. A. Fridell and N. A. Meanwell, *J. Med. Chem.*, **2014**, *57*, 1643-1672.
 65. S. Li, D. Cohen-Karni, L. T. Beringer, C. Wu, E. Kallick, H. Edington, M. J. Passineau and S. Averick, *Polymer*, **2016**, *99*, 7-12.
 66. P. Targett-Adams, E. J. S. Graham, J. Middleton, A. Palmer, S. M. Shaw, H. Lavender, P. Brain, T. D. Tran, L. H. Jones, F. Wakenhut, B. Stammen, D. Pryde, C. Pickford and M. Westby, *J. Virol.*, **2011**, *85*, 6353-6368.
 67. F. Penin, V. Brass, N. Appel, S. Ramboarina, R. Montserret, D. Ficheux,

- H. E. Blum, R. Bartenschlager and D. Moradpour, *J. Biol. Chem.*, **2004**, 279, 40835-40843.
68. C. A. Coulson, *Nature*, **1969**, 221, 1106-1110.
 69. J. Shi, L. Zhou, F. Amblard, D. R. Bobeck, H. Zhang, P. Liu, L. Bondada, T. R. McBrayer, P. M. Tharnish, T. Whitaker, S. J. Coats and R. F. Schinazi, *Bioorg. Med. Chem. Lett.*, **2012**, 22, 3488-3491.
 70. B. T. Guan, X. Y. Lu, Y. Zheng, D. G. Yu, T. Wu, K. L. Li, B. J. Li and Z. J. Shi, *Org Lett*, **2010**, 12, 396-399.
 71. K. J. Blight, A. A. Kolykhalov and C. M. Rice, *Science*, **2000**, 290, 1972-1974.
 72. T. C. Chou, *Pharmacol. Rev.*, **2006**, 58, 621-681.
 73. T.-C. Chou, *Cancer Res.*, **2010**, 70, 440.
 74. R. Schinazi, P. Halfon, P. Marcellin and T. Asselah, *Liver Int.*, **2014**, 34 Suppl 1, 69-78.
 75. D. R. Piper, S. R. Duff, H. C. Eliason, W. J. Frazee, E. A. Frey, M. Fuerstenau-Sharp, C. Jachec, B. D. Marks, B. A. Pollok, M. S. Shekhani, D. V. Thompson, P. Whitney, K. W. Vogel and S. D. Hess, *Assay. Drug. Dev. Technol.*, **2008**, 6, 213-223.
 76. V. Lohmann, F. Korner, J. Koch, U. Herian, L. Theilmann and R. Bartenschlager, *Science*, **1999**, 285, 110-113.
 77. T. Phan, R. K. Beran, C. Peters, I. C. Lorenz and B. D. Lindenbach, *J. Virol.*, **2009**, 83, 8379-8395.
 78. A. Geddawy, Y. F. Ibrahim, N. M. Elbahie and M. A. Ibrahim, *J. Transl. Int. Med.*, **2017**, 5, 8-17.
 79. C. Wang, J. H. Sun, D. R. O'Boyle, 2nd, P. Nower, L. Valera, S. Roberts, R. A. Fridell and M. Gao, *Antimicrob. Agents. Chemother.*, **2013**, 57, 2054-2065.
 80. M. O. Silva, M. Treitel, D. J. Graham, S. Curry, M. J. Frontera, P. McMonagle, S. Gupta, E. Hughes, R. Chase, F. Lahser, R. J. O. Barnard, A. Y. M. Howe and J. A. Howe, *J. Hepatol.*, **2013**, 59, 31-37.
 81. T. T. Cheung, J. W. Yan Chiu, M. F. Yuen, K. S. Ling Lam, B. M. Yung

Cheung, H.-P. Feng, W. W. Yeh, J. Wang, W. Li, X. M. Zhao, Z. Wang and S. Mu, *Clinical Therapeutics*, **2018**, *40*, 719-732.e711.

국문초록

C 형 간염 바이러스 (HCV) 감염은 간경화 및 간암으로 이어질 수 있으며, 결국 사망에 이를 수 있는 심각한 질환이다. 최근 HCV의 여러 유전자형을 표적으로 하는 직접 작용 제제들 (DAA)을 개발하기 위한 노력이 집중되어왔다. 특히, 비 구조 단백질 5A (NS5A)는 HCV 증식에 필수적이므로, 여러 제약회사에서 NS5A를 타겟으로 하는 항HCV 약물을 많이 개발하고 있다. 우리는 이 논문에서, 바이아릴 설펜 (biaryl sulfone) 또는 황산염 (biaryl sulfate) 중심과 치환된 플루오렌 (fluorene) 중심골격을 가진 새로운 C 형 간염 바이러스 비 구조 5A (NS5A)단백질 억제제를 개발하였다.

첫째, 우리는 황산염 코어 구조를 함유 한 HCV NS5A 억제제의 합성을 위해, 불화 황 (VI) 불화 교환 (SuFEx) 반응으로 알려진 아릴 설폰닐 플루오라이드 (aryl sulfonyl fluoride)와 아릴 실릴 에테르 (aryl silyl ether)사이의 고효율 화학적 커플링 반응을 이용하여 합성하였다. SuFEx화학에 기초하여 합성한 억제제 중, 몇몇 화합물은 GT-1b에 대한 두 자리 pM 수준의 EC_{50} 값 및 HCV GT-2a 균주에 대한 nM 수준보다 낮은 EC_{50} 값활성을 나타내었다. 황산염 중심골격의 각 면에 이미다졸 (imidazole) 및 아마이드 (amide)부분을 함유하는 비대칭 억제제 또한 합성하였다. 설페이트 또는 설펜 코어 구조의 다양한 치환 패턴을 함유하는 억제제에 대한 구조-활성 관계 (SAR) 연구를 통해, 아마이드 잔기를 함유한 **BMK-21014** 또는 이미다졸 잔기를 함유하는 **BMK-21025** 은 매우 높은 저해활성을 보여주었다. **BMK-21014** 는 유전자형 1b (GT-1b)와 2a (GT-2a)에 대해, 두자리 수 pM 수준의

저해 활성도를 나타냈다. **BMK-21025** 는 GT-1b에 비해 두 자리수의 pM 및 GT-2a에 대한 nM보다 낮은 EC₅₀ 를 보여주었다. 또한, **BMK-21014** 및 **BMK-21025** 는 hERG 리간드 결합 분석에서 심장 독성을 나타내지 않았으며, 에임스 (Ames) 시험에서 돌연변이 유발 가능성을 나타내지 않았다. 이들 화합물은 비구조 단백질 5B (NS5B) 억제제인 sofosbuvir (Sovaldi®) 약물과의 병용 치료에서 부가 효과가 있는 것으로 나타났다. 이 연구의 결과를 바탕으로, 바이아릴 설페이트 중심 골격을 갖는 화합물이 효과적인 HCV 억제제가 될 수 있음을 보여 주었다.

한편, 최근에 개발된 NS5A 억제제들은 돌연변이에 의해 생기는 저해제 내성이 큰 이슈로 부각되고 있다. 특정 유전자형과 낮은 저항 장벽에 대한 낮은 저해 활성도를 극복하기 위해, 우리는 NS5A 저해제의 다양한 유도체를 개발하고 *in vitro* 및 *in vivo* 분석 시스템을 사용하여 HCV 증식에 미치는 영향을 조사했다. 그 중에서, 유전자형 3a와 약물 내성 돌연변이에 효과적인 화합물 **BMK-21054** 와 **BMK-21075** 를 개발할 수 있었다. 이러한 결과를 바탕으로, 우리는 플루오렌 중심골격과 치환된 L-프롤린 유도체를 가진 NS5A 억제제가 다양한 HCV 유전자형과 돌연변이 억제에 중요한 역할을 한다는 것을 증명할 수 있었다.

주요어: HCV, NS5A 저해제, 항바이러스제, 바이알릴설페이트, SuFEx, 구조-활성 관계, 플루오렌, 돌연변이 저항성